

---

## RECENT RESEARCH ACTIVITIES

---

### **Development of a model system for tree growth under shortened annual cycle condition using artificial climate chambers**

**(Laboratory of Biomass Morphogenesis and Information, RISH, Kyoto University)**

**Kei'ichi Baba**

Generally, wood forms annual rings in the temperate region. The wood structures in a ring are synchronized to seasons. For example, large vessels of ring-porous wood are formed in the spring but thick-walled tracheids in conifer wood are formed in late summer to autumn. Such an annual rhythm of tree growth offers researchers only one chance each year to harvest and/or apply treatments to the stem for the formation of specific type of cells or structures. This forces researchers to accomplish all their research activities within a short experimental window or prolong their experiments to multiple years to accomplish their study objectives. Wood research would progress tremendously if such time constraints could be alleviated.

We established a shortened annual cycle system using growth chambers with leaf changes as the indicator [1]. It comprises three stages and includes dormancy and dormancy-breaks every 4-5 months. Thus, we compared the three cycles to examine annual rings and wood tissue formed in the shortened system with those formed in the field conditions and when lacking dormancy with fixed condition in the growth room [2]. The wood tissue grown under the shortened system consisted of three growth rings. Similar structures were observed around the ring-boundaries of the wood in a field-grown stem but were missing in the wood grown in conditions lacking dormancy even with growth periods similar to those of the shortened system. This result suggests that this shortened system could be adopted as a model for physiological research of wood and studying annual ring formation.

Tree shape in a shortened system could be useful as a model of tree aging. Miniaturized poplar trees with a multiple branching architecture similar to that of much older field-grown trees were developed using the shortened annual cycle system [3]. Poplars grown under the non-dormant condition had no branches and formed a simple shape with a single stem and leaves. In the shortened system, we observed the simultaneous breaking of dormancy of several buds, resulting in architectural complexity. Our results suggest that apical dominance is lost in the shortened annual system as dormancy is broken. In contrast, apical dominance persisted in the trees grown under the condition without dormancy. Moreover, observation of the phloem structure of the trees grown under the shortened system showed a more matured structure in the bast fiber cluster than that seen in trees grown under conditions without dormancy [4].

#### **Acknowledgements**

Financial support for this work was provided by the Research Institute for Sustainable Humanosphere, Kyoto University (Mission-1) and by JSPS KAKENHI Grant Number 18K05761. We would like to thank Editage ([www.editage.jp](http://www.editage.jp)) for assistance in English language editing.

#### **References**

- [1] Kurita, Y., Baba, K., Ohnishi, M., Anegawa, A., Shichijo, C., Kosuge, K., Fukaki, H. and Mimura, T., "Establishment of a shortened annual cycle system; a tool for the analysis of annual re-translocation of phosphorus in the deciduous woody plant (*Populus alba* L. ).", *J Plant Res*, vol. 127, no. 4, pp. 545-551, 2014.
- [2] Baba, K., Kurita, Y. and Mimura, T., "Wood structure of *Populus alba* formed in a shortened annual cycle system." *J Wood Sci*, vol. 64, no. 1, pp. 1-5, 2018.
- [3] Baba, K., Kurita, Y. and Mimura, T., "Architectural morphogenesis of poplar grown in a shortened annual cycle system." *Sustain Humanosphere*, no.13, pp. 1-4, 2017.
- [4] Baba, K., Kurita, Y. and Mimura, T., "Tissue structure of poplar stem grown under shortened annual cycle system." The 59<sup>th</sup> Annual meeting of the Japanese Society of Plant Physiologist, 2018.

## RECENT RESEARCH ACTIVITIES

**Production and identification of antiviral compounds from lignocellulosic biomass**

**(Laboratory of Biomass Conversion<sup>1</sup> & Center for Exploratory Research on the Humanosphere<sup>2</sup>, RISH, Kyoto University, Institute for Frontier Life and Medical Sciences<sup>3</sup>, Kyoto University)**

**Takashi Watanabe<sup>1</sup>, Ruibo Li<sup>1</sup>, Chihiro Kimura<sup>1</sup>, Ryota Ouda<sup>2,3</sup>,  
Ryo Narita<sup>2,3</sup>, Hiroshi Nishimura<sup>1</sup>, and Takashi Fujita<sup>3</sup>**

There is an increasing demand to establish sustainable society by replacing fossil resources to renewable bioresources. Biomass is the alternative carbon resources contributing reduction of green house gas emission and the energy crisis owing to depletion of fossil fuels. To establish the biomass-based society, production of value-added products is required in addition to production of biofuels, materials and commodity chemicals from biomass. In addition to the demand from the resource depletion and green house gas emission, we are now facing the crisis of pathogenic virus infection due to the global warming and globalization of transportation. If we could produce antiviral compounds from lignocellulosic biomass such as waste wood and agricultural residues, the process contributes to the establishment of biorefinery and suppression of expansion of pathogenic viruses. In the first step of the research strategy, we studied antiviral compounds involved in pyroligneous acids (PAs).

PAs, also called wood vinegar, pyroligneous liquor, pyrolysis bio-oil, or liquid smoke, are the crude condensate of smoke produced through carbonization, and consist of a pyrolyzate of cellulose, hemicelluloses, and lignin. Wood and bamboo PAs are complex mixtures of water, alcohols, organic acids, esters, aldehydes, ketones, phenolics, and nitrogen compounds. Acetic acid is the primary component of wood and bamboo PAs. We have been analyzing antiviral activities of PAs from hardwood, softwood and bamboo against EMCV to identify the compound responsible for the biological activity.<sup>1,2</sup> All the PAs except for Japanese red pine wood exhibited strong antiviral activity. Twenty-five kind of phenolic derivatives in the PAs were identified and quantified. An assessment of the antiviral activity of all the phenolic compounds against EMCV demonstrated that they are strongly dependent on the functional groups and their relative positions attached to the aromatic ring. More potent antiviral activities were determined for catechol and its derivatives. The antiviral activities of phenolic compounds with methyl groups are higher than those of compounds with methoxyl groups.<sup>1</sup>

These results present a new strategy to optimize the production of antiviral agents from PAs by monitoring the concentration of each phenol derivative from different plant origins. Understanding the structure-activity relationship of phenol derivatives will lead to the synthesis of more effective agents for virus-inactivation treatments. In addition to the analysis of PAs, research on production of antiviral compounds by microwave catalytic reactions of woody biomass and sugarcane bagasse is in progress.

**Acknowledgements**

We acknowledge Mission 5-1-1 Research Programs and ADAM, of Research Institute for Sustainable Humanosphere (RISH), Kyoto University. We indebted coworkers and collaborators of the research programs, Dr. Shinsuke Marumoto, Dr. Seiji P. Yamamoto and Emer. Prof. Mitsuyoshi Yatagai.

**References**

- [1] Li, R., R. Narita, H. Nishimura, S. Marumoto, S. P. Yamamoto, R. Ouda, M. Yatagai, T. Fujita and T. Watanabe, Antiviral activity of phenolic derivatives in pyroligneous acid from hardwood, softwood, and bamboo, *ACS Sustain. Chem. & Eng.*, **6**, 119-126 (2018).
- [2] Marumoto, S., S. Yamamoto, H. Nishimura, K. Onomoto, M. Yatagai, K. Yazaki, T. Fujita and T. Watanabe, Identification of germicidal compound against picornavirus in bamboo pyroligneous acid, *J. Agric. Food Chem.*, **60**, 9106-9011 (2012).

## RECENT RESEARCH ACTIVITIES

**Structure, biosynthesis, and bioengineering of lignocellulose and phenylpropanoid metabolites for future biorefinery****(Laboratory of Metabolic Science of Forest Plants and Microorganisms,  
RISH, Kyoto University)****Toshiaki Umezawa, Yuki Tobimatsu, Shiro Suzuki, and Masaomi Yamamura**

It is becoming increasingly important to establish a sustainable society by reducing our heavy reliance on fossil resources. As lignocellulosic biomass represents the most abundant renewable and carbon-neutral resources on earth, technologies to improve their utilizations are key for realizing the goal. In this context, we investigate the structure, biosynthesis and bioengineering of lignocellulose using various model plants and biomass crops. In addition, we are interested in understanding the biosynthesis of plant-derived phenylpropanoid metabolites which display various useful biological activities. Our program typically integrates research ideas and approaches based on chemistry, biochemistry, and molecular biology.

Among a wide variety of biomass feedstocks, grass biomass crops, such as *Erianthus*, *sorghum*, sugarcane, and bamboo, have attracted particular attention due to their high biomass productivity and superior environmental adaptability. To explore new breeding strategies to improve the production of useful fuels and materials from grass biomass, we seek to develop transgenic rice plants that produce biomass with improved utilization properties. Our research particularly focuses on manipulating lignin, a phenylpropanoid polymer accounting for 15-30 wt% of lignocellulosic biomass.

We have developed various rice transgenic lines in which specific genes encoding enzymes and transcription factors functioning in the lignin biosynthetic pathway are down- and/or up-regulated. Some of our developed transgenic lines appeared to display notably enhanced biomass properties that can be exploited for productions of bioenergy and biomaterials. In parallel, we are working on selective breeding of grass crop varieties, such as *Erianthus* spp. and *Sorghum* spp., with superior lignins suited for bioenergy and biomaterial productions.

In addition, aiming at biological production of useful phytochemicals, we have been characterizing plant and microbial enzymes/genes involved in formations of bioactive phenylpropanoids such as lignans and norlignans. Our recent projects include elucidation of the biosynthesis of antitumor podophyllotoxin in *Anthriscus sylvestris*, unravelling crystal structures of hinokiresinol synthases, unique enzymes responsible for the enantioselective formation of bioactive norlignans, and identification of enzymes/genes involved in the formation of estrogenic mammalian lignans (enterolignans) via human intestinal bacteria.

**Selected Publications (FY2017)**

- [1] Takeda Y, Koshiba T, Tobimatsu Y, Suzuki S, Murakami S, Yamamura M, Rahman Md M, Takano T, Hattori T, Sakamoto M, Umezawa. Regulation of *CONIFERALDEHYDE 5-HYDROXYLASE* expression to modulate cell wall lignin structure in rice. *Planta* **246**:337-349 (2017).
- [2] Lam PY, Tobimatsu Y, Takeda Y, Suzuki S, Yamamura M, Umezawa T, Lo C. Disrupting Flavone Synthase II alters lignin and improves biomass digestibility. *Plant Physiology* **174**:972-985 (2017).
- [3] Tarmadi D, Yoshimura T, Tobimatsu Y, Yamamura M, Umezawa T. Effects of lignins as diet components on the physiological activities of a lower termite, *Coptotermes formosanus* Shiraki. *Journal of Insect Physiology* **103**:57-63 (2017).
- [4] Tarmadi D, Yoshimura T, Tobimatsu Y, Yamamura M, Miyamoto T, Miyagawa Y, Umezawa T. The effects of various lignocelluloses and lignins on physiological responses of a lower termite, *Coptotermes formosanus*. *Journal of Wood Science* **63**:464-472 (2017).
- [5] Cui S, Wada S, Tobimatsu Y, Takeda Y, Saucet S, Takano T, Umezawa T, Shirasu K, Yoshida S. Host lignin composition affects haustorium induction in the parasitic plants *Phtheirospermum japonicum* and *Striga hermonthica*. *New Phytologist* **218**:710-723 (2018).
- [6] Tarmadi D, Tobimatsu Y, Yamamura M, Miyamoto T, Miyagawa Y, Umezawa T, Yoshimura T. NMR studies on lignocellulose deconstructions in the digestive system of the lower termite *Coptotermes formosanus* Shiraki. *Scientific Reports* **8**: 1290 (2018).
- [7] Umezawa T. Lignin modification in planta for valorization. *Phytochemistry Reviews*, in press (2018).
- [8] Miyamoto T, Yamamura M, Tobimatsu Y, Suzuki S, Kojima M, Takabe K, Terajima Y, Mihashi A, Kobayashi Y, Umezawa T. A comparative study of the biomass properties of *Erianthus* and sugarcane: lignocellulose structure, alkaline delignification rate, and enzymatic saccharification efficiency. *Bioscience Biotechnology and Biochemistry*, in press (2018).

---

 RECENT RESEARCH ACTIVITIES
 

---

**Analysis of gene expression in field grown soybean**
**(Laboratory of Plant Gene Expression, RISH, Kyoto University)**
**Akifumi Sugiyama and Kazufumi Yazaki**

Plants synthesize specialized metabolites which can be counted up to 200,000 to 1,000,000 compounds. These compounds are active in defense against both biotic and abiotic stresses as well as the interactions with other organisms. Among these metabolites, flavonoids, with more than 8,000 compounds, are a chemically and functionally well-characterized group. For example, flavonoids are known to function in the regulation of auxin transport, protection against UV exposure, and modulation of ROS (reactive oxygen species). In addition to these functions in plants, flavonoids are secreted from plant roots and shown to play important roles in rhizosphere biological communications.

Flavonoid synthesis is well characterized: chalcone synthase (CHS) converts 4-coumaroyl-CoA to naringenin chalcone or, to isoliquiritigenin together with chalcone reductase (CHR). Chalcone isomerase (CHI) isomerizes naringenin chalcone to naringenin and isoliquiritigenin to liquiritigenin.

Isoflavones are a class of flavonoids, which occur predominantly in legume species. The isoflavone biosynthesis pathway is also well characterized, and known to be derived from the central flavonoid biosynthesis pathway. P450 protein, isoflavone synthase (IFS), catalyses the first reaction in isoflavone biosynthesis pathway to form 2-hydroxyisoflavanone. 2-Hydroxyisoflavanone is dehydrated to produce daidzein and genistein. This reaction is mediated either spontaneously or via 2-hydroxyisoflavanone dehydratase (HID). Soybean (*Glycine max* (L.) Merr.) synthesizes daidzein and genistein, which are further glucosylated in the cytosol to daidzin and genistin by UDP-glucose: isoflavone 7-O-glucosyltransferase (IF7GT) and malonylated to malonyldaidzin/genistin by malonyl-CoA: isoflavone 7-O-glucoside 6''-O-malonyltransferase (IF7MaT). These products are presumably accumulated in vacuoles via unknown mechanisms. These isoflavone aglycones are suggested to be secreted from roots into the rhizosphere via two different pathways: membrane transport mediated by an ABC (ATP binding cassette)-type transporter, and secreted as isoflavone glucosides, which then to be hydrolysed to aglycones, daidzein and genistein, by an apoplast-localized ICHG (isoflavone conjugates hydrolysing beta-glucosidase). It is well known that Isoflavones in the soybean rhizosphere were shown to induce the expression of nod genes of *Bradyrhizobium japonicum*, which in turn initiate the nodule formation in the soybean roots to fix atmospheric nitrogen.

The major form of isoflavone in soybean root tissue is malonyldaidzin, but the major secreted form of isoflavone is daidzein. We previously showed that the secretion of isoflavones was developmentally regulated in hydroponic culture. Higher secretion of daidzein was observed during the vegetative stages than during the reproductive stages (Sugiyama et al. 2016). To expand our understanding of isoflavone synthesis and secretion, we analyzed isoflavone biosynthesis and contents during soybean growth in the field (Sugiyama et al. 2017). Differential expression of isoflavone biosynthesis genes was observed.

**References**

- [1] A Sugiyama, Y Yamazaki, K Yamashita, S Takahashi, T Nakayama, K Yazaki, "Developmental and nutritional regulation of isoflavone secretion from soybean roots" *Bioscience, biotechnology, and biochemistry* 80 (1), 89-94, 2016.
- [2] A Sugiyama, Y Yamazaki, S Hamamoto, H Takase, K Yazaki, "Synthesis and secretion of isoflavones by field-grown soybean" *Plant and Cell Physiology* 58 (9), 1594-1600, 2017.

## RECENT RESEARCH ACTIVITIES

**Global distribution of short vertical scale gravity waves potential energy observed from COSMIC GPS radio occultation****(Laboratory of Atmospheric Sensing and Diagnosis, RISH, Kyoto University)****Noersomadi, Toshitaka Tsuda, and Hiroyuki Hashiguchi**

We retrieved temperature profile with a high vertical resolution using the full spectrum inversion or Wave Optics (WO) method from Constellation Observing System for Meteorology Ionosphere and Climate (COSMIC) Global Positioning System (GPS) Radio Occultation (RO) measurement. We analyzed the vertical wavenumber spectra of gravity waves (GWs) from the normalized temperature perturbations in the 20-27 km height range considering reasonably stable layer regardless of season and latitude. We integrated the wavenumber spectra at range 0.5 km to 1.75 km of vertical wavelength ( $\lambda_z$ ) to obtain the gravity waves potential energy ( $E_p$ ), which was not studied using conventional COSMIC GPS-RO data retrieved by Geometrical Optics (GO). Figure 1 shows the ratio  $E_p$  to the model value by saturated GW theory during November-December-January (NDJ) and June-July-August (JJA). The ratio of  $E_p$  with the saturated GW model spectrum was relatively stable in the Southern Hemisphere, ranging from 0.4 to 0.6, but in the Northern Hemisphere it showed large variations from 0.3 to 1.2, depending on topography (i.e. Tibetan Plateau in 90°-150°, 30°-60°N, mountainous region in 170°-230°, 70°N) and showed a clear contrast between winter and summer. In particular, the ratio exceeded 1.0 in winter at middle latitudes in the Northern Hemisphere in region 90°-150°, indicating an important effect of topography. It is also noteworthy that the ratio of  $E_p$  in the tropics was steadily large at 1.0-1.2 regardless of season and longitude. In particular, over the Equator the ratio was 1.2-1.3 throughout a year.

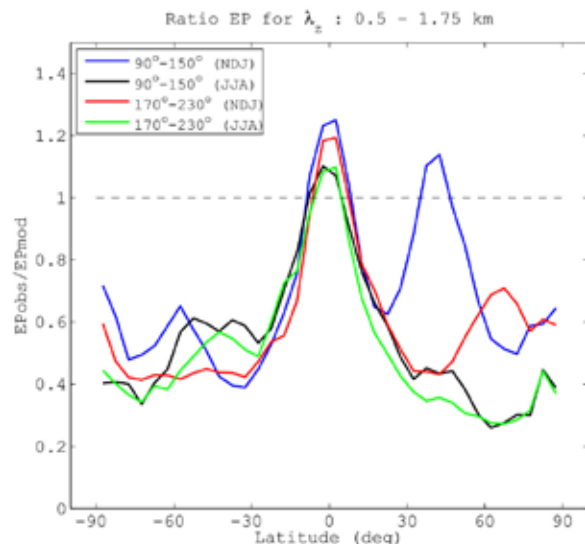


Figure 1. Ratio of the observed  $E_p$  to the model value by saturated gravity wave theory.

**Acknowledgements**

Noersomadi would like to grateful to the Program of Research and Innovation in Science and Technology (RISET-Pro), Ministry of Research, Technology, and Higher Education (RISTEKDIKTI) of Indonesia as the sponsor for his Ph.D.

**References**

Noersomadi and T. Tsuda, "Global distribution of vertical wavenumber spectra in the lower stratosphere observed using high-vertical-resolution temperature profiles from COSMIC GPS radio occultation", *Ann. Geophys.*, vol. 34, pp. 203-213, doi:10.5194/angeo-34-203-2016, 2016.

## RECENT RESEARCH ACTIVITIES

### Exploring sub-daily to seasonal variations in methane exchange in a single-crop rice paddy in central Japan

(Laboratory of Atmospheric Environmental Information Analysis, RISH, Kyoto University)

Kenshi Takahashi

Methane ( $\text{CH}_4$ ) is an important greenhouse gas, accounting for about 20% of the total direct radiative forcing from long-lived greenhouse gases since pre-industrial times. Rice paddy fields are known as a major source of  $\text{CH}_4$  in the terrestrial atmosphere. Many studies have thus investigated the source strength and environmental controls on  $\text{CH}_4$  exchange in rice paddies using the chamber technique and pot experiments. Despite these efforts, there is still large uncertainty regarding the global  $\text{CH}_4$  emissions from rice paddies. It is important to understand the transport pathways from the anoxic soil where  $\text{CH}_4$  is produced to the atmosphere, as well as the environmental controls on the transport processes. We applied the eddy covariance technique to observe ecosystem-scale  $\text{CH}_4$  exchange in a rice paddy field in central Japan (Kanto Region) in both the growing and post-harvest seasons. Our objectives were: 1) to clarify the environmental controls on ecosystem-scale  $\text{CH}_4$  exchange to infer the main transport pathways for the different stages of cultivation, and 2) to quantify the total annual  $\text{CH}_4$  exchange in the rice paddy field.

Our observations showed that, before heading of rice plant, the  $\text{CH}_4$  emission was dependent of soil temperature and wind speed. The soil temperature dependence can be due to an increase in  $\text{CH}_4$  production, higher molecular diffusion, and higher conductance within rice plant at higher soil temperature. An occurrence of ebullitive emission was also indicated from the wind speed-dependent data. After heading was completed, relative humidity and water temperature influenced the  $\text{CH}_4$  emission rates. Clear diurnal variations in the  $\text{CH}_4$  emission were also observed, and their amplitudes were dependent of the stages of cultivation ( $0.03 \mu\text{mol m}^{-2} \text{s}^{-1}$  in the late pre-heading stage and  $0.13 \mu\text{mol m}^{-2} \text{s}^{-1}$  in the post-heading stage). Induced convective throughflow within the rice aerenchyma after the change in plant structure was attributable to this variation in environmental controls after the heading.

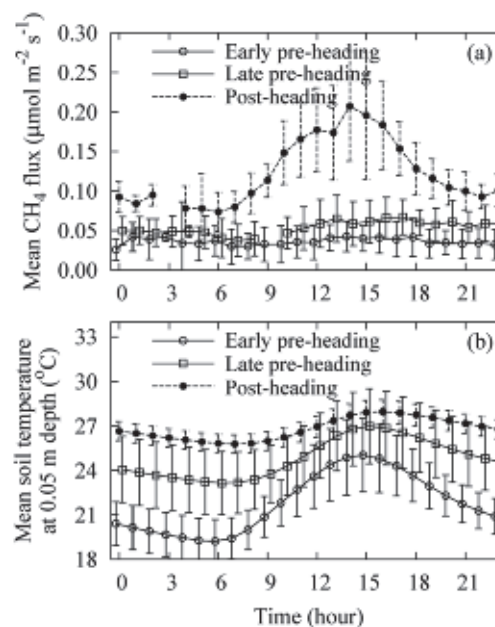


Figure 1. Mean diurnal variations in (a)  $\text{CH}_4$  flux and (b) soil temperature at 0.05m depth for the early pre-heading period (May 23-June 23, 2012, open circle), the late pre-heading period (June 28-July 29, 2012, open square), and post-heading period (July 30-August 27, 2012, solid circle). The averaged data points are shown only when the number of original data points is more than five. The error bars represent standard deviation. For clarity, data points are slightly shifted in the x-axis direction.

#### References

Iwata, H., M. Mano, K. Ono, T. Tokida, T. Kawazoe, Y. Kosugi, A. Sakabe, K. Takahashi, and A. Mityata, "Exploring sub-daily to seasonal variations in methane exchange in a single-crop rice paddy in central Japan", *Atmospheric Environment*, 179, 156-165, doi: 10.1016/j.atmosenv.2018.02.015, 2018.

## RECENT RESEARCH ACTIVITIES

**Equatorial Plasma Bubble (EPB) to atmosphere relationship found from day-to-day variation of GPS scintillation and GAIA assimilation data****(Laboratory of Radar Atmospheric Science, RISH, Kyoto University)****Mamoru Yamamoto**

Equatorial plasma bubble (EPB) is one of intense ionospheric phenomena that occur in the low-latitude and equatorial ionosphere. EPB is the phenomenon in which depletion of ionospheric plasma at the bottom side F-region becomes unstable, and rapidly grows and upwells to an altitude of up to 1000 km. The growth mechanism of EPBs is understood via the Rayleigh-Taylor instability. However, studies of day-to-day variability in EPB activity are few.

We tried to elucidate the relationship between EPBs and the behavior of the lower atmosphere by a combination of observations and simulations. This study is based on the previous study in which the GPS scintillation index and the tropospheric cloud-top temperature are used as proxies for EPB-activity and atmospheric perturbations, respectively, and a correlation was found between their day-to-day variations [Ogawa et al. 2009]. In this paper we maintained the same GPS scintillation data but substituted the atmospheric data via an assimilation run of the Ground-to-topside model of Atmosphere and Ionosphere for Aeronomy (GAIA). Cross-correlation between the EPB activity and the atmospheric temperature is similar to the results in the previous study (Figure 1). The new findings from our study include 1) an enhanced correlation between the EPB activity and the neutral atmosphere is found in horizontally and vertically large areas, 2) the longitudinal disturbance of atmospheric temperature and wind velocity during the EPB-active days is enhanced, and 3) the enhancement of atmospheric disturbance during the EPB-active days shows a similarity to the characteristics of large-scale wave structures in the ionosphere (Figure 2). These results more clearly support couplings between EPBs and the neutral atmosphere [Yamamoto et al. 2018].

**References**

- [1] Ogawa T, Miyoshi Y, Otsuka Y, Nakamura T, Shiokawa K (2009) Equatorial GPS ionospheric scintillations over Kototabang, Indonesia and their relation to atmospheric waves from below. *Earth, Planets and Space*, 61:397-410.
- [2] Yamamoto, M., Y. Otsuka, H. Jin, Y. Miyoshi (2018) Relationship between day-to-day variability of equatorial plasma bubble activity from GPS scintillation and atmospheric properties from GAIA assimilation, *Progress in Earth and Planetary Science*, 5:26, doi: 10.1186/s40645-018-0184-7.

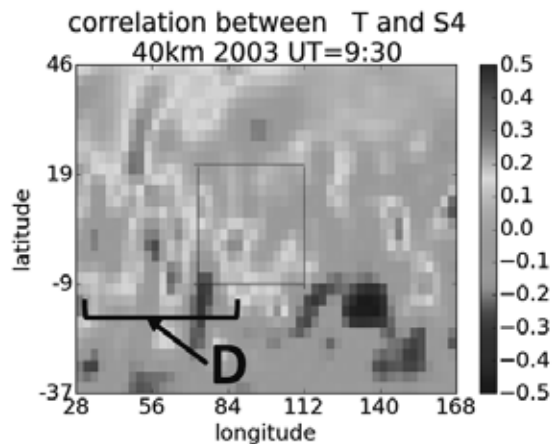


Figure 1. Correlation between day-to-day variation of GPS S4 index and GAIA temperature at 2hPa (~40 km in altitude) show high-correlation region (marked by “D”) in the low-latitude region with North-South elongated structures.

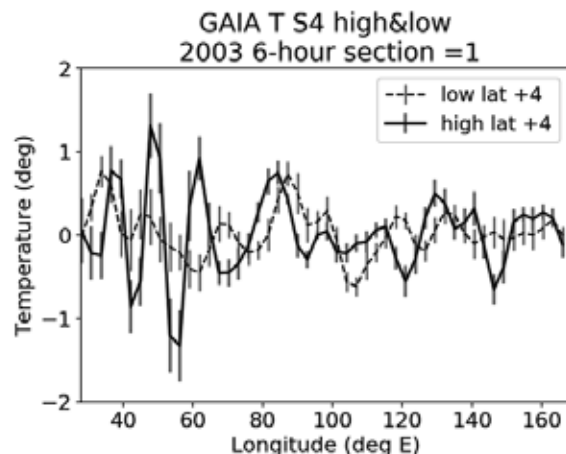


Figure 2. GAIA temperature on EPB-active days (solid) show enhanced longitudinal variation compared to the data on EPB-inactive days.

---

 RECENT RESEARCH ACTIVITIES
 

---

**Water-free process for natural polymer aerogel**
**(Laboratory of Fiber Multiplication, RISH, Kyoto University)**
**Satoko Okubayashi**

Polymers widely found in nature such cellulose, chitin, polypeptide, rubber are of great interests as source of bioplastics that are promising alternative materials of petrochemical polymers. Especially their nano-scaled products such nanofiber, nanowhisker and nanoparticle have unique features so called “Nano effects” that come up from extremely large surface area of the nanomaterials. A representative application of the Nano effects is to enhance mechanical properties of base plastics by assembling with the nano substances. In order to obtain a new filler material for lighter and stronger composite, we have attempted to prepare sponge-like cellulose aerogel that is the lightest three-dimensional sustainable biopolymer, using chemical treatment and supercritical fluid extraction for the last decade. The process basically consists of (1) preparation of cellulose solvent-gel using strong hydrogen bond acceptor, tetrabutyl ammonium fluoride, (2) substitution of the solvent with alcohol that is easily removed by supercritical CO<sub>2</sub>, and (3) extraction of the alcohol in gel by supercritical CO<sub>2</sub> that is well-used as a non-aqueous medium having significantly low surface tension to maintain porous aerogel structure. We optimized the experimental conditions and obtained a cellulose aerogel having 30-40 mg/cm<sup>3</sup> of density and 0.8-3.1 kPa of compressive modulus depending on cellulose dose by this process [1].

Recently, the process above was simplified by skipping substitution process (2). This improvement not only saved time for whole process but also reduced the shrinkage of the gel, resulting in more uniform and smaller pores of the aerogel [2]. The process set with (1) and (3) was also undertaken for cellulose nanofiber disintegrated by mechanical treatment without any chemicals and dispersed in water taking medical applications into account. Any sponge-like material was not obtained from the cellulose nanofiber dispersed in water, although a sheet-like material was found in a high pressure-vessel after supercritical CO<sub>2</sub> extraction. On the other hands, adding a silk protein, sericin into the aqueous solution containing cellulose nanofiber promoted its gelation and the bulky aerogel was prepared as their scanning electron microscopic images are shown in Figure 1 [2].

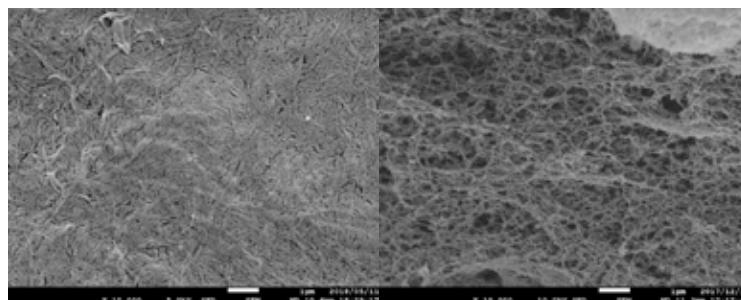


Figure 1. SEM images of cellulose nanofibers disintegrated by mechanical treatment in water with (left) and without (right) sericin after supercritical CO<sub>2</sub> extraction

At present, we have been preparing an aerogel of another silk protein, fibroin from the nanofiber disintegrated in water by mechanical treatment followed by supercritical CO<sub>2</sub> extraction. The fibroin aerogel is going to be tested for tissue scaffold, and influences of the aerogel morphology e.g. pore size, pore volume, specific surface area on the formation of new viable tissue will be investigated.

**Acknowledgements**

Part of the works were supported by KAKENHI Grant-in-Aid for Scientific Research (C) 18550190, 22550196, and JSPS Joint Research Projects in 2010-2012.

**References**

- [1] Y. Koyama, “Preparation of nonligneous cellulosic aerogel using high pressure CO<sub>2</sub>”, *Master Thesis at Graduate School of Science and Technology, Kyoto Institute of Technology*, 2013.
- [2] S. Ueeda, Y. Okahisa, E. Kotani, S. Okubayashi, “Preparation of natural polymer aerogel using supercritical carbon dioxide”, *Proceedings of the 71<sup>st</sup> Annual Meeting at The Textile Machinery Society of Japan*, p65, 2018.



---

## RECENT RESEARCH ACTIVITIES

---

### No evidence for presence of the red imported fire ant in Osaka Nanko area

(Laboratory of Ecosystem Management and Conservation Ecology,  
RISH, Kyoto University)

Chin-Cheng Yang

The red imported fire ants (hereafter refer to as the fire ant), *Solenopsis invicta*, one of the world's worst invasive ants, have been discovered in numerous container yards and in-land warehouses at a total of 12 prefectures in Japan since May 2017. Despite intensive survey within various port regions, it remains questionable if field population of the fire ant exists outside the survey perimeter, simply because little attempt has been made. As the invasion of fire ant is believed at very early stage, knowledge of this invasive ant such as geographic distribution in Japan is urgently needed as delimitation of an invasive species' distribution is key to eradication success. Supported by RISH Mission 1 research grant, my lab has conducted a detailed survey for the presence of fire ant within areas located in close proximity of the Osaka Nanko Port, one of the seaports with reported fire ant infestations. Here I reported results of the survey effort.

#### Why Nanko area, and how survey was carried out

Nanko area is of particular interest because two fire ant queens were once found in one of the container yards of this area during July 2017 (within a colony refuse pile where ant workers discard uneaten food and other wastes with corpses). This is believed as a sign indicative of the presence of a mature colony. A total of 15 sites around the port were selected for survey based on the known nesting preference of the fire ant, which includes park, school, lawns and fields. Two prevailing survey methods were utilized: a standard lure station (fixed amount of potato chip or hotdog slice in a 50cc centrifuge) and visual surveillance. The lure stations were separated by 10m interval and was placed for 40mins along the roadside. Stations were brought back to the lab, and ants found in the centrifuge tubes were subject to species identification under microscope.

#### No fire ant detected in our study sites in Nanko area

While virtually all lure stations were found positive with ants, none of them are fire ants. The top five dominant species discovered in the lure station include *Tetramorium tsushimae*, *Monomorium chinense*, *Pheidole noda* and *Formica japonica*. These five species generally are considered as dominant species in urban environment and share similar food preference (protein/lipid) as the fire ant (except *F. japonica*). A number of ant mounds were found during the visual inspection, with most of which belonging to either *F. japonica* or *Camponotus japonicas*. Conclusively, the survey results of this study suggest that no field population of fire ant, at least in our study sites, exists, a conclusion consistent to separate survey effort by Dr. Ueda at Osaka Prefecture University. Furthermore, biotic resistance seems to be a main contributing factor to prevent fire ant from establishment in this area where native ants are quite abundant and dominant.

#### Acknowledgements

The author acknowledges Ms. Melody Man, Mr. Calvin Utomo, Mr Juntaek Shim and Mr. Ayumu Tanase for their help in the field. Gratitude goes to the RISH Mission 1 Committee.

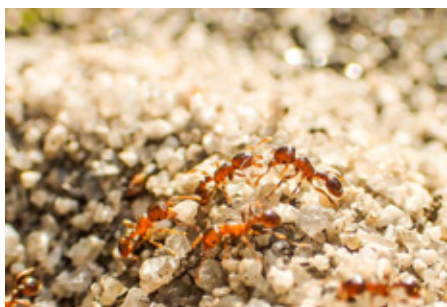


Figure 1. Workers of *Tetramorium tsushimae* nearby the nest opening.



Figure 2. A worker of *Formica japonica* leaving the nest for foraging.

## RECENT RESEARCH ACTIVITIES

## Optically transparent cellulose nanofiber nanocomposites via Pickering emulsion method

(Laboratory of Active Bio-based Materials, RISH, Kyoto University)

Subir Kumar Biswas

CNF-reinforced optically transparent composites of high-performance have been developed a decade ago.<sup>1</sup> The composites were fabricated by impregnating acrylic resin monomer into the CNF-sheet. The CNF-sheet is very stiff due to the hydrogen (H) bonding among the nanofibers and hence, its resin impregnated composite is difficult to mold into a three-dimensionally (3D) curved material. To accomplish 3D-molding with optical transparency, CNF-suspension could be mixed with liquid resin, however, hydrophilic CNF-suspension and hydrophobic acrylic resin are typically immiscible. These drawbacks virtually hinder the fabrication of CNF-reinforced high-performance transparent materials that could be used in many exciting applications, such as contact lenses, substrate for curved displays, microlens arrays and so on.

To overcome above two limitations, a Pickering emulsification process is developed. First, CNF-suspension was mixed with acrylic resin monomer (ABPE-10) at a concentration of 10% CNFs to the resin followed by vigorous agitation in a high-speed blender (37,000 rpm). The obtained emulsion was vacuum-filtered to get a CNFs/resin mat. The mat was then hot-pressed by placing between respective substrates to fabricate planar, 3D-molded, or micro-patterned composites (Fig. 1). The thermal, mechanical and optical properties of the composites were evaluated.

During emulsion formation, numerous resin droplets of 0.3-10  $\mu\text{m}$  in diameter have been produced. The droplets are covered and stabilized by the suspended CNF-network in the emulsion. Interestingly, after vacuum-filtration a CNF/resin mat with self-assembled 'nacre-like' structure has been obtained (Fig. 1). The nacre-like alternating CNF-resin structure reduces the H-bonding between the CNFs and allows to fabricate a lens-shaped transparent material after hot-pressing. The fabricated materials uniquely combines high optical transparency (regular transmittance 82% at 600 nm wavelength), high strength and toughness (15 and 24-times than neat acrylic resin, respectively), and a drastically low thermal expansion (1/24th of the neat acrylic resin) at a CNF content of 14-20%.

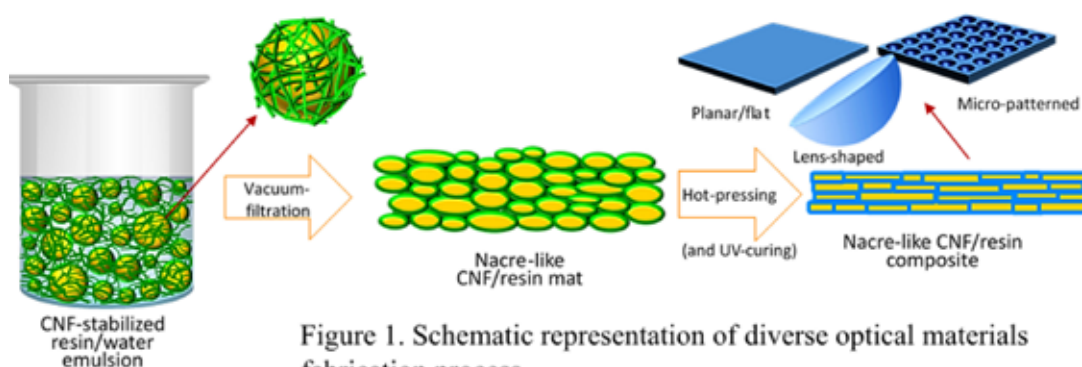


Figure 1. Schematic representation of diverse optical materials fabrication process.

### References

- [1] Yano H, Sugiyama J, Nakagaito A.N., Nogi M, Matsuura T, Hikita M, Handa K, "Optically transparent composites reinforced with networks of bacterial nanofibers", *Advanced Materials*, vol.17, no.2, 153-155, 2005.

---

**RECENT RESEARCH ACTIVITIES**

---

**Application of impact elastic waves in liquid to impregnation of wood****(Laboratory of Sustainable Materials, RISH, Kyoto University)****Soichi Tanaka, Kenji Umemura, and Kozo Kanayama****Introduction**

Chemical treatment, or introduction of chemicals into wood, is one of the major methods to enhance the performance and reliability of wood and wood-based materials. In the conventional treatment, however, distribution of chemicals in wood was irregular, leading to the inadequate performance and reliability. This irregularity can be categorized to macroscopic irregularity, indicating that the chemically treated wood includes the untreated cells in its structure; and microscopic irregularity, indicating that each cell includes the untreated regions in its amorphous structure. The macroscopic irregularity is mainly caused by the obstacle that blocks the liquid flow, e.g., the aspirated pits in tracheid of coniferous wood. This study focuses on the impact elastic waves transmitted through liquid to penetrate the obstacle as follows. If the liquid fills up the cell cavities between the wood surface and the tip of the liquid permeation in wood, or the obstacles, the abrupt increase in the liquid pressure from one to another on the wood surface is expected to cause the damping oscillation in the liquid pressure at the obstacles, leading to penetrate them. The purpose of this study is to promote the liquid permeation into wood by applying the impact elastic wave in the liquid. The test equipment was fabricated, and distilled water was used as a liquid. The temporal variability of the liquid pressure was examined to confirm the generation of the waves in liquid. The effect of the waves on the liquid permeation into wood was also examined.

**Experiment**

To generate impact elastic wave, a vessel (named  $V_A$ ) filled with liquid at an ordinary pressure (0.1 MPa) was connected by a valve to another vessel (named  $V_B$ ) filled with liquid at higher pressure (1.1 MPa). The temporal variability in liquid pressure in  $V_A$  was measured using the pressure gauge (named PG) after the valve was opened with various rate. The temporal variability was analyzed by a theory being based on the fluid dynamics.

To examine liquid permeation, wood samples with a dimension of 15 mm (T)  $\times$  15 mm (R)  $\times$  100 mm (L) were prepared from a block of yellow cedar (*Chamaecyparis nootkatensis* Spach). The samples at oven-dry state were injected by the liquid after vacuuming, and subsequently remained to be immersed in the liquid for 48 h. The sample after immersed was fixed to the region closed to  $P_G$  in the  $V_A$  with an ordinary pressure. The valve was opened with various rate after the inside of  $V_B$  was pressurized to 1.1 MPa. Amount of the liquid taken up to the sample was measured for each rate.

**Results and discussion**

The pressure at  $P_G$  without sample showed damping oscillation behavior when the valve was opened quickly, called quick pressurization. With sample in the quick pressurization, the pressure showed the similar behavior. By slow opening of the valve, called slow pressurization, the pressure gradually increased to a constant value. These findings indicate that the impact elastic waves occurred by the quick pressurization. The amount of the liquid taken up to the sample, however, showed no significant difference between the quick and slow pressurization. Analysis of the pressure variation suggests that the impact elastic waves in this experiment was not so much large as affecting the penetration of the obstacle in wood. To enhance the energy of the elastic wave, the amount of liquid passing through the valve per unit of time should be larger.

---

 RECENT RESEARCH ACTIVITIES
 

---

## Experimental seismic response of a full-scale Japanese conventional wooden post and beam building

(Laboratory of Structural Function, RISH, Kyoto University)

Hiroshi Isoda and Kotaro Sumida

### Introduction

While Japanese conventional wooden post and beam buildings have been designed to perform well with regard to life safety requirements in regions of moderate to high seismicity, it was found these types of low-rise structures have sustained significant structural and nonstructural damage in recent earthquakes, such as 2016 Kumamoto Earthquake. However, load path and dynamic response in post and beam construction arising during earthquake shaking are not well understood.

We have conducted some shake table tests to discuss the dynamic characteristic and the seismic performance of a full-scale, two-story, Japanese conventional wooden post and beam townhouse buildings. These test buildings have different seismic performance (Figure 1) and the damages observed from the tests were compared with the damage observed near seismic station (KiK-net, Mashiki-town, Kumamoto).

### Research subjects

#### Damage comparison with test buildings

Shake table tests were conducted for the building in accordance with the minimum requirement of the Building Standard Law of Japan. As a result of the tests, the extent of damage almost agreed with the result of the survey in the disaster area, and this test building which complied with the standard law did not collapse even two mainshocks were input (Figure 2).

#### High performance building twice the minimum requirement

On the other hand, the test building with high seismic capacity performed quite well during all earthquakes and there was no damage to structural components but some failure on gypsum boards or sidings. The inter-story drift was 80 mm, which is below the safety limit even input more than 20 major earthquakes recorded in Japan.

### Future plan

In the place 350 m away from KiK-net station, the building based on the new standard after 2000 collapsed, but other buildings following the old standard around it did not collapse (Figure 3). The cause of collapsed house seems to be the local site effect of ground motion or inadequate seismic design or construction, and further consideration is required for this cause.

### References

[1] BRI (Building Research Institute) and NILIM (National Institute for Land and Infrastructure Management), “2016 Kumamoto Earthquake Building Survey Report”, 2016.  
<http://www.nilim.go.jp/lab/bcg/siryou/tnn/tnn0929.htm>.



Figure 1. Test buildings with different seismic performance.

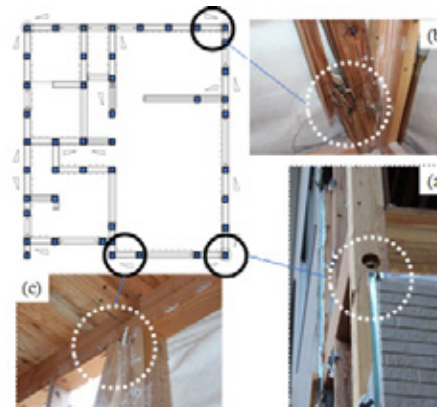


Figure 2. Observed damage to the test building with minimum requirement.

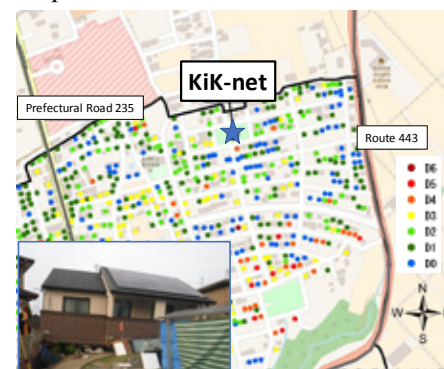


Figure 3. Collapsed building near the KiK-net station.

---

 RECENT RESEARCH ACTIVITIES
 

---

**Establishment of mass cultures of wood-attacking beetles**
**(Laboratory of Innovative Humano-habitability, RISH, Kyoto University)**
**Izumi Fujimoto and Tsuyoshi Yoshimura**

The recent increase in global wood imports and exports has accelerated the invasion of wood-attacking beetles into new areas. In addition, housing structures in Japan have been shifting to air-tight, high-insulation systems to save energy and achieve stable temperature conditions inside the home. These trends increase the risk of infestation and growth of wood-attacking beetle species, both domestic and exotic. To study the ecology of insect pests and develop effective management systems, establishment of mass cultures of target species is indispensable. We have been trying for many years to establish mass cultures of economically and culturally important wood-attacking beetles in the Deterioration Organisms Laboratory (DOL) of the Research Institute for Sustainable Humanosphere (RISH) for many years, and recently succeeded in specific efforts.

***Nicobium hirtum* – a most important pest for wooden cultural products**

*Nicobium hirtum* is a species of “Death-watch beetle” and is well known as the most important pest for wooden cultural products in Japan. However, its ecology is still a mystery due to the lack of mass culture. We obtained *N. hirtum*-infested timbers and maintained the colony for several years with an artificial diet originally designed for *Lyctus* beetles. Finally, some adults who emerged from the timbers laid eggs, and the larvae grew to produce healthy adults. Thus, we have established the first mass culture of *N. hirtum* and have started ecological studies on this beetle.

***Heterobostrychus aequalis* – a possible pest for hardwood timbers**

*Heterobostrychus aequalis* is an exotic species of “False powder-post beetle” and constitutes an important wood pest in the Asian tropics. Recently, infestation by *H. aequalis* has been increasing in Japan. We began a mass culture of the beetle using artificial diets in 2010. The mass culture has been well maintained, and we are now ready for laboratory experiments with *H. aequalis* larvae and adults.

***Lyctus* species other than *L. brunneus* and *L. africanus***

*Lyctus brunneus* and *L. africanus* are the 2 economically important species of “True powder-post beetle” in Japan. They cause serious problems in service timbers/composite materials, and are available at DOL. However, other related species, such as *L. sineisis* and *Lyctoxylon dentatum*, are also sometime found in Japan. We collected fresh larvae of these insects from infested timbers and have been trying since 2014 to establish mass cultures of these insects using artificial diets. The mass cultures of these two beetle species are now close to being fully established.

**Acknowledgements**

The authors acknowledge Professor Emeritus Masahiro Sakai, Ehime University, for providing *N. hirtum*-attacked timbers. The authors are also grateful to Dr. Lee-Jin Bong, National Health Research Institute, Taiwan, for her efforts to maintain an artificial culture of *H. aequalis* from attacked timbers when she was at RISH as a Mission Research Fellow.



Figure 1. An adult and a larva of *Nicobium hirtum* obtained from a mass culture.

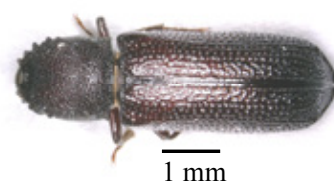


Figure 2. An adult of *Heterobostrychus aequalis* obtained from a mass culture.

---

 RECENT RESEARCH ACTIVITIES
 

---

**Simulations and modeling of geospace environment**
**(Laboratory of Computer Space Science, RISH, Kyoto University)**
**Yoshiharu Omura and Yusuke Ebihara**

We have investigated the properties of whistler mode wave-particle interactions at oblique wave normal angles to the background magnetic field. We find that electromagnetic energy of waves at frequencies below half the electron cyclotron frequency can flow nearly parallel to the ambient magnetic field. We thereby confirm that the gyroaveraging method, which averages the cyclotron motion to the gyrocenter and reduces the simulation from two-dimensional to one-dimensional, is valid for oblique wave-particle interaction [1]. We have conducted a self-consistent hybrid simulation, successfully reproducing electromagnetic ion cyclotron (EMIC) emissions with falling tone frequencies. The hybrid simulation is implemented with a parabolic ambient magnetic field [2]. We have also carried out a series of self-consistent electron hybrid code simulations for the dependence of chorus generation process on the temperature anisotropy and density of energetic electrons in the Earth's inner magnetosphere. We find that the chorus generation processes reproduced in the simulation results are consistently explained by the nonlinear wave growth theory [3].

When a substorm occurs, a bright aurora travels westward quickly. This is called a westward traveling surge. Using computer simulation, we found the reason why the bright aurora travels westward. A key parameter is the ionospheric conductivity depending on the upward field-aligned current. When we increased the ionospheric conductivity in the downward field-aligned current (although this situation is unrealistic), the bright aurora travels eastward [4]. We also show the pathway of energy from the solar wind to the ionosphere during the substorm expansion. The conversion of energy among electromagnetic energy, kinetic energy, and thermal energy is also shown [5]. In 1770, very bright aurora dominated by red color was witnessed in Japan and China. Using computer simulation, we investigated possible cause of the bright red aurora. Electrons with energy less than 100 eV should selectively precipitate into the ionosphere from 32 to 42 invariant latitudes to explain contemporary documents and paintings. The low energy electrons may originate in the plasmasphere, which could be accelerated to several tens of eV [6].

**References**

- [1] Hsieh, Y.-K., and Y. Omura, Study of wave-particle interactions for whistler mode waves at oblique angles by utilizing the gyroaveraging method. *Radio Science*, 52, 1268-1281, <https://doi.org/10.1002/2017RS006245>, 2017.
- [2] Shoji, M., and Y. Omura, Nonlinear generation mechanism of EMIC falling tone emissions. *Journal of Geophysical Research: Space Physics*, 122, 9924-9933, <https://doi.org/10.1002/2017JA023883>, 2017.
- [3] Katoh, Y., Y. Omura, Y. Miyake, H. Usui, and H. Nakashima, Dependence of generation of whistler mode chorus emissions on the temperature anisotropy and density of energetic electrons in the Earth's inner magnetosphere. *Journal of Geophysical Research: Space Physics*, 123, <https://doi.org/10.1002/2017JA024801>, 2018.
- [4] Ebihara, Y., and T. Tanaka, Why does substorm-associated auroral surge travel westward?, *Plasma Physics and Controlled Fusion*, 60, 014024, 2018..
- [5] Ebihara, Y., and T. Tanaka, Energy flow exciting field-aligned current at substorm expansion onset, *Journal of Geophysical Research: Space Physics*, 122, [doi:10.1002/2017JA024294](https://doi.org/10.1002/2017JA024294), 2017.
- [6] Ebihara, Y., H. Hayakawa, K. Iwahashi, H. Tamazawa, A. D. Kawamura., H. Isobe, Possible cause of extremely bright aurora witnessed in East Asia on 17 September 1770, *Space Weather*, 15, [doi:10.1002/2017SW001693](https://doi.org/10.1002/2017SW001693), 2017.

## RECENT RESEARCH ACTIVITIES

## Wireless power transfer R&amp;D for smart, flexible, and accommodating society

(Laboratory of Applied Radio Engineering for Humanosphere, RISH, Kyoto University)

Naoki Shinohara, Tomohiko Mitani, Yohei Ishikawa, Junji Miyakoshi,  
and Shin Koyama

Our laboratory joins a JST Center of Innovation (COI) Project named ‘The Last 5X innovation R&D center for a Smart, Happy, and Resilient Society’ in Kyoto University from FY2013[1]. The Last 5X indicates that it is to achieve a cordless environment at home within 5 meters from a wall, outside monitoring within a distance from 50 meters to 5 kilometers, sharing information on a daily basis with family members and friends living far from you (up to 500 km) by using 5 technologies (electric power transmission, communication, sensing, device, ICT) that connect the 5 elements of people, information, energy, health, and the environment at the same time.

Our R&D team is developing various Wireless Power Transfer (WPT) systems for the aim of the COI (Fig.1). In 2017, we developed a wearable rectenna (rectifying antenna) to drive a wireless sensor by microwave wireless power, whose aim was a nursing and child care application[2]. A part of these works is supported by RISH mission 5-2. In parallel, toward a commercial WPT application, we proposed a special permission of a field WPT experiment to MIC(Ministry of Internal Affairs and Communications) and got it as ‘sandbox (special region)’ to carry out the field WPT experiment at Seikacho town hall, Kyoto. We also got a sandbox for a microwave charging system of an electro-mobility at the same place at the same time. After the field experiments at the sandbox, we will apply the WPT system as a commercial system in next step.

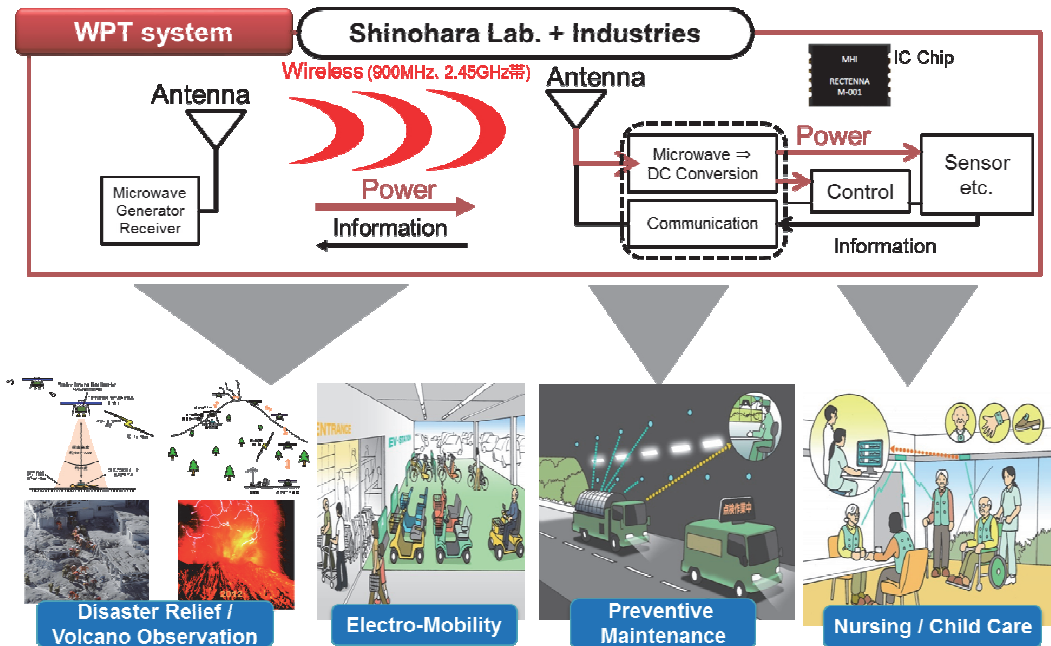


Fig. 1: Developing WPT systems and their applications by Shinohara Lab. and collaborative industries.

## References

- [1] Kyoto University COI <http://www.coi.kyoto-u.ac.jp/en>  
 [2] Y. Tanaka, et al., “Development of Wireless Sensor Powered by Microwave Wireless Power Transfer (in Japanese)”, submitting to IEICE Trans. B, 2018.

---

## RECENT RESEARCH ACTIVITIES

---

### **Novel space environment monitor, instrument, and space mission concepts**

**(Laboratory of Space Systems and Astronautics, RISH, Kyoto University)**

**Hiroshi Yamakawa, Hirotsugu Kojima, and Yoshikatsu Ueda**

#### **Space debris observation, modelling, and mitigation**

The space debris problem is tackled from observation (space situational awareness), trajectory evolution, and mitigation points of view. 1) A method to identify the size, shape, and rotation features, and to determine the trajectory of known space debris using range Doppler data of MU (Middle and Upper) Radar, RISH, Kyoto University, is investigated with successful observation results. 2) A study to investigate space debris trajectory evolution focusing on objects smaller than 1 cm has been started to shed light on geomagnetic field effects. 3) An on-orbit space debris observing system is studied assuming an optical sensor onboard a satellite. The required specifications of optical sensors and ranges of observable space debris are investigated for application to removal sequence.

#### **Electromagnetic space propulsion systems**

Recently, new propulsion systems that utilize electromagnetic forces acting on a charged spacecraft were proposed. The Lorentz force that acts when a charged object goes across the Earth's magnetic field and the Coulomb force that acts on among the charged objects can be employed to control the orbit of charged spacecraft or space debris by controlling the electrostatic potential of the object with charged particle emitters. One of our studies is to evaluate feasibility and performance of such "electromagnetic orbital control" regarding both orbital dynamics and plasma physics by using numerical simulation on the super computer system of Kyoto University. We 1) proposed a new charging model that enables to compute the surface potential fast and precisely by considering a velocity distribution of emitted particles, 2) proposed a new secondary electron emission model for particle simulations that can simulate much like the actual physics than conventional methods, and 3) revealed the thrust performance of an electric solar wind sail, a novel propulsion system which obtains its thrust by deflecting the ions in solar wind with numerous positively charged tethers.

#### **Miniaturization of plasma wave receiver system**

Plasma wave receiver is one of the essential instruments for space environment exploration; however, conventional receiver has a problem in its large weight and size. In order to overcome this problem, we have been miniaturized plasma wave receiver by developing Application-Specific Integrated Circuits (ASIC) for plasma wave receivers. We succeeded in developing miniaturized plasma wave receiver by realizing analog circuit, which is especially large part of the receiver, using ASIC. This miniaturized receiver will be onboard the SS-520-3 sounding rocket, which will launch in the not-too-distant future to resolve the cause of ion outflow phenomena at the cusp region. In addition, we aim to develop a mixed-signal ASIC chip for one-chip plasma wave receiver. The mixed-signal ASIC chip includes all analog and digital circuits for plasma wave receiver. One-chip plasma wave receiver allows to reduce weight and size of the instruments drastically, and it will contribute for increasing opportunities of plasma wave observation.

#### **Theoretical study of fine bubble and its application research**

Fine bubble (FB, less than 1 micro meter) technology is standardized as ISO/TC 281 and its basic and application research is conducted by many researchers. Basic properties and assumed generation mechanisms are now making clear. There is still remained problems of integrated theory of FB such as generation and stabilization. And we also need to apply FB technology to various application field with its detailed theory. As for integrating basic properties, we conduct various measurement such as ultrasonic attenuation of FB water, as measuring electrical potential of FB and as comparison with nano-particles in water. We also try to do application experiment in agricultural field as international collaboration study.



---

ABSTRACTS (PH D THESIS)

---

**Study on conservation of archaeological waterlogged wood in Vietnam**

**(Graduate School of Agriculture,  
Laboratory of Biomass Morphogenesis and Information, RISH, Kyoto University)**

**Nguyen Duc Thanh**

Archaeological waterlogged wood (WW) is one significant part of the archaeological resource because it provides evidence for the primary raw material used for structures, artifacts, and fuel throughout most of human existence. Therefore, conservation of cultural heritage is fundamental for conveying culture, traditions, ways of thinking and behaving to future generations. The preservation has an impressive impact on society from a political, sociological and anthropological point of view. The conservation treatments aim to prolong the life of cultural properties, without impairing the information and value they contain.

There are several archaeological sites have been discovered in Vietnam such as the ancient shipwrecks under the seabed in the south of Vietnam, wooden artifacts under the ground in the Thang Long heritage site - Hanoi, Bach Dang stake yard - Quang Ninh, and so on. Among them, the Thang Long Imperial Citadel site is one of the most important heritage sites, and it was named on the World Heritage list by UNESCO's World Heritage Committee in 2010. During the archaeological investigation, a significant proportion of wooden artifacts was unearthed from the Thang Long archaeological site. Some of them remain buried *in-situ* while others were salvaged from the site. These cultural properties are continually threatened by environmental impacts since the long-term protections are not implemented. Given the current condition of heritage, it is recommended that the immediate conservation treatment should be taken into account for preserving these artifacts. The conservation of cultural relics at Thang Long Imperial Citadel site, therefore, is one of the important plans put forth by the Government of Vietnam.

Conservation of archaeological WW is often a difficult subject in Vietnam. This is because general preservation methods cannot be applied for Vietnamese tropical WW. Therefore, this study aimed to establish appropriate preservation technology for the WW obtained from the Thang Long Imperial Citadel site, Hanoi, Vietnam.

Chapter 1 introduced the research background, objective and outline of the study. Additionally, the chapter also introduced conservation treatment methods currently applied to WW.

Chapter 2 summarizes the species identification and physicochemical properties of 15 waterlogged hardwood samples obtained from Thang Long archaeological site. The anatomical features showed that those samples were belonging to 10 different genera. The measurements on physical and chemical characteristics of WW showed different levels of wood degradation. Chemical analysis also confirmed the degree of wood degradation. Interestingly, the deterioration of *Erythrophleum fordii* Oliv. wood was very limited even after several hundred years of burial.

In Chapter 3, the natural durability of the *E. fordii* wood against white rot fungi was performed to elucidate the excellent state of preservation of this timber in the soil, and for determining appropriate procedures to conserve this timber. The results revealed high structural rigidity of *E. fordii* timber. The *E. fordii* wood fiber consisted of heavily lignified thick-walled fibers with the fiber lumina almost completely closed. 2D HSQC NMR evaluation revealed the *E. fordii* wood to have a heavily condensed lignin structure that reflected by the durability classes [1].

General preservation treatment methods using PEG4000, trehalose, and keratin was tested (Chapter 4). The results showed that the dimensional stability of WW was significantly improved after the treatments. The anti-shrink efficiency (ASE) values of the WW treated with keratin ranged between 72.5% and 96.2% depending on the species and degree of wood degradation. These values varied from 82.4% to 96.9% for the WW treated with PEG4000 or trehalose. Microscopic observations showed that the chemically treated woods maintained their original cell structures, forms, and shapes. It was also revealed that the reinforcement of cell walls by the feather keratin treatment was different from those observed for the PEG4000 or trehalose treatments. It was observed that PEG4000 and trehalose primarily filled the wood

---

## ABSTRACTS (PH D THESIS)

---

voids, while keratin predominantly absorbed on the cell walls and middle lamella. Based on the improved dimensional stability of wood, shortened impregnation time, removability of chemical, and aesthetic results obtained from the treatment, keratin showed a good performance in average as a preservation materials [2].

In order to establish the suitable treatment conditions for Vietnamese WW, steady-state diffusion coefficients of PEG4000, trehalose, and feather keratin through eight WW species were carried out (Chapter 5). The diffusion coefficients were strongly affected by wood species, the anisotropic structures of wood, conservation agents. Based on diffusion coefficient, expected impregnation time for dip-diffusion treatments can be estimated. A new method utilizing the *in-situ* crosslinking reaction of the hydrophilic polymer to enhance recoverability of WW from unexpected drying was developed (Chapter 6). The results showed that treatment with cross-linked PAANA resulted in excellent shape recovery of WW after multiple drying-rewetting cycles, while the recovery was not complete in the untreated samples [3]. The cross-linking PAANA treatment could be used to provide resistance and recovery after unexpected drying, and may be used either as the primary conservation method or as a pretreatment in conjunction with other established conservation methods.

In summary, the species identification and physicochemical properties of 15 WW samples were examined. It is revealed that the *E. fordii* (called as Lim wood) commonly excavated from the site is extremely resistant to degradation. The condensed type lignin is abundant, and the wood is made from the thick wall wood fibers with fibers lumina were completely closed. General preservation treatment methods using PEG, trehalose, and feather keratin was applied for conservation of small WW samples. Among chemical investigations, keratin exhibited high performance in average as a preservation material. It was clarified that the diffusion coefficient of preservatives depends on wood species, and pointed out the necessity of deciding treatment conditions for each tree species. Finally, a new method of protecting excavated wood from unexpected drying by utilizing the *in-situ* crosslinking reaction of the hydrophilic polymer was developed. The results of this study can be applied practically for the conservation of WW in Vietnam. However, inherent limitations of WW materials, several species have not been explicitly explored within this study. Moreover, since the anisotropic structure of wood and the degree of deterioration varies widely (even though wood samples are cut from the same beams), future study is required to examine additional tests for different WW species and samples with different degrees of wood degradation.

### Acknowledgements

The author appreciates supervisor Professor Junji Sugiyama (Laboratory of Biomass Morphogenesis and Information (LBMI), Research Institute for Sustainable Humanosphere (RISH), Kyoto University) for his invaluable enlightenment and guidance, kind encouragement and patience. Grateful appreciation is made to graduate committee members: Professor Takashi Watanabe (RISH, Kyoto University), Professor Tsuyoshi Yoshimura (RISH, Kyoto University) and Dr. Yohsei Kohdzuma (Nara National Research Institute for Cultural Properties (NNRICP), Nara) for examining and finalizing dissertation. Special thanks to Ms. Do Thi Ngoc Bich (Vietnam National University of Forestry) and Associate Professor Akiko Tashiro (Hokkaido University) for setting up the initial contact to the research group of waterlogged wood conservation. Last but not least, sincere thanks to the members of LBMI, RISH and Center for Archaeological Operations, NNRICP for their supports and friendship.

### References

- [1] Nguyen T.D, Kohdzuma Y, Endo R, Sugiyama J (2018) "Evaluation of chemical treatments on dimensional stabilization of archaeological waterlogged hardwoods obtained from the Thang Long Imperial Citadel site, Vietnam" *Journal of Wood Science*. DOI: 10.1007/s10086-018-1719-7.
- [2] Nguyen T.D, Nishimura H, Imai T, Watanabe T, Kohdzuma Y, Sugiyama J (2018) "Natural durability of the culturally and historically important timber: *Erythrophleum fordii* wood against white-rot fungi" *Journal of Wood Science*. DOI: 10.1007/s10086-018-1704-1.
- [3] Nguyen T.D, Sakakibara K, Imai T, Tsujii Y, Kohdzuma Y, Sugiyama J (2017) "Shrinkage and swelling behavior of archaeological waterlogged wood preserved with slightly crosslinked sodium polyacrylate" *Journal of Wood Science*. DOI: 10.1007/s10086-018-1696-x.

## ABSTRACTS (PH D THESIS)

**Development of particleboard made from sweet sorghum bagasse and citric acid**

(Graduate School of Agriculture,  
Laboratory of Sustainable Materials, RISH, Kyoto University)

**Sukma Surya Kusumah**

Sweet sorghum bagasse as a non-wood lignocellulose material that contain high hemicellulose (33.95%) [1] is a promising substitute wood material for the manufacture of particleboard. The high content of hemicellulose probably would make sweet sorghum bagasse react effectively with citric acid as a natural adhesive, hence the particleboard made from sweet sorghum bagasse bonded with citric acid would have good bondability. Therefore, the objective of this study is to utilize sweet sorghum bagasse in the manufacturing of environmentally friendly particleboard bonded with citric acid. The optimization of the manufacturing conditions of particleboard such as pre-treatment of particles before hot pressing condition, citric acid contents, pressing temperature and time that influence the physical properties of particleboard were investigated. The improvement of the particleboard physical properties was observed by addition of sucrose.

**Optimization of manufacturing conditions**

Pre-treatment optimization of particles before pressing were decided by investigation of pre-drying and non drying treatment of sprayed particles to observe the effect of the pre-pressing moisture content of sprayed particles on the physical properties of the particleboards [1]. In addition, the effect of the citric acid (CA) content on the physical properties of the particleboards was investigated. The boards were manufactured under the pressing conditions of 200 °C for 10 min. The citric acid content was varied in the range of 0 to 30 wt% [1]. The board size and target density were 300 x 300 x 9 mm and 0.8 g/cm<sup>3</sup>, respectively. Particleboards manufactured using phenol formaldehyde (PF) resin and polymeric 4,4'-methylenediphenyl isocyanate (pMDI) were used as references. The physical properties of boards prepared using pre-dried particles were superior to those of the boards prepared using non-dried particles [1]. The physical properties of boards were improved with increasing citric acid content up to 20 wt% [1]. The physical properties of boards bonded with 20 wt% citric acid satisfied the requirement of the JIS A 5908 (2003) 18 type [1]. In addition, the physical properties of the board were comparable to those of boards bonded using PF resin and pMDI. Infrared (IR) spectral analysis suggested the presence of ester linkages, indicating that the carboxyl groups of citric acid had reacted with the hydroxyl groups of the sweet sorghum bagasse to give the boards good physical properties [1]. Consequently, it was concluded that pre-drying treatment of the particles and a citric acid content of 20 wt% were effective in manufacturing particleboards composed of sweet sorghum bagasse and citric acid. In addition, the pressing temperature and time condition which used in this step was only one condition at high pressing temperature of 200 °C and long pressing time relatively for 10 min. Therefore, the second step was carried out the particleboard manufacturing with the several pressing temperatures (i.e. 140, 160, 180, 200, 220 °C ) and times (i.e. 2, 5, 7, 10, 15 minutes) [2].

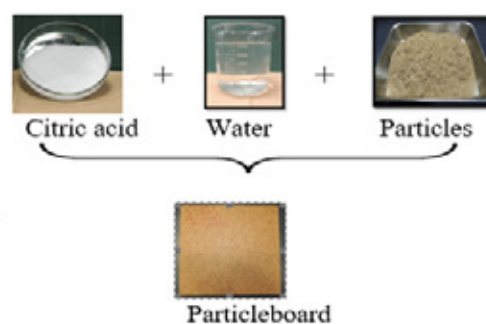


Figure 1. The production of particleboard from sweet sorghum bagasse and citric acid.

The effects of pressing temperature and time on physical properties such as dry-bending (DB), internal bond strength (IB), and thickness swelling (TS) of particleboard were investigated. Wet bending (WB), screw-holding power (SH), biological durability, and formaldehyde emission of particleboard manufactured under effective pressing temperature and time were also evaluated. The results showed that the effective pressing temperature and time were 200 °C and 10 min, respectively [2]. It was clarified that

---

## ABSTRACTS (PH D THESIS)

---

DB, IB, and TS satisfied the type 18 requirements of the JIS A 5908 (2003), and its dimensional stability was comparable to those of particleboard bonded with PF and pMDI [2]. However, the SH of particleboard did not satisfy type 18 of JIS [2]. Particleboard manufactured under effective pressing conditions had good biological durability and low formaldehyde emission [2]. Based on the results of infrared spectra (IR) measurement, the degree of ester linkages increased with increased pressing temperature and time. On the other hand, high content of citric acid i.e. 20 wt% seem to be probably the particleboard become brittle, hence MOR and screw holding power were lower than those of particleboard bonded with PF and or pMDI. Therefore, the improvement of those properties were observed by adding sucrose to the adhesion system in manufacturing of particleboard, hence the content of citric acid will be reduced.

### **Improvement of the particleboard physical properties by addition of sucrose**

The effects of the ratio (i.e. 100:0, 75:25, 50:50, 25:75, 20:80, 15:85, 10:90, 0:100) between citric acid (CA) and sucrose (SU) on the physical properties of the particleboards were investigated [3]. Based on the effective conditions of particleboard manufacturing as discussed in the optimization of manufacturing conditions, the particleboards were manufactured using pre-drying treatment particles before hot pressing and pressed under 200 °C for 10 min. Those particleboards were bonded with 20 wt% of CA-Su-based adhesive under several weight ratios of CA to SU. The mechanical properties of particleboards bonded with CA-SU based adhesive under 15/85 and 10/90 ratio of CA to Su were superior to those of the particleboard under other conditions of the ratio [3]. In addition, the physical properties of the particleboard bonded with CA-SU based adhesive under 15/85 and 10/90 ratio of CA to SU were comparable to those of particleboard bonded using phenol formaldehyde (PF) resin and satisfied the requirement of the 18 type JIS A 5908 (2003) [3]. The brittleness of the particleboards were decreased effectively by adding sucrose. The low formaldehyde emission and good biological durability against termite and decay were obtained by particleboard under effective ratio of CA to Su [3]. According to the results of thermal analysis and infrared spectra measurement, the ester linkages was generated by the reaction between CA, Su and SSB components [3].

### **Conclusions**

Development of particleboard using sweet sorghum bagasse, citric acid, and sucrose had some benefit values of environmental and technical aspects. Utilization of sweet sorghum bagasse in the manufacturing of particleboard could reserve the carbon for long term. In addition, citric acid, sucrose as sustainable natural resources have well prospective to substitute petroleum resources for particleboard adhesive. Technically, the particleboard had good physical properties, free from formaldehyde emission and good durability against termite and decay.

### **Acknowledgements**

The authors would like to thank the Science and Technology Research Partnership for Sustainable Development (SATREPS), Sakigake-Kyoto University and Ministry of Research, Technology and Higher Education of the Republic of Indonesia, the Indonesian Institute of Sciences (LIPI) for support of the study.

### **References**

- [1] Kusumah S.S., Umemura K., Yoshioka K., Miyafuji H., Kanayama K., *Ind. Crop Prod.*, 84:34-42, 2016.
- [2] Kusumah S.S., Umemura, K., Guswenrivo, I., Yoshimura, T., and Kanayama, K., *J Wood Sci.* 63(2), 161-172, 2017.
- [3] Kusumah S.S., Arinana, Hadi YS, Guswenrivo, I., Yoshimura, T., Umemura, K., Tanaka, S and Kanayama, K., *BioResources* 12(4), 7498-7514, 2017.

---

ABSTRACTS (PH D THESIS)

---

**Role of lignin in nutritional physiology of a lower termite, *Coptotermes formosanus* Shiraki (Isoptera: Rhinotermitidae)**

**(Graduate School of Agriculture Faculty of Agriculture,  
Division of Forest and Biomaterials Science,  
Laboratory of Innovative and Humano-habitability, RISH, Kyoto University)**

**Didi Tarmadi**

The mechanisms of the decomposition of polysaccharides by termites have been well-documented. However, there is almost no information regarding the role of lignin in the nutritional physiology of wood-feeding insects. Studies on the role of lignin in the nutritional physiology of wood-feeding insects would improve our understanding of natural lignocellulose-decomposition mechanisms, and contribute to the development of sustainable technology to convert lignocellulosic biomass to valuable fuels and materials.

The present study therefore aimed to investigate the role of lignin in nutritional physiology of a lower termite, *Coptotermes formosanus* Shiraki.

The study observed the ability of *C. formosanus* to decompose natural lignin polymers from Japanese cedar (*Cryptomeria japonica*) (softwood), Japanese beech (*Fagus crenata*) (hardwood), and rice straw (*Oryza sativa* L. ssp. *japonica* cv. Nipponbare) (grass) by using high-resolution multidimensional nuclear magnetic resonance (NMR) techniques. The study also investigated the dietary effects of lignins on the physiological responses of *C. formosanus* workers as well as on their gut microbial community profiles by using automated ribosomal intergenic spacer analysis (ARISA).

High-resolution NMR structural data suggested preferential removal of syringyl aromatic units in hardwood lignins, but non-acylated guaiacyl units as well as triclin end-units in grass lignins. In addition, the data suggest that termites and/or their gut symbionts may favor degradation of C–C-bonded  $\beta$ – $\beta$  and  $\beta$ –5 lignin inter-monomeric units over degradation of ether-bonded  $\beta$ –O–4 units, which is in contrast to what has been observed in typical lignin biodegradation undertaken by wood-decaying fungi.

The three purified lignins (milled wood lignins, MWLs), regardless of their structural differences, have no negative effect on termites' survival or body mass or the survival of all the three protists (*Pseudotrichonympha grassii*, *Holomastigotoides hartmanni*, and *Spirotrichonympha leidyi*) in their hindguts. In addition, the three MWL diets resulted in much lower termite survival compared to starvation conditions. Those results suggested that lignins are hardly utilized as a nutrient source by *C. formosanus* workers and are even rather detrimental to termites when used as a sole food source.

The study showed that lignins, regardless of their source (softwood, hardwood, and grass), have markedly positive effects on the survival of *C. formosanus* workers as well as the maintenance of the major protists *P. grassii* and *H. hartmanni* in their hindguts when fed with polysaccharide diets. The results strongly suggested that the presence of lignins in lignocelluloses is crucial to maintaining the physiological activities of *C. formosanus* workers.

Fractional analysis on ARISA profiling data obtained for workers fed on polysaccharide diets with and without lignins suggested that lignin when served with polysaccharides give marked effect on the bacterial pools in the hindgut of *C. formosanus* workers. Taken together with the author's previous findings, the results obtained from ARISA support the view that lignin takes an important role to maintain the gut microbial communities during the lignocellulose digestions in lower termites' digestive system.

Overall, the results support the view that lignin polymers are at least partially decomposed during their passage through the termite gut digestive system, although polysaccharide decomposition clearly dominates

---

## ABSTRACTS (PH D THESIS)

---

the overall lignocellulose deconstruction process and the majority of lignin polymers remain intact in the digestive residues. It was also found that lignins give marked positive effects on the survival of *C. formosanus* workers as well as on their maintenance of hindgut protists when served with polysaccharide diets. Furthermore, it was suggested that the gut bacterial community profiles are also affected by dietary lignins. This study has provided evidence that the presence of lignin is crucial to maintaining the physiological activities and a wholesome hindgut digestive system of *C. formosanus* workers for their efficient lignocellulose decomposition.

### **Acknowledgements**

The author thanks Professor Toshiaki Umezawa, Dr. Yuki Tobimatsu, Dr. Masaomi Yamamura, Dr. Rie Takada, Dr. Takuji Miyamoto, Dr. Yasuyuki Miyagawa, Ms. Keiko Tsuchida, Ms. Naoko Tsue, and Ms. Megumi Ozaki [Metabolic Science of Forest Plants & Microorganisms, RISH, Kyoto University] for providing of research facilities; their scientific advises and technical assistance in the experiments, and critical writing and reading of the publications. The author also thanks the Shiga Prefecture Agricultural Technology Promotion Center for providing rice straw samples, and Prof. Hironori Kaji and Ms. Ayaka Maeno [Institute for Chemical Research (ICR), Kyoto University] for their support in the NMR experiments, and Mr. Akio Adachi and Dr. Izumi Fujimoto [Laboratory of Innovative Humano-habitability, RISH, Kyoto University] for preparing the wood samples and termites used in this study.

---

 ABSTRACTS (PH D THESIS)
 

---

**Termite ectoparasitic fungi in Japan:  
distribution, prevalence, and molecular detection**

**(Graduate School of Agriculture, Laboratory of Innovative humano-habitability,  
RISH, Kyoto University)**

**Ikhsan Guswenrivo**

Termites are widely spread eusocial insects with 3,106 known species, of which 183 are considered pests and 83 cause significant damage to wooden structures. In the natural environment, subterranean termites live in soil with relatively high humidity. These conditions can expose termites to parasites such as fungi. The relationships between termites and fungi are generally divided into two categories: symbiotic mutualism and pathogenic relationships. Termite-fungus interaction is a topic that has attracted researchers for more than fifty years and extensive research has been carried out to reveal the power of entomopathogenic fungi against termite attacks, and 20 species have been tested for their pathogenicity, but none of the researches has focused on ectoparasitic fungi. Ectoparasitic fungi are fungi that attach to and live on the body surface of their hosts. There are 22 species of ectoparasitic fungi obligate parasite to termite, of which *Laboulbeniopsis termitarius* Thaxt and *Antennopsis gallica* Buchli & Heim are the most commonly found on termite cuticle. Ectoparasitic fungi have been reported to have the ability to reduce a termite's lifespan. However, the effects of ectoparasitic fungi on termite activity remain unclear due to their inability to grow in laboratory conditions. On the other hand, ectoparasitic fungi as a whole can be found in a wide distribution region, from tropical to temperate areas, but none of the reports has mentioned Japan, while the detection of ectoparasitic fungi are mainly based on manual observation.

Therefore, the present study aims to find *L. termitarius* and *A. gallica* species associated with *Reticulitermes speratus* (Kolbe), which is a termite widely distributed in Japan. Furthermore, the PCR-based assay to detect termite-associated ectoparasitic fungi was created for effective detection of the ectoparasitic fungi together with trials for cultivation of the fungi in the laboratory. Furthermore, as termite colonies are often infected by multiple ectoparasitic fungi, including the two tested species, a multiplex PCR assay was further designed to allow simultaneous detection of *L. termitarius* and *A. gallica*.

*Laboulbeniopsis termitarius* Thaxt is the most commonly found ectoparasitic fungi on termite body with varieties of termite species as its hosts. It is reported to be found in wide areas, but none of the report has mentioned about Japan. *Laboulbeniopsis termitarius* morphologically can be characterized by the unique shape and size. They have small body size, barely longer than termite setae, and attach to body surface of termites. *Laboulbeniopsis termitarius* can be identified from three main body structures namely: foot cell, stalk, and sporogonium. The other ectoparasitic fungi is *Antennopsis* sp. In 1952 Buchli and Heim described *Antennopsis gallica* on *Reticulitermes lucifungus* Rossi in southern France, proposed the genus *Antennopsis*, and placed it in a new order, Gloeohaustoriales, of the class Hyphomycetes. Presently the genus *Antennopsis* contains three species: *Antennopsis gallica* Heim and Buchli, *A. grassei* Buchli and *A. gayi* Buchli. Each species of *Antennopsis* is specific to a specific termite species.

The ectoparasitic fungi *L. termitarius* and *A. gallica* were collected from the body surface of *Reticulitermes speratus* (Kolbe) (Isoptera: Rhinotermitidae), collected from Uji, Kyoto Prefecture, Japan. These are the first record of these fungi from Japan. Moreover, the distribution of *L. termitarius* and *A. gallica* in *Reticulitermes* spp. colonies in Japan was observed. Meanwhile, the infection rate and strength of *L. termitarius* and *A. gallica* were discussed with references to effects of environmental factors at the collection sites. In total of 63 colonies of *Reticulitermes* spp. were collected from seventeen locations (from Hokkaido Prefecture to Okinawa Prefecture) in Japan. Five hundred workers and twenty soldiers from each colony were examined individually to see the infection of *L. termitarius* and *A. gallica*. The survey showed that *L. termitarius* distributed in whole Japan and *A. gallica* had a little bit restricted distribution. The infection rate of workers of *Reticulitermes* spp. varied among all locations: 0.10 - 16.10% for *L. termitarius* and 0 - 66.40% for *A. gallica*. No infected soldiers was observed. The negative relationship between temperature and infection rate was speculated in both the fungi. Rearing the colonies in the laboratory

---

## ABSTRACTS (PH D THESIS)

---

might result in the spreading of the fungi in the colonies. The both fungi grew on any body parts of the termites. The trials for isolation and cultivation of *L. termitarius* and *A. gallica* with eight media did not succeed under the laboratory conditions.

Visual observation under a dissecting microscope is a common method for screening for such fungi, it generally requires a large number of termites and is thus very time consuming. Therefore, development of a fast and efficient protocol to detect fungi infection on the termite *R. speratus* was targeted. Species-specific primers were designed based on sequence data, and amplified using a number of universal fungus primer pairs that target partial sequences of the 18s rRNA gene of the two fungi. To detect these fungi in a robust yet economic manner, we then developed a multiplex nested PCR assay using species-specific primers. Results suggested that both fungi could be successfully detected, even in cases where *L. termitarius* was at low titer (e.g., a single thallus per termite). The new method described here is recommended for future surveys of these two fungi, as it is more sensitive, species-specific, and faster than visual observation, and is likely to facilitate a better understanding of these fungi and their dynamics in host populations.

### Acknowledgements

The author would like to express his deepest gratitude and sincere appreciation to Dr. Hiroki Sato (Department of Forest Entomology, Forestry and Forest Products Research Institute Japan) and Junior Associate Professor Chin-Cheng Scotty Yang (Research Institute for Sustainable Humanosphere (RISH), Kyoto University) for all the invaluable enlightenment and guidance, kind encouragement, advices and constructive discussions during academic activities, reviewing and commenting this study. I would like to express my great appreciation to Professor Yoichi Honda (Graduate School of Agriculture, Kyoto University) for valuable advices, comments and discussions. I would also like to thanks to Dr. Izumi Fujimoto and Shu-Ping Tseng (RISH) for all the helpful assistance, scientific and valuable advices comments and discussion. I would also thank to Professor Junji Sugiyama, Associate Professor Tomoya Imai and Professor Hiroyuki Yano (RISH) for the use of the lab equipment during this study. I also thank to Dr. Toru Miura (Hokkaido University), Dr. Yasuji Kurimoto (Akita Prefectural University), Dr. Kengo Mikame (Niigata University), Dr. Wakako Ohmura (Forestry and Forest Products Research Institute), Mr. Hiroshi Kurishaki (Toyama Prefectural Agriculture, Forestry and Fisheries Research Center), Mr. Takeshi Katada (Kaneko Construction Co.), Mr. Shigeru Hashimoto (Tokushima Agriculture, Forestry and Fisheries Technology Support Center), Mr. Masao Yamashima (Alpine Enterprise Co.) and Prof. Yoko Takematsu (Yamaguchi University) for providing us termite colonies. This work was financially supported in part by a Monbukagakaku Sho (MEXT; Ministry of education, Culture, Sports, Science, and Technology) Scholarship and a Japan Society for the Promotion of Science (JSPS) Kakenhi grant, no. 15H04528.



---

**ABSTRACTS (PH D THESIS)**

---

**Study on variation of radiation belt electron fluxes  
through nonlinear wave-particle interactions****(Graduate School of Engineering, Department of Electrical Engineering,  
Laboratory of Computer Simulation for Humanospheric Sciences,  
RISH, Kyoto University)****Yuko Kubota**

Using results of test particle simulations of a large number of electrons interacting with either whistler-mode chorus emissions or electromagnetic ion cyclotron (EMIC) emissions, we evaluate formation and loss processes of the outer radiation belt consisting of MeV electrons quantitatively. Both emissions are generated by energetic charged particles injected into the inner magnetosphere. They are characterized by large wave amplitudes, rising-tone frequencies, and coherent circularly polarized waves. We find that chorus emissions play a key role in radiation belt dynamics as a generator of MeV electrons and that EMIC emissions with rising-tone frequencies are effective in scattering of relativistic electrons into the atmosphere. Nonlinear cyclotron resonance with these waves causes rapid variation of the radiation belt electrons, which is in good agreement of observational results.

In the case of interaction with whistler-mode chorus emissions, we use two chorus wave models for the test particle simulations. One assumes an optimized wave amplitude and the other assumes a time dependent wave amplitude that characterizes subpackets. Using the results of the test particle simulations, we numerically obtain Green's functions to model evolution of the electron distribution function after all of the possible interactions with the waves. In both wave models with and without subpackets, electrons undergoing the cyclotron resonance with the waves are efficiently accelerated by nonlinear wave trapping. Since the strong modulation of the wave amplitude (in the case of the waves with subpackets) affects dynamics of resonant electrons, the electrons are detrapped from the wave potential or entrapped into it more frequently than those interacting with the waves without subpackets. As a result of interaction with the waves with subpackets, the number of electrons undergoing the acceleration is increased, while the acceleration efficiency in energy is decreased because of shorter interaction time. In forming the relativistic electron flux, the total acceleration efficiencies for the two different wave models are not much different.

We modify the numerical Green's function method with the simplified model of chorus waves uniform in longitude since the data obtained by spacecraft shows magnetic local time (MLT) dependency of chorus emissions. Using the revised Green's function method, we follow the long-time evolution of global distribution function of energetic electrons interacting with the chorus waves localized in longitude. Electron acceleration process slows down temporarily because relativistic electrons go through the wave generation region due to the longitudinal drift in a time scale of a few minutes. After another few minutes, they come back to the wave generation region, resulting in re-acceleration. We find that the fluxes of the electrons after an hour interaction quantitatively agree with the results obtained by Van Allen Probes.

Tracing trajectories of relativistic radiation belt electrons interacting with EMIC rising-tone emissions, we find that some electrons are trapped by wave potentials and efficiently guided down to lower pitch angles. We also find a nonlinear scattering process named SLPA (Scattering at Low Pitch Angle) totally different from the nonlinear wave trapping. The nonlinear wave trapping, occurring for high pitch angles away from the loss cone, scatters some of resonant electrons to lower pitch angles, and a fraction of the electrons is further transported into the loss cone by SLPA after being released from the wave trapping. These scattering processes can work in any cases with proton-band or helium-band and inside or outside the plasmopause. Monitoring fluxes of electrons being lost into the atmosphere, we find efficient relativistic electron precipitation. The characteristics of the precipitating electron fluxes as a function of kinetic energy vary significantly depending on the wave frequency range and the plasma density. The nonlinear wave trapping and SLPA can expand the resonant ranges in energy and pitch angle if the wave amplitudes are larger, resulting in increase of the number of the precipitated electrons. In comparison between the effects of waves with and without subpackets, we find that fluxes of precipitated electrons are strongly modulated

---

## ABSTRACTS (PH D THESIS)

---

because of the amplitude variation of the subpacket structures. We clarify that the combined scattering process causes significant depletion of the outer radiation belt. In the time evolution of an electron distribution observed locally in longitude, we find echoes of the electron depletion by the localized EMIC emissions.

### References

- [1] Kubota, Y., Y. Omura, and D. Summers (2015), Relativistic electron precipitation induced by EMIC-triggered emissions in a dipole magnetosphere, *J. Geophys. Res. Space Physics*, *120*, 4384-4399, doi:10.1002/2015JA021017.
- [2] Kubota, Y., and Y. Omura (2017), Rapid precipitation of radiation belt electrons induced by EMIC rising tone emissions localized in longitude inside and outside the plasmopause, *J. Geophys. Res. Space Physics*, *122*, 293-309, doi:10.1002/2016JA023267.
- [3] Kubota, Y., Y. Omura, C. Kletzing, and G. Reeves (2018), Generation process of large- amplitude upper band chorus emissions observed by Van Allen Probes, *J. Geophys. Res. Space Physics*, *in press*.
- [4] Kubota, Y., and Y. Omura, Nonlinear dynamics of radiation belt electrons interacting with chorus emissions localized in longitude, submitted to *J. Geophys. Res. Space Physics*.
- [5] Omura, Y., Y. Miyashita, M. Yoshikawa, D. Summers, M. Hikishima, Y. Ebihara, and Y. Kubota (2015), Formation process of relativistic electron flux through interaction with chorus emissions in the Earth's inner magnetosphere, *J. Geophys. Res. Space Physics*, *120*, 9545-9562, doi:10.1002/2015JA021563.

---

**ABSTRACTS (PH D THESIS)**

---

**Study on nonlinear acceleration of electrons  
by oblique whistler mode waves**

**(Graduate School of Engineering, Department of Electrical Engineering,  
Laboratory of Computer Simulation for Humanospheric Sciences,  
RISH, Kyoto University)**

**Yikai Hsieh**

Whistler mode wave-particle interactions are significant phenomena causing electron accelerations and precipitations in the Earth's inner magnetosphere. The waves also play important roles in radiation belt dynamics. Whistler mode chorus emissions propagating at an oblique angle are frequently observed by satellites. The structure and propagation of oblique whistler mode waves are much more complicated than that of parallel waves. Hence, the dynamics of oblique wave-particle interactions are very different from parallel ones. To reveal the nonlinear dynamics of oblique wave-particle interactions is the purpose of the present thesis.

First, we analyze propagation conditions of an obliquely propagating coherent wave by solving the cold plasma dispersion relation and develop a wave model with the whistler mode dispersion relation. We find that in conditions that wave frequency less than half the cyclotron frequency or wave normal angle smaller than  $15^\circ$ , the wave group velocity propagates nearly parallel to the background magnetic field. Under this nearly parallel propagating feature, a one-dimensional simulation is able to calculate wave-particle interactions of oblique whistler mode wave. We also compare the dispersion relation between the exact form and the quasi-longitudinal approximation, which is usually applied in oblique wave-particle interactions. The comparison shows that the approximation is not available for wave with high frequencies or with wave normal angles near the resonance cone angle.

Second, we confirm that the gyroaveraging method, which averages the cyclotron motion to the gyrocenter and reduces the simulation from two-dimensional to one-dimensional, is valid for oblique wave-particle interaction. Multiple resonances appear for oblique propagation but not for parallel propagation. We calculate the possible range of resonances with the first-order resonance condition as a function of electron kinetic energy and equatorial pitch angle. To reveal the physical processes and the efficiency of electron acceleration by multiple resonances, we assume a simple uniform wave model with constant amplitude and frequency in space and time. We perform test particle simulations with electrons starting at specific equatorial pitch angles and kinetic energies. The simulation results show that multiple resonances contribute to acceleration and pitch angle scattering of energetic electrons.

Third, we focus on interactions between relativistic electrons and a whistler mode chorus packet propagating at oblique angles. We trace evolution of a delta function of relativistic electrons in a phase space of kinetic energy and equatorial pitch angle and obtain numerical Green's functions of the chorus wave-particle interactions. Examining the Green's functions in a wide range of kinetic energies, we find that Landau resonance can accelerate MeV electrons efficiently and that higher  $n$ th resonances such as  $n = -1$  and  $n = 2$  also contribute to acceleration of electrons at high equatorial pitch angles (about  $70^\circ$ ) and high energies (about 2 MeV). We investigate the rate of energy gain of the cyclotron resonance acceleration and the Landau resonance acceleration and find that the perpendicular component of wave electric field dominates both accelerations for MeV electrons. Furthermore, the proximity between the parallel phase velocity and parallel group velocity of oblique whistler mode waves and the nonlinear trapping condition make the interaction time of Landau resonance much longer than that of  $n = 1$  cyclotron resonance, resulting in efficient acceleration of MeV electrons.

Fourth, we demonstrate the effective acceleration by test particle simulations with parameters for the Earth's inner magnetosphere at  $L = 5$  and a small wave normal angle  $10^\circ$ . Analyzing the wave electric fields and the resonant currents for Landau resonance, we find that effective wave damping takes place at around half the electron gyrofrequency. Furthermore, we confirm that this damping is dominated by

---

## ABSTRACTS (PH D THESIS)

---

parallel components of resonant currents for electrons with a few keV, and perpendicular components of resonant currents for electrons with tens of keV. The simulation results reveal that nonlinear damping through Landau resonance is one of the mechanisms dividing chorus emissions into the upper band and the lower band.

In the present study we address the nonlinear processes of oblique wave-particle interactions. By carefully analyzing the results of test particle simulations, we confirm the importance of the effective electron acceleration and wave damping through Landau resonance under the condition of the Earth's inner magnetosphere.

### References

- [1] Hsieh, Y.-K., & Omura, Y. (2017). Study of wave-particle interactions for whistler mode waves at oblique angles by utilizing the gyroaveraging method. *Radio Science*, 52. <https://doi.org/10.1002/2017RS006245>
- [2] Hsieh, Y.-K., & Omura, Y. (2017). Nonlinear dynamics of electrons interacting with oblique whistler-mode chorus in the magnetosphere. *Journal of Geophysical Research: Space Physics*, 122, 675-694. <https://doi.org/10.1002/2016JA023255>
- [3] Hsieh, Y.-K., & Omura, Y. Nonlinear damping of oblique whistler mode waves through Landau resonance. Submitted to *Journal of Geophysical Research: Space Physics*.

---

**ABSTRACTS (PH D THESIS)**

---

**Integral study of GaN amplifiers and antenna technique  
for high power microwave transmission****(Graduate School of Engineering, Laboratory of Applied Radio Engineering for  
Humanosphere, RISH, Kyoto University)****Naoki Hasegawa**

The microwave transmission recently requires a high power RF circuit and antenna system based on continuous wave (CW) for wireless power supply and space satellite applications. The GaN amplifiers and antenna technologies are necessary for the high power microwave transmission. In the modern works, these technological fields have been considered as the different field. In this work, the integration of the design methods of GaN amplifier and RF antenna technologies is studied. In addition, the GaN amplifier and RF antenna are comprehensively designed for the high efficiency and effective microwave transmission. In particular, the following programs are discussed in this work: the high power GaN amplifier design based on a combiner technique for CW operation; the high efficiency GaN amplifier design and integration with an antenna for beam combining in a free space based on active array antenna techniques; the sidelobe reduction based on the active antenna techniques.

In the study of high power GaN amplifier design based on a combiner technique for CW operation, a GaN amplifier is firstly designed and fabricated at C-band (7.1 GHz) frequency on CW condition. The fabricated GaN amplifiers are combined by a 20-way radial combiner based on a waveguide circuit (Fig.1). The assembled 20-way high power GaN amplifier is assumed to use for a grand base station for satellite application. In the measurement of properties of the 20-way high power GaN amplifier, 179.8 W RF output power is observed in 7.1 GHz frequency and CW condition, which stand comparison with conventional GaN amplifiers operated in pulse condition. This research achievement contributes to high power microwave transmission based on large-scale aperture antenna system with a high power amplifier.

For the effective microwave transmission, the beam combining in free space based on active array antenna techniques is required. It is necessary for the active array antenna to design a high efficiency GaN amplifier and integrate with an antenna element. In this work, the high efficiency GaN amplifier with more than 60 % power-added efficiency (PAE) is design and fabricated by a harmonic tuning technique at C-band frequency (5.8 GHz). In this techniques, the second harmonic is treated by a harmonic tuning circuit, which makes an improvement of more than 10 point PAE at comparing the amplifier without the harmonic circuit in this work. In addition, an antenna design method for loss reduction in integration with amplifier is proposed. In this method, the impedance ratio of antenna to GaN HEMT is reduced, which contribute to high efficiency active antenna design. In fabrication of the active antenna, the integration loss is reduced at comparing conventional studies.

The low sidelobe techniques are necessary for compatibility of the high power microwave transmission system with other wireless system and ambient environment. In this work, the new beam controlling approach based on the active array antenna technique is proposed. It is possible to control the saturated output power levels of amplifier by operated DC drain bias voltage. In this approach, this amplifier property is used for a sidelobe reduction based on active array antenna, which makes possible tunably to control the sidelobe level. In an experiment, the sidelobe reduction with one dimension active array antenna based on this technique is demonstrated.

This comprehensive studies of high power and high efficiency GaN amplifiers and antenna is expected for development of the high power microwave transmission. This research is hope to contribute the progressive social system with the microwave transmission technology.

ABSTRACTS (PH D THESIS)

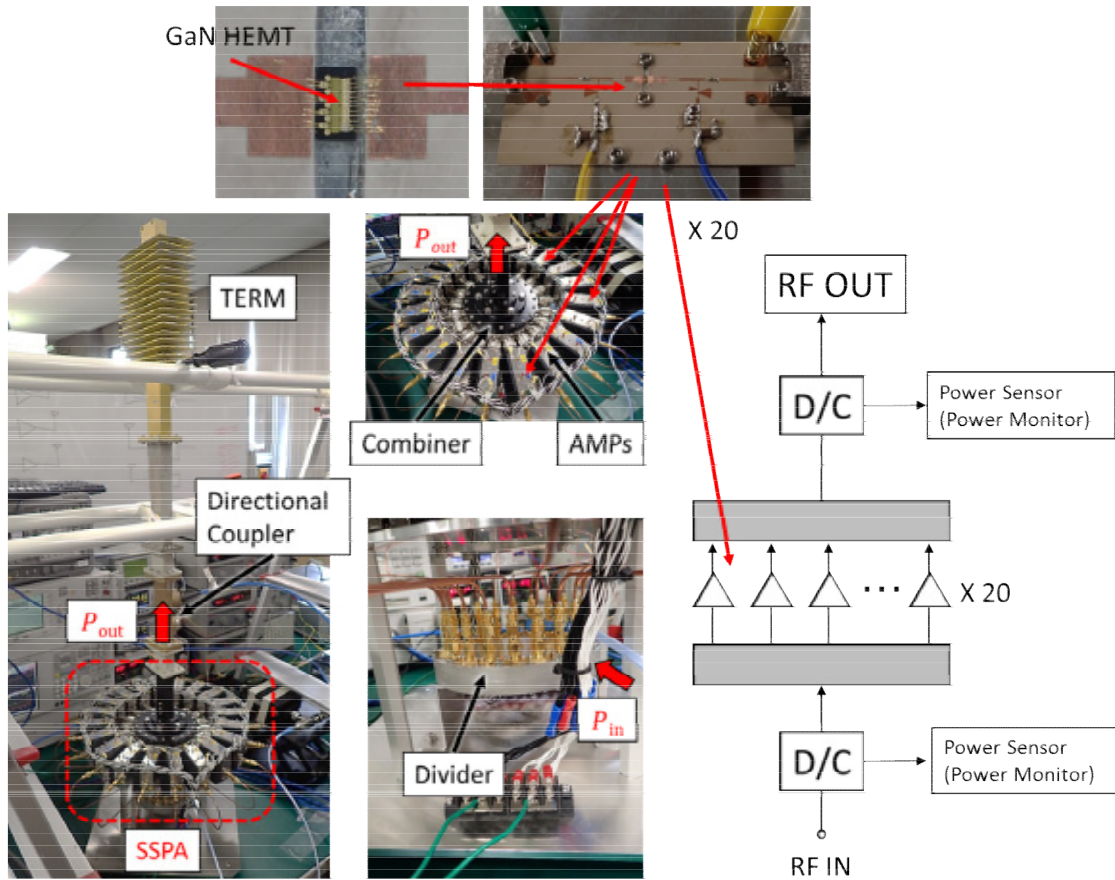


Fig.1: Developed 20-Combined C-band GaN amplifier (179.8 W).

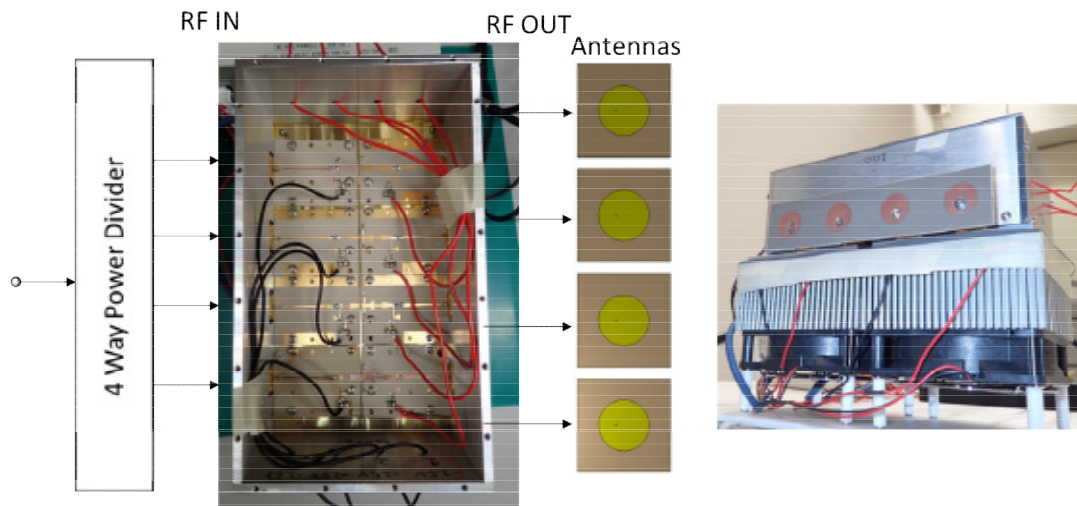


Fig.2: Developed array antenna with GaN amplifiers for sidelobe reduction.

## ABSTRACTS (PH D THESIS)

## Study on active spacecraft charging model and its application to space propulsion system

(Graduate School of Engineering,  
Laboratory of Space Systems and Astronautics, RISH, Kyoto University)

Kento Hoshi

### Introduction

Spacecraft charging is one of the most common problems in designing spacecraft. Although the amount of charging varies according to the surrounding environment and the material properties of the spacecraft surface, it is practically impossible to avoid charging because ambient plasmas are present everywhere in space. Recently, a variety of new space propulsion systems utilize spacecraft charging, that is, orbital control techniques that utilize electrostatic and electromagnetic forces have been proposed. These orbital control methods provide propellant-less spacecraft orbital control and a very lightweight propulsion system compared with conventional chemical and electrical propulsion systems. These previous works, however, studied the problem from the standpoint of orbital dynamics, and typically assumed some feasible value of surface charge and then computed orbital trajectories or relative motions between two spacecrafts. To evaluate the performance and feasibility of such systems, it is necessary to understand active spacecraft charging. The purpose of this thesis is to model active spacecraft charging and the related phenomenon for evaluating the performance under realistic conditions from the perspective of plasma physics.

### Active spacecraft charging model

Active spacecraft charging is simulated with full particle-in-cell (PIC) simulation to investigate the potential characteristics of the actively charged spacecraft. The electrostatic potential characteristics with a geostationary plasma environment are revealed. A new active charging model that considers the velocity distribution of beam particles is then proposed. Figure 1 shows the concept of the new model. Due to the finite temperature, the velocity distribution of beam particles has a spread around a beam velocity which corresponds to the accelerating potential. To consider the returning current, we define the velocity which corresponds to the spacecraft's potential. If the particle's velocity is slower than it, the particle will return to the spacecraft's surface. The potential of active charging can be calculated numerically and quickly using the new model; in contrast, the conventional model can only express active charging qualitatively, and particle-in-cell simulations require a very high computational load. The numerical solution of the new model is in very good agreement with the results of the full PIC simulation for a cubic spacecraft model with electron beam emission.

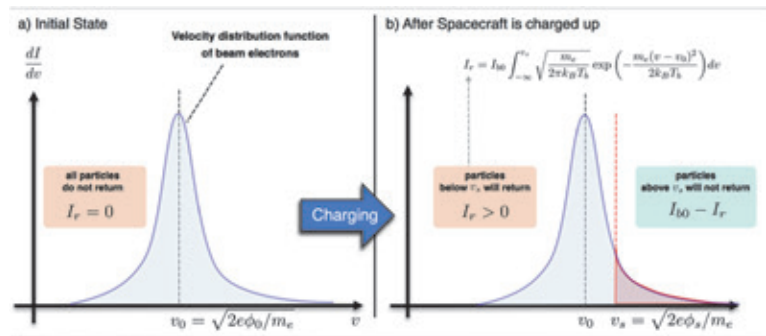


Fig.1: A new returning current model for active spacecraft charging.

### A new probability-based secondary electron emission model

Secondary electron emission (SEE) was also investigated, which is one of the dominant factors that affect spacecraft charging. To realistically simulate an interaction between an electron and a material, three different processes of SEE should be considered in the simulation model. However, to correctly include all processes in charging simulations requires some computational techniques. Particularly, probability-based SEE models enable realistic simulation, but these models are difficult to use in a general particle simulation code due to their complexity and because they include experiment-dependent parameters. Since these models were mainly developed to be used for the simulation of an interaction between mono-energetic electron beam

## ABSTRACTS (PH D THESIS)

and an object's surface, they require experimental data of emission energy distribution and yield by electron beam impact to fit the parameters. Here we propose a new probability-based SEE model that is suitable for particle-based simulations. Figure 2 depicts the concept of the new SEE model. The new model has flexibility in the use of yield models of each emission process and can be easily implemented for particle-based simulations. This model was employed for a spacecraft charging simulation using a three-dimensional (3D) PIC code and its effect on charging was investigated. As a result, the secondary electron current significantly was varied depending on the ambient plasma temperature because the amount of elastic and inelastic backscattering current was strongly dependent on the temperature. The model enables the ratio of each secondary current to be automatically adjusted without any experimental parameter fittings.

### Thrust Evaluation of Electric Solar Wind Sail

An electric solar wind sail, called E-sail, is a recently proposed propulsion device that consists of 50–100 conductive tethers with lengths of 10–20km and thicknesses of 0.1–1 $\mu$ m, as shown in Fig. 3. The E-sail was first proposed by Janhunen 2004 [1]. The main body of the spacecraft expands the tethers to form a sail-like structure. E-sail has electron guns to maintain a positive surface potential on the order of several kilovolts, in order to deflect solar wind protons. The tethers obtain the momentum of these deflected protons via Coulomb scattering and use it as their propulsive force. The system requires electron sources and electrical power for the electron guns to produce thrust. The E-sail is expected to be used as a new propellant-less space propulsion device. In this thesis, the thrust characteristics of the E-sail are investigated. The thrust obtained from the PIC simulation was lower than the thrust estimations obtained in previous studies. The PIC simulation indicated that ambient electrons strongly shield the electrostatic potential of the tether of the E-sail, and the strong shield effect causes a greater thrust reduction than has been obtained in previous studies. In addition, previous expressions of the thrust estimation were modified using the shielded potential structure derived from the present simulation results. The modified thrust estimation agreed very well with the thrust obtained from the PIC simulation.

### Acknowledgements

The present study was supported by a JSPS Kakenhi Grant-in-Aid for JSPS Fellows No. 15J08941. The computations in the present study were performed using the Kyoto-daigaku Denpa-kagaku Keisanki-jikken (KDK) system at RISH of Kyoto University.

### References

[1] Janhunen, P., "Electric Sail for Spacecraft Propulsion," *Journal of Propulsion and Power*, vol. 20, pp. 763-764, 2004.

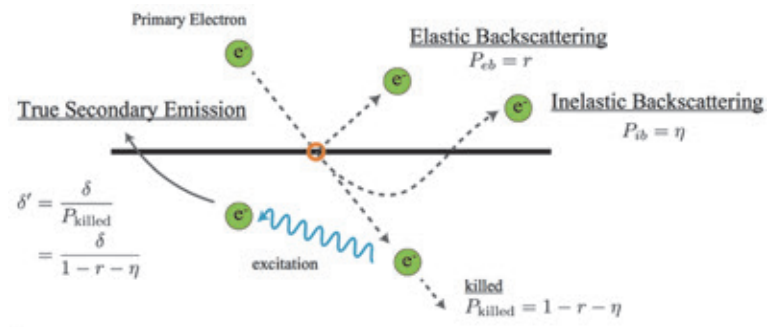


Fig. 2: A new probability-based SEE model for particle simulations.

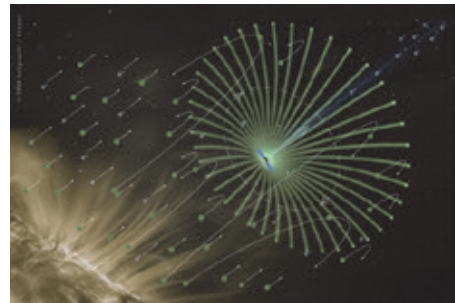


Fig. 3: An artistic image of E-sail.  
[©www.electric-sailing.fi]



## ABSTRACTS (MASTER THESIS)

**Computer vision application for quantitative analysis of anatomical features in Fagaceae woods****(Graduate School of Agriculture,  
Laboratory of Biomass Morphogenesis and Information, RISH, Kyoto University)****Takahiro Kegasa****Introduction**

Fagaceae plants grow within Japan naturally and these species are excavated from some ruins. Therefore, it is conceivable that they had been used in dairy life since ancient time. Fagaceae plants have various anatomical features such as porosity; porous-wood, diffuse-wood and radial-wood, hence it is easy to classify by genus [1]. On the other hand, it is very difficult to identify species because anatomical characteristics are quite similar among genus or subgenus. In recent years, computer vision system is commonly used for face recognition and so on. Then wood recognition using this system has been studied for the purpose of identification of tree species of wooden cultural properties or safe trading of logs and timber. The purpose of my master study is to extract possible anatomical features among Fagaceae that may allow us identification or classification at species level by means of the computer vision, which are not able to obtain by our visual inspection.

**Experiment**

Wood samples of 18 Fagaceae species were selected from the xylarium collection at RISH, Kyoto University. The optical microscopic images were obtained using Olympus BX51 equipped with a digital camera. The database consists of 540 microscopic images, namely 30 images per 1 species. SIFT-LDA were calculated by Scale-invariant feature transform (SIFT) followed by linear discriminant analysis (LDA). SIFT-LDA feature vectors were analyzed by some statistical analyses such as cluster analysis and multiple regression analysis.

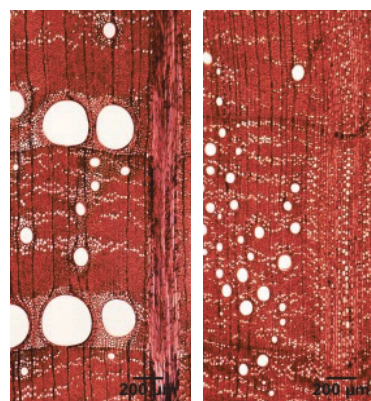


Fig. 1: Microscopic images of Fagaceae species.

Left: *Quercus acutissima*

Right: *Quercus phillyraeoides*

**Results and discussion**

High accuracy up to 99.44% by SVM discriminator using SIFT-LDA features calculated from 4.5  $\mu\text{m}/\text{pixel}$  images. In addition, k-means unsupervised clustering based on the dataset, a dendrogram of taxonomically accurate at the subgenus and section levels were obtained. In the dendrogram, *Quercus phillyraeoides* of radial-porous wood belongs to subgenus *Quercus* in which ring-porous species are dominant. It is because section Ilex containing *Quercus phillyraeoides* and section Cerris have similar arrangement of vessels and axial parenchyma cells in the latewood (Fig.1). Furthermore, the regression analysis using SIFT-LDA and estimated anatomical features suggested that frequency, porosity and aspect ratio of vessel elements are important factors for identifying species in Fagaceae.

**References**

[1] Shimaji Ken, "Anatomical studies on the phylogenetic interrelationship of the genera in the Fagaceae.", *Bull. Tokyo Univ. Forests*, 57, pp. 1-64, 1962.

## ABSTRACTS (MASTER THESIS)

**Screening of candidate enzymes involved in the biosynthesis of lipid-related metabolites and proteomic analysis of intracellular proteins from the selective white-rot fungus *Ceriporiopsis subvermispora* against exogenous addition of vanillin**

**(Graduate School of Agriculture,  
Laboratory of Biomass Conversion, RISH, Kyoto University)**

**Hikari Akiyoshi**

A white-rot fungus, *Ceriporiopsis subvermispora*, is characterized as one of the best bio-pulping fungi because it can selectively degrade lignin without serious damage to cellulose. This fungus extracellularly produces a series of itaconic acid derivatives, ceriporic acids A-C, having a long alkyl and alkenyl side chain at the C3 position [1]. In particular, ceriporic acid B suppresses iron redox reactions to inhibit the production of cellulolytic hydroxyl radicals by the Fenton reaction [2-3]. Moreover, we found that the production of ceriporic acids was increased when *C. subvermispora* was grown on a glucose-containing synthetic medium supplemented with vanillin, one of the key intermediates found during lignin biodegradation. The biosynthetic pathway of ceriporic acids remains to be elucidated although its model pathway is proposed [4]. In this study, we tried to screen candidate genes involved in the biosynthesis of ceriporic acids and also to express them heterologously.

On the other hands, we also performed fluorescence two-dimensional difference gel electrophoresis (2D-DIGE) using intracellular proteins from *C. subvermispora* grown in the presence and absence of vanillin [5]. Peptide mass fingerprinting identified numerous intracellular proteins that were involved in metabolism, cellular processes, signaling, and so on. These results will shed light on the molecular mechanism of the selective lignin degradation of *C. subvermispora*.

**References**

- [1] Amirta, R., Fujimori, K., Shirai, N., Honda, Y., Watanabe, T., 2003. Ceriporic acid C, a hexadecenylitaconate produced by a lignin-degrading fungus, *Ceriporiopsis subvermispora*. *Chem. Phys. Lipids* **126**, 121-131.
- [2] Watanabe, T., Teranishi, H., Honda, Y., Kuwahara, M., 2002. A selective lignin-degrading fungus, *Ceriporiopsis subvermispora*, produces alkylitaconates that inhibit the production of a cellulolytic active oxygen species, hydroxyl radical in the presence of iron and H<sub>2</sub>O<sub>2</sub>. *Biochem. Biophys. Res. Commun.* **297**, 918-923.
- [3] Ohashi, Y., Kan, Y., Watanabe, T., Honda, Y., Watanabe, T., 2007. Redox silencing of the Fenton reaction system by an alkylitaconic acid, ceriporic acid B produced by a selective lignin-degrading fungus, *Ceriporiopsis subvermispora*. *Org. Biomol. Chem.* **5**, 840-847.
- [4] Gutierrez, A., del Rio, J.C., Martinez-Inigo, M.J., Martinez, M.J., Martinez, A.T., 2002. Production of new unsaturated lipids during wood decay by ligninolytic basidiomycetes. *Appl. Environ. Microbiol.* **68**, 1344-1350.
- [5] Watanabe, T., Yoshioka, K., Kido, A., Lee, J., Akiyoshi, H., Watanabe, T., 2017. Preparation of intracellular proteins from a white-rot fungus surrounded by polysaccharide sheath and optimization of their two-dimensional electrophoresis for proteomic studies. *J. Microbiol. Methods.* **142**, 63-70.

## ABSTRACTS (MASTER THESIS)

**NMR analysis of interaction site between  
carbohydrate binding module of cellulase and lignin****(Graduate School of Agriculture,  
Laboratory of Biomass Conversion, RISH, Kyoto University)****Yuki Tokunaga**

Human society has rapidly developed through exploitation of fossil resources. However due to the population explosion and economic growth, energy consumption increased to such an extent causing depletion of readily accessible oil. In addition, excessive use of oil resources disturbs atmospheric equilibrium causing global warming. To solve these problems toward establishment of sustainable society, utilization of renewable resources is strongly required. Cellulose is the most abundant biopolymer on the earth, and it provides glucose, a source for chemicals production by fermentation technology. For production of glucose from lignocellulosic biomass, enzymatic saccharification with cellulase is commonly used [1]. Typical fungal cellulase consists of catalytic domain (CD) and carbohydrate binding modules (CBMs). CBMs play a role to bring the catalytic domain in close proximity to the substrate to improve efficiency of the saccharification [2]. However, CBMs have affinity to lignin and the resultant non-productive binding of cellulase to lignin through CBMs strongly inhibits the activity of enzyme [3]. Nevertheless, the interaction mechanism has not been clearly understood, which makes the saccharification of lignocellulose more difficult. Understanding of the interaction between CBMs and lignin is pivotal to accomplish the effective enzymatic saccharification. To investigate the interaction of CBMs, point-mutagenesis has been applied [4], but the available information is limited near the mutation site and influenced by conformation changes caused by the replacement of amino acids. In this thesis, the interaction between CBM and lignin was analyzed using NMR. As a lignin sample, milled wood lignins (MWLs) from Japanese cedar and *Eucalyptus globulus* were used. From the NMR analysis and binding affinity measurement, the mechanism of non-productive binding was discussed.

**References**

- [1] H. Jorgensen *et al*, "Enzymatic conversion of lignocellulose into fermentable sugars: challenges and opportunities", *Biofuels Bioprod. Bioref.*, no. 1, pp. 119-134, 2007.
- [2] A. B. Boraston *et al*, "Carbohydrate-binding modules: fine-tuning polysaccharide recognition", *Biochem. J.*, vol. 382, pp. 769-781, 2004.
- [3] J. Rahikainen *et al*, "Inhibition of Enzymatic Hydrolysis by Residual Lignins From Softwood-Study of Enzyme Binding and Inactivation on Lignin-Rich Surface", *Biotechnology*, vol. 108, no. 12, pp.2823-2834, 2011.
- [4] M. Linder *et al*, "The difference in affinity between two fungal cellulose-binding domains is dominated by a single amino acid substitution" *FEBS Letters*, vol. 372, pp. 96-98, 1995.

---

ABSTRACTS (MASTER THESIS)

---

**Production of deuterated aromatic compounds from lignin  
by microwave catalytic reactions**

**(Graduate School of Agriculture,  
Laboratory of Biomass Conversion, RISH, Kyoto University)**

**SungHo Choi**

Conversion of lignocellulosic biomass is emerging as one of the most important technologies for sustainable production of renewable fuels and chemicals due to its widespread availability, large quantity, non-competitiveness with food supply, potential as platform for green chemicals and high mitigation effects on GHG emissions. In conversion of lignocellulosic biomass, increase in conversion efficiency with low energy input is essential. Microwave heating is attractive for this purpose due to its rapid heating behavior toward the materials with high permittivity loss. In some chemical reactions, acceleration of reaction rate by microwave heating has been reported, and mechanisms for the phenomena have been discussed in terms of thermal and non-thermal effects. In this research, deuterated aromatic chemicals were produced from lignin by microwave catalytic reactions. The reaction efficiency was compared between microwave and conventional heating using the same reaction vessel and temperature profile.

Copper oxide /H<sub>2</sub>O<sub>2</sub> reactions were applied to the degradation of lignin from Japanese cedar wood. It was confirmed that the microwave significantly accelerated production of vanillin compared with conventional heating.<sup>1</sup> When the reactions were carried out using deuterated solvents, incorporation of deuterium into vanillin was found. The yield of deuterated vanillin by microwave irradiation was slightly higher than that of non- deuterated vanillin. The promoting effects of vanillin formation was found both for deuterated and non- deuterated reaction systems. Acidolysis reactions with deuterated and non-deuterated solvents were also applied to lignins from Japanese cedar and *Eucalyptus globulus* wood, and incorporation of deuterium into the lignin monomers were found. The yield of deuterated diketone compound produced by microwave reactions were higher than that of non-deuterated vanillin but the differences between microwave and conventional heating was slight. The mechanism for deuteration and effects of microwave reactions on the aromatic monomer formation was discussed.

## References

- [1] Qu, C., M. Kaneko, K. Kashimura, K. Tanaka, S. Ozawa and T. Watanabe, Direct production of vanillin from wood particles by copper oxide-peroxide reaction promoted by electric and magnetic fields of microwaves. *ACS Sustain. Chem. Eng.*, **5**, 11551-11557 (2017).

## ABSTRACTS (MASTER THESIS)

**Studies on lytic polysaccharide monooxygenase (LPMO) from the selective white rot fungus, *Ceriporiopsis subvermispota*****(Graduate School of Agriculture,  
Laboratory of Biomass Conversion, RISH, Kyoto University)****Yu Iseki**

In the commence of the period sifted from fossil-based economy to biomass-based economy, woody biomass will be leading materials because of the large quantity, non-competing with food supply and the renewable. However due to lignocellulose binding to lignin and both being recalcitrance, the exploitation of woody biomass is challenging. A selective white rot fungus, *Ceriporiopsis subvermispota* is known as a basidiomycete decomposing preferentially lignin without significant damage to cellulose and separating cellulose from lignin<sup>1</sup>. The selectivity for lignin degradation depends on culture conditions and both simultaneous and selective degradation has been observed during the wood decay by the fungus. *C. subvermispota* secretes cellulolytic enzymes, cellobiohydrolase, endoglucanase and  $\beta$ -glucosidase. In addition to the hydrolases, the fungus possesses the genes encoding lytic polysaccharide monooxygenases (LPMOs) which are known to boost cellulolytic enzyme activities on cellulose<sup>2</sup>. LPMOs are copper-dependent enzymes that oxidize  $\beta$ -1,4-glycoside bond in the C1 or C4 position, or in the both positions of terminal sugar. Typical LPMOs require an electron donor such as ascorbic acid, cellobiose dehydrogenase and phenols. Recent studies suggested that lignin can serve as electron donor for LPMOs particularly in the presence of high-molecular-weight lignin and low-molecular-weight lignin but the redox mechanism is not well understood<sup>3</sup>. In this study, LPMO from *C. subvermispota* was expressed in *Pichia pastoris*, purified and characterized by focusing its cellulolytic activities in the presence of electron donor and lignin.

Recombinant LPMO from *C. subvermispota* was expressed in *P. pastoris* and purified using hydrophobic interaction, anion exchange chromatography and size exclusion chromatography. Cellopentaose were incubated with LPMO in the presence of ascorbic acid or milled wood lignin (MWL) or phenolic lignin  $\beta$ -O-4 model compound. Products were analyzed by LC and FT-ICR-MS. LPMO decomposed cellopentaose in the presence of ascorbic acid and MWL. The reaction with lignin model compound also gave the same reaction products. Detailed structures of the reaction products were identified by FT-ICR-MS.

**References**

- [1] Watanabe, T., H. Teranishi, Y. Honda and M. Kuwahara, "A selective lignin-degrading fungus, *Ceriporiopsis subvermispota* produces alkylitaconates that inhibit the production of a cellulolytic active oxygen species, hydroxyl radical in the presence of iron and H<sub>2</sub>O<sub>2</sub>", *Biochem. Biophys. Res. Commun.*, **297**, 918-923, 2002.
- [2] Hori, C., Gaskell, J., Igarashi, K., *et al.*, "Temporal alterations in the secretome of the selective ligninolytic fungus *Ceriporiopsis subvermispota* during growth on aspen wood reveal this organism's strategy for degrading lignocellulose," *Appl. Environ. Microbiol.*, **80**, 2062-2070, 2014.
- [3] Westereng, B., Cannerlla, D., Ageer, J.W., *et al.*, "Enzymatic cellulose oxidation is linked to lignin by long-range electron transfer," *Sci. Rep.*, **5**, 18561, 2015.

---

ABSTRACTS (MASTER THESIS)

---

**Fractionation and analyses of lignin-carbohydrate complexes in woody biomass**

**(Graduate School of Agriculture,  
Laboratory of Biomass Conversion, RISH, Kyoto University)**

**Shziuka Sakon**

Woody biomass consists of lignin, cellulose, and hemicellulose. Lignin is a recalcitrant aromatic polymer which has a three-dimensional network structure in wood cell walls. Lignin is promising as a chemical raw material because aromatic rings can utilize as raw materials for various chemical products. Here, we focus on Lignin-Carbohydrate Complexes (LCCs), which have covalent bonds between polysaccharide and lignin [1]. The abundance of LCCs is small in wood cell walls, but significantly important in physical and chemical properties. Thus, a better understanding about LCCs is necessary to develop an efficient conversion system of woody biomass. In this study, we try to fractionate and analyze LCCs from hardwood. We separated an LCC fraction in combination with enzymatic digestion, solvent extraction, and column chromatography, and analyzed by 2D-HSQC NMR.

**References**

[1] Nishimura, H., Kamiya, A., Nagata, T., Katahira, M., Watanabe, T. Direct evidence for alpha ether linkage between lignin and carbohydrates in wood cell walls. *Sci. Rep.* 8:6538 (2018).

## ABSTRACTS (MASTER THESIS)

**X-ray crystal structure analysis of *cis*-hinokiresinol synthase  $\beta$  subunit****(Division of Applied Life Sciences, Graduate School of Agriculture, Laboratory of Metabolic Science of Forest Plants and Microorganisms, RISH, Kyoto University)****Atsushi Azuma****Abstract**

Norlignans are a natural phenolic compound with diphenylpentane carbon skeleton (C<sub>6</sub>-C<sub>5</sub>-C<sub>6</sub>) and are found mainly in conifers and monocotyledons<sup>1</sup>. Norlignans and related compounds have various biological activities such as antifungal and antiprotozoal activities<sup>2</sup>. Moreover, norlignans are accumulated abundantly in the heartwood region of woody plants and known as substances attributed to heartwood coloration of *Cryptomeria japonica* and *Chamaecyparis obtusa*<sup>2</sup>. Hinokiresinols have the simplest structure among norlignans and *cis/trans*-isomers which are found in monocots/dicots and conifers, respectively<sup>3,4</sup>. Both hinokiresinols have antifungal activity as phytoalexins to be produced in response to stresses<sup>3</sup>. The biosynthetic pathway of hinokiresinols and the existence of *cis/trans*-hinokiresinol synthases have been revealed by using *Asparagus officinalis* and *C. japonica* cells<sup>5,6</sup>. In the biosynthetic pathway of *cis/trans*-hinokiresinols, it is demonstrated that *p*-coumaryl *p*-coumarate is catalyzed by *cis*-hinokiresinol synthase to form *cis*-hinokiresinol in *A. officinalis* and *trans*-hinokiresinol synthase to produce *trans*-hinokiresinol in *C. japonica* without any additional cofactors<sup>5,6</sup>. Previously, (*Z*)-hinokiresinol synthase, produced in *A. officinalis*, was found to be composed of two distinct subunits, HRS $\alpha$  and HRS $\beta$ . Interestingly, recombinant HRS $\alpha$  or HRS $\beta$  can catalyze the formation of (*E*)-hinokiresinol while the mixture of both recombinant subunits produces (*Z*)-hinokiresinol with >99% (+)-enantiomer excess<sup>7</sup>. To clarify these unique molecular mechanisms, elucidation of the structures of two subunits with X-ray crystallographic analysis is essential.

In this study, recombinant HRS $\beta$  expressed in *E. coli* BL21(DE3)pLysS was purified by IMAC and anionic exchanging chromatography, and crystalized. The diffraction data on the crystals were collected by CCD detector in SPring-8, and single-wavelength anomalous dispersion analysis with the heavy-atom replacement was performed to determine the structure of HRS $\beta$ . Calculating the figure of merit and the structure refinement were performed using the PHENIX, and the initial model was built by the program Coot. In addition, the crystal structures of HRS $\beta$  complexes with substrate analogs were compared with apo-HRS $\beta$  structure.

As a result, the crystal structure of recombinant HRS $\beta$  was solved at 2.6 Å by the single-wavelength anomalous dispersion, and the final model was refined at 2.2 Å for the first time. In addition, the crystal structures of complexes of HRS $\beta$  with substrate analogs were refined.

**Acknowledgements**

The author would like to thank Professor Dr. Bunzo Mikami, Graduate School of Agriculture, Kyoto University, for his warm supports. A part of this study was conducted using the facilities in the DASH/FBAS at RISH, Kyoto University.

**References**

- [1] Suzuki S *et al.*, *J Wood Sci* 53: 273-284 (2007).
- [2] Suzuki S *et al.*, *J Chem Soc, Perkin trans 1*, 3252-3257 (2001).
- [3] Suzuki S *et al.*, *Proc Natl Acad Sci USA* 104:21008-2113 (2007).
- [4] Song MC *et al.*, *Arch Pharm Res* 30:1392-1397 (2007).
- [5] Suzuki S *et al.*, *Chem Commun* 1088-1089 (2002).
- [6] Suzuki S *et al.*, *Chem Commun* 2838-2839 (2004).
- [7] Yamamura M *et al.*, *Org Biomol Chem* 8:1106-1100 (2010).

## ABSTRACTS (MASTER THESIS)

## Studies of lignan *O*-demethylase from a human intestinal bacterium, *Blautia producta* ATCC27340

(Division of Applied Life Sciences, Graduate School of Agriculture, Laboratory of Metabolic Science of Forest Plants and Microorganisms, RISH, Kyoto University)

Nami Hisadome

### Abstract

A lignan glycoside, secoisolariciresinol diglucoside (SDG), is one of the most abundant dietary lignans. After oral administration of SDG, SDG is converted into the mammalian lignans, enterodiol (ED) and enterolactone (EL), by human intestinal bacteria [1] (Figure. 1). The mammalian lignans are lignan-type phytoestrogens and contribute the reduction of risk of breast cancer in females. Elucidation of the formation mechanism for mammalian lignans could be useful for further reduction of risk of breast cancer. In addition, the *O*-demethylation and dehydroxylation of aromatic rings in mammalian lignan formation attract a great attention because these reactions are essential for eliminating methoxyl substitutions in aromatic monomers or oligomers derived from depolymerized lignin in lignin biorefineries. To date, few human intestinal bacterial species including *Eubacterium limosum* and *Blautia producta*, have been known to catalyze *O*-demethylation, and very recently a tetrahydrofolate-dependent secoisolariciresinol (SIR) *O*-demethylase has been identified in *E. limosum* ZL-II [2]. Thus far, other *O*-demethylases have not been identified, and much information remain elusive. Therefore, we aimed at identifying a lignan *O*-demethylase in *B. producta* ATCC27340.

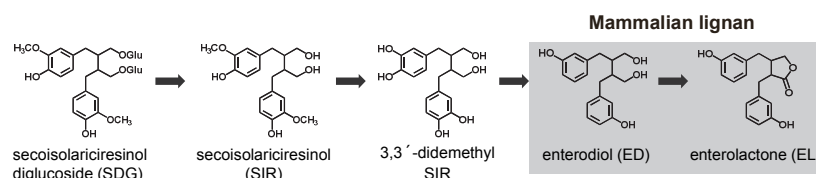


Figure 1. SDG transformation by human intestinal bacteria

The author's previous bioinformatic study suggested that the lignan *O*-demethylase reaction was catalyzed by a tetrahydrofolate-dependent *O*-demethylase system, composed of methyltransferase I (MT I), methyltransferase II (MT II), a corrinoid protein (CP), and an activating enzyme (AE) [3], which is independently reported of [2]. Furthermore, the author found an *O*-demethylase gene cluster encoding the four components in *B. producta* ATCC27340 genomic sequences [3]. In this present study, the author shows that lignan *O*-demethylation occurred in liquid culture of the bacterium and that the recombinant proteins expressed in *Escherichia coli* catalyzed *O*-demethylation of SIR.

### Acknowledgements

The author would like to thank Professor Dr. Ryutaro Utsumi, Agriculture of Kindai University, for his warm supports. The author wishes to thank Professor Dr. Daisuke Shibata, Kazusa DNA Research Institute, for his kindest advice. The author also wishes to thank Associate Professor Dr. Takeshi Ara, Kagome Tomato Discoveries Faculty/Graduate School of Agriculture, Kyoto University, for his valuable advice in bioinformatics analyses. A part of this study was conducted using the facilities in the DASH/FBAS at RISH, Kyoto University.

### References

- [1] Jin et al., Transformation of trachelogenin, an aglycone of tracheloside from sanfflower seeds to phytoestrogenic (-)-enterolactone by human intestinal bacteria. *Food Chem* 134: 74-80 (2012).
- [2] Chen et al., Cloning, expression, and characterization of a four-component *O*-demethylase from human intestinal bacterium *Eubacterium limosum* ZL-II. *Appl Microbiol Biotechnol* 100:9111-9124 (2016).
- [3] Nami Hisadome, Mining of lignan *O*-demethylase from bacteria, Undergraduate thesis, Faculty of Agriculture, Kindai University, Nara, Japan (2015).



## ABSTRACTS (MASTER THESIS)

**Functional characterization of *p*-coumaroyl-CoA:monolignol transferase genes involved in lignin biosynthesis in rice****(Graduate School of Agriculture, Laboratory of Metabolic Science of Forest Plants and Microorganisms, RISH, Kyoto University)****Takuto Tanaka****Abstract**

Among the variety of biomass feedstocks under consideration for biorefinery, grass biomass crops, such as *Erianthus*, sorghum, switchgrass and bamboo, have attracted considerable attention especially because of their superior biomass productivities. It is thus becoming increasingly important to facilitate our understanding of the biosynthesis, structures, and properties of grass lignocellulose to optimize their production and properties for biorefinery applications.

Lignin is a complex aromatic polymer produced in plant cell walls and accounts for 15-30% by weight of lignocellulose. Grass lignins have unique structural features that are prominently different from eudicot and gymnosperm lignins. One of the distinguishing features is the partial attachment of *p*-coumarates (*p*CAs) on the  $\gamma$ -positions of the phenylpropanoid sidechains. Such lignin  $\gamma$ -coumaroylation arises from the incorporation of monolignol-*p*CA conjugates which may be generated by *p*-coumaroyl-CoA:monolignol transferase, PMT, a member of the BAHD (BEAT, AHCT, HCBT, and DAT) acyltransferase (AT) family [1,2]. Currently, the physiological function of *p*-coumaroylated lignins in grass cell walls remains poorly understood. In addition, it is yet largely unknown how such lignin *p*-coumaroylation affects the biomass utilization properties of grass lignocellulose.

In this thesis, the author attempted to identify rice PMTs responsible for lignification in rice, and also to obtain novel *PMT*-deficient rice mutants that could be useful to study the elusive functions and properties of *p*-coumaroylated lignins. To these ends, the author first conducted genetic and biochemical characterizations of rice BAHD AT proteins and identified one new putative PMT, i.e., OsAT3, in addition to the previously identified OsAT4 [1]. The author demonstrated that both OsAT3 and OsAT4 show *in vitro* PMT activity to convert monolignols into the corresponding monolignol-*p*CA conjugates. Accordingly, by using the CRISPR/Cas9 genome editing system, the author successfully generated rice mutants deficient either in *OsAT3* or in *OsAT4*, and demonstrated, through in-depth structural analyses using 2D NMR, that both of the mutants produced altered lignins with decreased *p*CA levels. Collectively, these results establish the *in planta* functions of OsAT3 and OsAT4 as PMTs to generate *p*-coumaroylated lignins in rice cell walls. Further comprehensive analyses of the *PMT*-deficient mutants developed in this study should facilitate our understanding of the elusive physiological role of *p*-coumaroylated lignins in grass cell walls. Besides, various physical and chemical properties as well as biomass utilization properties of the lignin-modified modified lignocellulose are worthy of further investigation.

**Acknowledgements**

A part of this study was conducted using the facilities in the DASH/FBAS at RISH, Kyoto University, and the NMR spectrometer in the JURC at ICR, Kyoto University.

**References**

- [1] Withers, S., Lu, F., Kim, H., Zhu, Y., Ralph, J., Wilkerson, C.G. (2012). Identification of grass-specific enzyme that acylates monolignols with *p*-coumarate. *J. Biol. Chem.* 287: 8347-8355.
- [2] Petrik, D.L., Karlen, S.D., Cass, C.L., Padmakshan, D., Lu, F., Liu, S., Le Bris, P., Antelme, S., Santoro, N., Wilkerson, C.G., Sibout, R., Lapierre, C., Ralph, J., Sedbrook, J.C. (2014). *p*-Coumaroyl-CoA:monolignol transferase (PMT) acts specifically in the lignin biosynthetic pathway in *Brachypodium distachyon*. *Plant J.* 77: 713-726.

---

ABSTRACTS (MASTER THESIS)

---

**Functional analysis of terpene synthase from hop**

**(Graduate School of Agriculture,  
Laboratory of Plant Gene Expression, RISH, Kyoto University)**

**Joji Kageyama**

Hop (*Humulus lupulus* L.) is a perennial vine plant (Cannabaceae) that is cultivated worldwide as been essential for beer brewing. Female flowers of hops are the indispensable ingredient of beer to contribute its characteristic flavor and bitterness to beer taste since the medieval period. These green flowers develop many yellow glandular trichomes called ‘lupulins’, which are the tissue for the accumulation of various terpenoids, bitter acids (prenylated phloroglucinols) [1, 2] and prenylated flavonoids [3].

Hop cultivars can be roughly divided into two groups, aromatic and bitter cultivars. Linalool is one of the most prominent monoterpenes as a marker compound of aromatic hop varieties. Although most important terpene synthases have been already isolated from hops in USA and Canada [4], linalool synthase gene has not yet been reported. In this study, we have isolate and characterize the linalool synthase of hop.

Using EST analysis of lupulin-rich part of the female flowers of an aroma hop cultivar, a novel terpene synthase-like gene was found among various terpene synthase genes having motifs highly preserved in most terpene synthases requiring  $Mg^{2+}$  for the enzymatic function. Then, we have characterized the enzyme activity of the candidate gene with the recombinant protein prepared in *Nicotiana benthamiana* and in an expression system of *Escherichia coli*. Consequently, the candidate gene synthesized linalool in the presence of GPP, and nerolidol in the presence of FPP.

Furthermore, we have investigated the expression level of linalool synthase in each organs of a hop plant. We have also done a chemical analysis of volatile components of hop cone using GC-MS to find various volatile terpenes, such as myrcene and humulene, while linalool content was almost undetectable when fresh lot of hop cones were used. The reason should be further studied.

### **Acknowledgements**

This study was supported by Dr. Tetsu Sugimura, Dr. Masaki Momose, Dr. Naoyuki Umemoto, Dr. Atsushi Murakami and Dr. Kazuaki Ohara of Kirin Co.; Dr. Ryosuke Munakata of RISH, Kyoto University; Dr. Kazutoshi Shindo of Ishikawa Prefecture University; Dr. Norihiko Misawa of Japan Women’s University; Dr. Tsuyoshi Nakagawa of Shimane University; Dr Hiroshi Kouchi of International Christian University; Dr. Shiro Suzuki of RISH, Kyoto University; and GC/MS provided by DASH/FBAS of RISH, Kyoto University.

### **References**

- [1] Okada Y, Ito K. (2001). Cloning and analysis of valerophenone synthase gene expressed specifically in lupulin gland of hop (*Humulus lupulus* L.). *Biosci. Biotechnol. Biochem.* 65, 150-155.
- [2] Tsurumaru Y, Sasaki K, Miyawaki T, Uto Y, Momma T, Umemoto N, Momose M, Yazaki K. (2012). *HlPT-1*, a membrane-bound prenyltransferase responsible for the biosynthesis of bitter acids in hops. *Biochem. Biophys. Res. Commun.* 417, 393-398.
- [3] Nagel J, Culley LK, Lu Y, Liu E, Matthews PD, Stevenes JF, Page JF. (2008). EST analysis of hop glandular trichomes identifies an *O*-methyltransferase that catalyzes the biosynthesis of xanthohumol. *Plant Cell.* 20, 186-200.
- [4] Wang G, Tian L, Aziz N, Broun P, Dai X, He J, King A, Zhao PX, Dixon RA. (2008). Terpene biosynthesis in glandular trichomes of hop. *Plant Physiol.* 148, 1254-1266.

---

ABSTRACTS (MASTER THESIS)

---

**Screening of caffeine metabolizing microbes from rhizosphere of coffee**

**(Graduate School of Agriculture,  
Laboratory of Plant Gene Expression, RISH, Kyoto University)**

**Tomo Kawakami**

Caffeine (1,3,7-trimethylxanthine) is one of the most popular plant specialized metabolite, and produced in such plants as coffee and tea. Since the identification of caffeine in 1819, function of caffeine to human has been intensively studied. Caffeine inhibits phosphodiesterase activity, which leads to the acceleration of cAMP signaling pathways. The physiological functions of caffeine in planta have also been reported: caffeine directly inhibits the development and growth of other organisms, such as bacteria, fungi, insects, mollusks as well as plants, which is referred to as allelopathy.

Caffeine also indirectly stimulates the plant defense response, which is often referred to as priming. It is reported that caffeine is secreted from caffeine-producing plants, suggesting the additional function in the rhizosphere, which is the small region around plant roots. Root of plants as coffee secretes caffeine into culture medium.

It was reported that the fungal community in coffee plant rhizosphere is enriched with *Trichoderma*, especially in in Ethiopian highlands [1]. *Trichoderma* family contains mycoparasites that kill phytopathogens primarily by coiling and destroying their hyphae. Recently, we reported the caffeine response of fungi, including 4 mycoparasitic *Trichoderma*, and 4 prey phytopathogens [2]. We showed that the allelopathic effect of caffeine on fungal growth and development in vitro was differential, i.e. stronger on pathogens than on *Trichoderma* species. We also showed that when confronting, the prey fungi immediately ceased the growth, whereas the predator fungi continued to grow [2] From these observations, we suggested that caffeine is a weapon in the arms race between plants and pathogens. In these interactions caffeine fosters enemy's enemy, for which we propose "caffeine fostering" as the role of caffeine [2].

In this study we analyzed the rhizosphere microbial communities of coffee plants and isolated bacteria which potentially metabolize caffeine in the rhizosphere of coffee plants. Isolated microorganism was differ depend on medium conditions.

**References**

- [1] Belimova, N. Hontzeas, V.I. Safronova, S.V. Demchinskaya, G. Piluzza, S. Bullitta, B.R. Glick. 2005. Cadmium-tolerant plant growth-promoting bacteria associated with the roots of Indian mustard (*Brassica juncea* L. Czern.). *Soil Biology & Biochemistry*, 37, 10.1016.
- [2] Sugiyama A, Sano CM, Yazaki K, Sano H. 2016. Caffeine fostering of mycoparasitic fungi against phytopathogens. *Plant Signal Behav*, 11(1), e1113362.

## ABSTRACTS (MASTER THESIS)

**A study on calibration techniques for water vapor  
Raman lidar using GNSS-PWV and meso-scale model**

(Graduate School of Informatics,  
Laboratory of Radar Atmospheric Science, RISH, Kyoto University)

**Hayato Kakihara**

The Raman lidar technique is useful for observing water-vapor profiles, which help the improvement of the accuracy of weather forecasts. In this study, we propose a new calibration technique for water-vapor Raman lidar using global navigation satellite system (GNSS)-derived precipitable water vapor (PWV) and grid point values from the Japan Meteorological Agency's meso-scale model (MSM-GPV). The analysis was accomplished by directly fitting the PWV to height-integrated water-vapor profiles combined with the MSM-GPV and the Raman lidar observation results. Because this new method can be applied to lidar signals lower than a limited height range due to weather conditions and lidar specifications, it will provide many opportunities for calibration, contributing to the long-term accuracy of measurements.

We demonstrated this method's potential by using the ultraviolet C region (UV-C) Raman lidar and GNSS observation data of the dense observation network around the Shigaraki MU Observatory (34°51' N, 136°06' E; 385 m a.s.l.) of the Research Institute for Sustainable Humanosphere (RISH), Kyoto University, Japan, in June and December 2016. The calibration factor differences between the proposed and conventional methods were within 5%.

The vertical and horizontal inhomogeneous water vapor factors were estimated by calculating the standard deviations of both the water vapor lidar profiles and the horizontal distribution of PWV from the dense GNSS network, respectively. Through a case study of the June and December data, we found differing vertical and horizontal characteristics of the water vapor inhomogeneity preceding rainfall. We investigated the statistical relationship between precipitation and PWV from June 2016 to August 2017 using a database around Shigaraki constructed in this study. The ratio of the observed PWV to the saturated PWV, estimated empirically from the MSM-GPV, was higher during rain events during May-October compared with those during November-April.

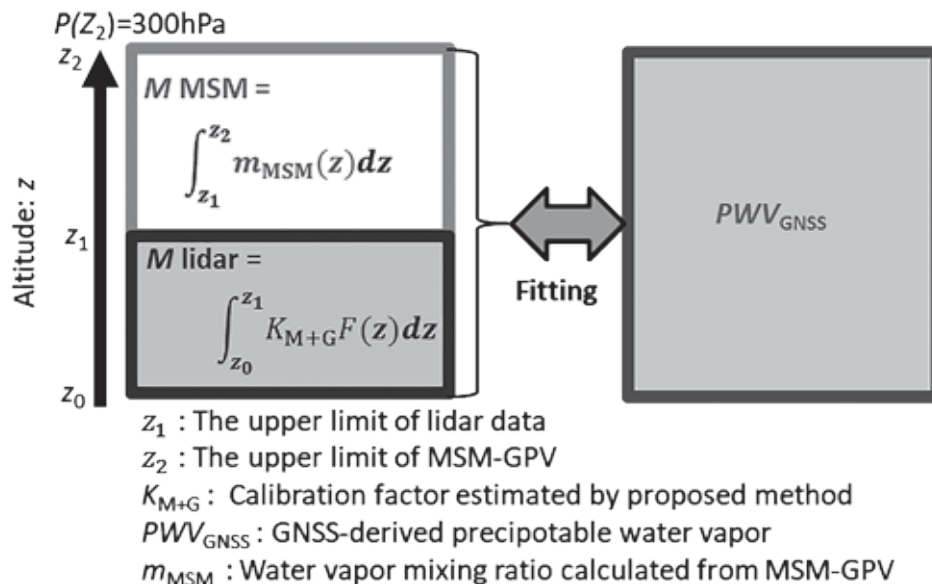


Figure 1. Schematic of new Raman lidar calibration method using GNSS-PWV and MSM. The function  $F(z)$  indicates the relative water vapor profile calculated from the Raman lidar signals for each molecule. The calibration factor  $K_{\text{M+G}}$  is estimated by fitting the GNSS-PWV to integrated water vapor profiles combined with the MSM and the results of the Raman lidar observation.

## ABSTRACTS (MASTER THESIS)

**Study on real-time aircraft clutter suppression using the MU radar**

(Graduate School of Informatics,  
Laboratory of Radar Atmospheric Science, RISH, Kyoto University)

**Kousuke Kubota**

The MU radar is the large VHF-band atmospheric radar to observe the lower, middle, and upper atmospheres in the Shigaraki MU Observatory. Strong clutter echoes from mountains or aircrafts sometimes cause problem of estimating wind velocity with atmospheric radars. In this study, we evaluated three methods of 1-constrained NC-DCMP (Norm-Constrained and Directionally Constrained Minimization of Power), 2-constrained NC-DCMP, and 2-step NC-DCMP, which are effective to suppress aircraft clutters [1]. The latter two requires the information of aircraft directions. We proposed a method to limit the scope of searching the directions using ADS-B Automatic Dependent Surveillance-Broadcast system.

First, the latitude, longitude, altitude, and velocity of aircrafts were decoded from 112 bit messages of ADS-B. In order to use their information with adaptive signal processing, they were converted to ENU coordinate, which is the orthogonal coordinate system with the MU radar as the origin. Moreover, we use MV filter to predict and complement the aircraft position because ADS-B information is intermittent [2].

Finally, we applied 1-constrained NC-DCMP, 2-constrained NC-DCMP, and 2-step NC-DCMP to the observation data of the MU radar, and evaluate the suppression performance for aircraft clutters. We indicated the correlation between 1-constrained NC-DCMP suppression performance for aircraft clutters and the average sight velocity of aircrafts by ADS-B. Suppression performance of 1-constrained NC-DCMP is worse when the Doppler velocity is faster. Moreover, if we use the optimized directions of aircraft clutters with 1st step of 2-step NC-DCMP, which is the procedure of subtracting reproduced aircraft clutters from the received signal, the suppression performance of 2-step NC-DCMP is improved about 5 dB more than that of 1-constrained NC-DCMP, which is the conventional method.

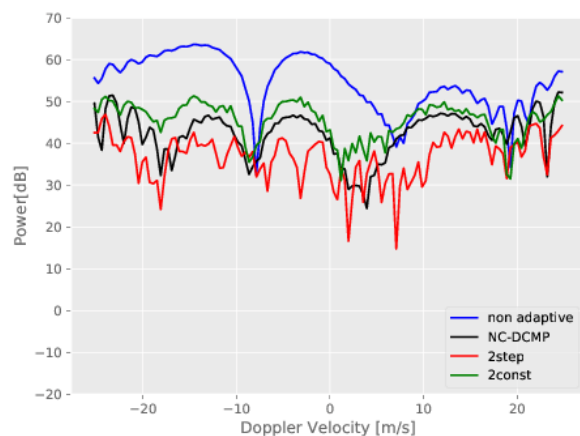


Figure 1. Comparison of three aircraft suppression methods with ADS-B.

## References

- [1] T. Hashimoto, K. Nishimura, M. Tsutsumi, K. Sato, and T. Sato, "A user parameter-free diagonal-loading scheme for clutter rejection on radar wind profiles", *Journal of Atmospheric and Oceanic Technology*, vol.34, no.5, pp.1139-1153, 2017.
- [2] A. Dutle, M. Moscato, L. Titolo, and C. Munoz, "A formal analysis of the compact position reporting algorithm", *Working Conference on Verified Software: Theories, Tools, and Experiments*, pp.19-34, Springer, 2017.

---

 ABSTRACTS (MASTER THESIS)
 

---

**Creation and utilization of the database of three-dimensional electron density distribution based on GPS-TEC tomographic analysis**

**(Graduate School of Informatics,  
Laboratory of Radar Atmospheric Science, RISH, Kyoto University)**

**Ryo Mizuno**

Accurate information of the ionospheric electron density distribution is necessary when correcting measurement errors of positioning with GPS receivers. On the other hand, the GPS is used to study structure of the ionosphere [1, 2]. We have developed three-dimensional (3D) tomography based on the GPS-TEC data. The real-time analysis of the 3D tomography of the ionosphere has just started from 2016. In this research, using the 3D ionospheric tomography analysis system developed by Suzuki [3], we created a database of analysis results of past GPS data and verified their accuracy. We also improved the area of the analysis range which is important when using this analysis result in other research.

In database creation, we could not effectively remove instrument bias of GPS data of a certain period. Therefore, we utilized absolute TEC data calculated by NICT for the tomographic analysis. By using a super computer, we also developed a software system to conduct the tomography by many core in parallel, and succeeded in shortening the analysis time by about 150 times.

In the verification of the analysis results from ionosonde and COSMIC occultation observation were compared with the analysis results of tomography. By performing this comparison, the regional and seasonal characteristics of the tomographic analysis are clarified. We found that tomography results showed good agreement with foF2 from ionosondes but height of the density peak was generally higher than the COSMIC occultation data.

For improve of the degree of freedom of the analysis range, we first developed a system that can display the analysis result as a vertical plane distribution on a line segment connecting arbitrary two points. Also, in order to expand the analysis area, we performed tomographic analysis by combining GPS data from Korea and Taiwan.

### References

- [1] S. Miyazaki and K. Heki: Crustal velocity field of southwest Japan: Subduction and arc-arc collision, *Journal of Geophysical Research: Solid Earth*, **106**, 4305-4326, 2001.
- [2] H. Tsuji, Y. Hatanaka, T. Sagiya, and M. Hashimoto: Coseismic crustal deformation from the 1994 hokkaido-toho-oki earthquake monitored by a nationwide continuous GPS array in Japan, *Geophysical Research Letters*, **22**, 1669-1672, 1995.
- [3] S. Suzuki: Development of real-time three dimensional analysis system of the ionosphere over Japan based on GPS-TEC observations, Master thesis, Graduate School of Informatics, 2016.

Table 1. Electron density ratio average and standard deviation of tomography and ionosonde in each season, each region.

ave,sta	Yearly	Feb.Mar.Apr.	May Jun.Jul.	Aug.Sep.Oct.	Nov.Dec.Jan.
Okinawa	1.032, 0.211	1.076, 0.268	1.097, 0.161	1.013, 0.185	0.950, 0.204
Yamagawa	1.064, 0.184	1.081, 0.238	1.101, 0.141	1.056, 0.151	1.000, 0.190
Kokubunji	0.975, 0.184	1.003, 0.241	1.026, 0.146	0.969, 0.136	0.903, 0.168
Wakkanai	0.750, 0.267	0.863, 0.306	0.787, 0.233	0.697, 0.198	0.610, 0.249

## ABSTRACTS (MASTER THESIS)

**Analysis of natural electric field and electron density for understanding medium-scale traveling ionospheric disturbances with sounding-rocket experiments****(Graduate School of Informatics,  
Laboratory of Radar Atmospheric Science, RISH, Kyoto University)****Keigo Nishida**

Medium-scale traveling ionospheric disturbance (MSTID) is an interesting phenomenon in the F-region. The MSTID is frequent in summer nighttime over Japan, showing wave structures with wavelengths of 100-200 km, periodicity of about 1 hour, and propagation toward the southwest. Although one hypothesis for the generation mechanism of MSTID is suggested by computer simulation [1], its confirmation by observation is necessary. We had a chance of launching the sounding rockets S-520-27 and S-310-42 to the MSTID region on July 20, 2013 from JAXA Uchinoura Space Center. This study aims to provide accurate data of natural electric field and plasma density from the sounding rocket S-520-27 experiment.

Natural electric field was measured by the double-probe sensor on the rocket. The data were analyzed with location and attitude data of the rocket and the geomagnetic field model. Accuracy of this new analysis is improved as we use the revised rocket attitude that is more accurate than before. Also, we propose an estimation method of electric field, which makes use of the orthogonality of the electric field to the geomagnetic field. Obtained natural electric field associated with MSTID was about 5 mV/m (Fig. 1).

Plasma density from this experiment, on the other hand, was measured by the rocket-ground dual-band beacon (DBB) experiment. First, total electron content (TEC) was derived from signal processing of the DBB. Secondly, distribution of plasma density was estimated by tomographic technique. We set the initial data by referring to the data from the impedance probe on the rocket and the three-dimensional GPS-TEC tomography based GEONET (Fig. 2). Wave-like structure of plasma density with wavelength of 100 km was found.

By comparison of the natural electric field and plasma density data, anti-correlation between the two elements was found. In the area of depleted plasma density, the electric field was northeastward, and its intensity became maximum. In conclusion, this study successfully derived natural electric field and plasma density distribution which are reasonable for ionosphere behavior and have potentiality for understanding electromagnetic interrelationship between the ionospheric E and F region.

**References**

[1] Yokoyama, T., Hysell, D., Otsuka, Y. and Yamamoto, M., *J. Geophys. Res.*, **114**, A03308, 2004.

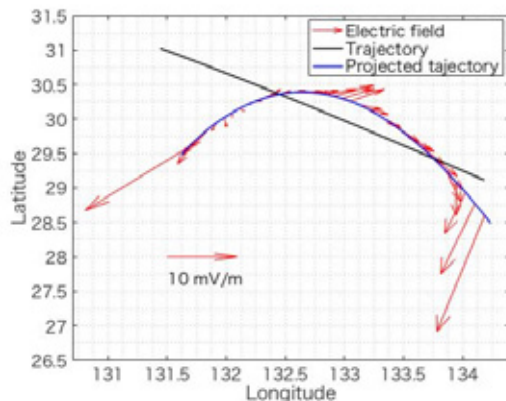


Fig.1: Electric field measurement by the double-probe on S-520-27 rocket.

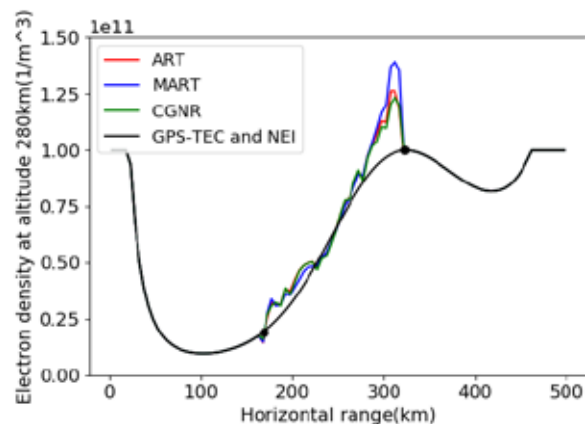


Fig.2: Tomography analysis results based on rocket-ground DBB experiment.

## ABSTRACTS (MASTER THESIS)

**Production and application of high-thermal-durability cellulose nanofibers**

(Graduate School of Agriculture,  
Laboratory of Active Bio-based Materials, RISH, Kyoto University)

Aya Miura

**Introduction**

Cellulose has poor thermal durability compared to inorganic materials, and degradation via depolymerization and discoloration starts around 230 °C. Therefore, the melt kneading of resins with cellulose is restricted to temperatures below 200 °C. In contrast, plastics such as polycarbonate and nylon 6 have high melting temperatures. By using chemical modification, we have succeeded in improving the thermal durability of cellulose nanofibers for reinforcement. Here, a new chemical modification method based on vinyl ester reagents was used to improve durability and for combining the modified cellulose nanofibers with polycarbonate resin at a processing temperature of 250 °C.

**Experiment**

Bleached kraft pulp (NBKP, moisture content of 10%) and bacterial cellulose (BC, water content of 91%) were used as material fibers. Acetylation and benzylation were performed at 70 °C with vinyl acetate and vinyl benzoate, respectively, dimethyl formamide solvent, and a K<sub>2</sub>CO<sub>3</sub> catalyst. The degree of substitution (DS) was determined with Fourier transform infrared spectroscopy (peak at 1730 cm<sup>-1</sup>). For the polycarbonate compound, nano-fibrillated NBKP or BC and polycarbonate resin powder (Mitsubishi Engineering Plastics, Iupilon) were dispersed in IPA solvent, and the filtrate was dried. Samples were then prepared by melt kneading at 240 °C using a twin-screw extruder, followed by injection molding at 260 °C. The physical properties were then evaluated.

**Results and discussion**

Acetylation of NBKP progressed more easily than benzylation, and, eventually, the DS became constant at 2.2 and 1.0, respectively. This can be attributed to the difference in steric hindrance. Thermal durability was evaluated via the 5% weight-loss temperature (5% WLT). It improved more from benzylation than from acetylation and depended on the structure of the ester group. The 5% WLT of NBKP by benzylation (DS 1.0) increased from 267 °C to 326 °C, and exhibited a similar heat resistance to that of benzyolated BC. It appeared that improved thermal durability of the hemicellulose was a factor. Similar results were obtained for acetylated BC.

By combining the polycarbonate resin with 5-wt-% benzyolated BC, the elastic modulus improved by a factor of 1.22 (Fig. 1), while maintaining the polycarbonate transparency (Fig. 2). The coefficient of linear thermal expansion decreased by 17.9%. When the benzyolated BC composite was compared to the acetylated BC composite, it was revealed that the degree of reinforcement depended on the structure of the ester group.

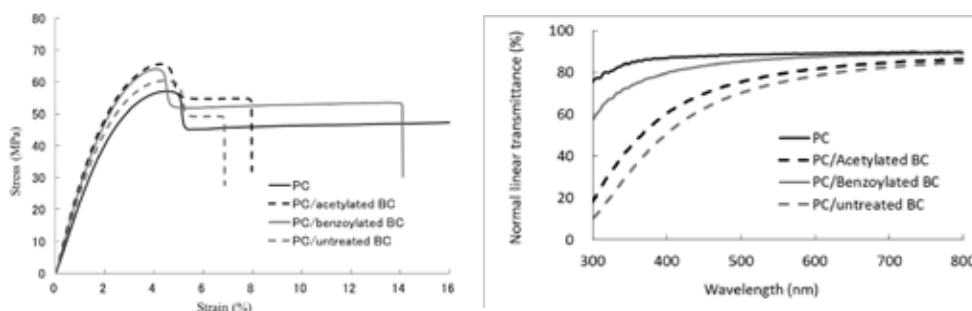


Fig. 1 Stress-strain curves of compounds. Fig. 2 Normal linear transmittance vs. wavelength.



## ABSTRACTS (MASTER THESIS)

## Mechanical properties of poly (vinyl alcohol)-cellulose nanofiber hydrogels prepared by repeated freeze-thaw treatment

(Graduate School of Agriculture,  
Laboratory of Active Bio-based Materials, RISH, Kyoto University)

Yuki Tomobe

### Introduction

Cellulose nanofiber (CNF) is a nanostructured material composed of cellulose fibrils featuring a high length-to-width ratio. It has novel structural properties and has been used as a reinforcing fiber in resin-based materials. CNF can be prepared from various cellulose sources, although plant biomass is often favored as a renewable resource. It is considered that the mechanical properties of CNF-resin composites depend on the dispersibility of CNF, the interfacial adhesion between CNF and the resin, and the nature of the CNF network. However, the actual mechanism of how CNF reinforces a resin is poorly understood. Therefore, in this study, poly(vinyl alcohol)-CNF hydrogels were prepared by repeated freeze-thaw treatment, and used to study the reinforcement mechanism. Poly(vinyl alcohol) (PVA) has good compatibility with CNF, and the gelation of PVA solution can be easily achieved. In particular, a freeze-thaw method has the advantages of being experimentally straightforward and does not require the use of potentially undesirable chemical crosslinking agents.<sup>1</sup> Gelation of PVA by the cyclic freeze-thaw treatment is driven by the phase separation that occurs as the solution freezes and the polymer is rejected from the growing ice crystallites.<sup>1</sup>

### Experiment

Pulp was prepared from the wood flour of Cypress (*Chamaecyparis obtusa*). CNF was isolated by grinding. PVA was added to a CNF suspension and the mixture was poured onto a plate. By repeated freeze-thaw treatment (liquid nitrogen atmosphere, 15 min/23°C, 60 min), gelation of the mixture was achieved. The tensile properties of the gels were measured.

### Results and discussion

The Young's modulus of PVA gels increased with increasing PVA content. By adding 1.3 vol% CNF, the Young's modulus increased significantly. This shows that a CNF network formed when CNF content was between 0.65 and 1.3 vol%. The Young's modulus of the PVA-CNF gels also increased as the PVA content increased. This trend of increasing Young's modulus with increased PVA content was more marked in the PVA-CNF gels than in the PVA gels. In other words, the modulus of the PVA-CNF gels increased more than expected as the PVA content increased. This suggests that the PVA network can reinforce the CNF network.

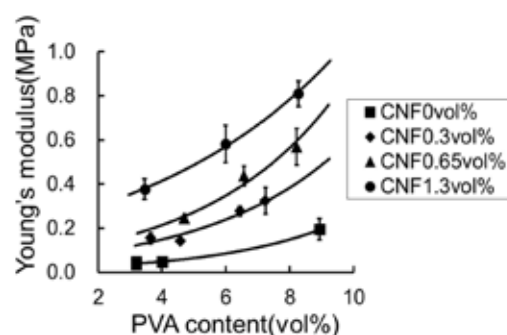


Figure 1. Relationship between Young's modulus of PVA/CNF hydrogels and PVA content.

### References

[1] Tiffany Abitbol, Timothy Johnstone, Thomas M. Quinnb and Derek G. Gray, "Reinforcement with cellulose nanocrystals of poly(vinyl alcohol) hydrogels prepared by cyclic freezing and thawing", *Soft Matter*, vol. 2011, no. 7, pp. 2373-2379.

## ABSTRACTS (MASTER THESIS)

**Cellulose nanofiber-reinforced composites using acrylic resin latex****(Graduate School of Agriculture,  
Laboratory of Active Bio-based Materials, RISH, Kyoto University)****Hiroki Yatsui****Introduction**

Cellulose nanofibers (CNFs) exhibit high strength and low thermal expansion and have been investigated and used as reinforcing components in composite materials. However, the hydrophilic nature of CNFs makes it difficult to mix them uniformly in hydrophobic resins. As a result, CNFs are frequently chemically modified to improve their affinity to resins. However, chemical modification of CNFs is very costly, which limits the extent of their application. The objective of this research was to reinforce hydrophobic resin with CNFs using latex that consisted of nanosized acrylic resin droplets.

**Experiment**

A TEMPO-oxidized CNF-water suspension and acrylic resin latex with nanosized droplets (~200 nm) were mixed using a blender. The mixture was filtered and the residue was dried to prepare CNF composite sheets. The mechanical properties and dynamic viscoelastic properties of the samples were studied.

**Results and discussion**

Nanospheres were found to keep their original shape in the transparent CNF-acrylic resin composites (Figure 1). The addition of CNF increased the Young's modulus and strength of the resin (Figure 2). The Young's modulus of the resin increased 380-fold with only 5% addition of CNF. The tensile strength of the resin also increased with increasing CNF content and it was nearly 9-fold higher for the nanocomposite with 5% CNF. The composites showed high electrical conductivity when they were mixed with silver nanowires. The electrical conductivities of the composites were found to change with stretching.

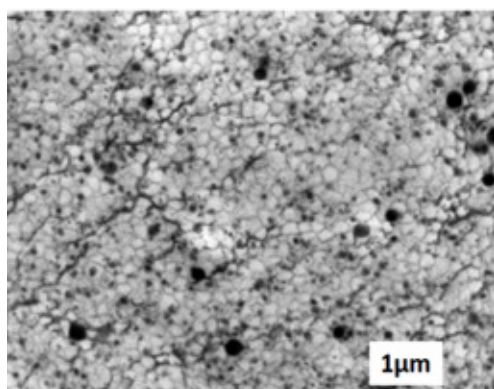


Figure 1. CNF-acrylic resin composite.  
(CNF: 2.5%, scale bar: 1 μm)

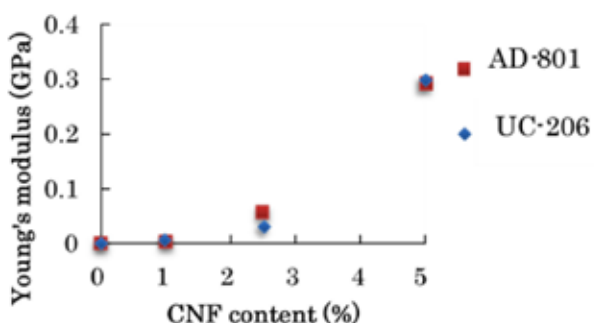


Figure 2. Young's modulus of composites

## ABSTRACTS (MASTER THESIS)

**Effect of calcium carbonate addition on adhesion properties of sucrose-ammonium dihydrogen phosphate adhesive for particleboard**

(Graduate School of Agriculture,  
Laboratory of Sustainable Materials, RISH, Kyoto University)

Jiahua Zhou

**Introduction**

As a novel natural adhesive, mixture of sucrose and ammonium dihydrogen phosphate (ADP) has been investigated. The particleboard bonded with the adhesive had excellent physical properties, but pH of the solution after thickness swelling (TS) test showed low value of 2.9. This means that the particleboard had acidic property. Generally, acidic property of the particleboard causes corrosion of metal material such as a nail. To resolve the problem, addition of calcium carbonate ( $\text{CaCO}_3$ ) which is sometimes used as a pH adjusting agent as well as a filler was attempted. In this study, the effect of  $\text{CaCO}_3$  addition on the adhesion properties of sucrose-ADP adhesive for particleboard was investigated.

**Materials and methods**

Sucrose and ADP (mixture ratio of 85: 15) were dissolved in distilled water and the solution was used as an adhesive.  $\text{CaCO}_3$  powder was added into the adhesive. The weight ratios of  $\text{CaCO}_3$  to the solid-based adhesive were from 0 to 20wt%. In Group A, the mixture solution was dried immediately after mixing, while in Group B the mixture solution was dried after 6 h of conditioning. The drying condition was 80°C for 12 h. The dried mixture was heat-treated in an oven at 180°C for 10 min. The heat-treated powder was immersed in boiling water for 4 h, and the insoluble matter rate was determined from the weight change before and after the boiling treatment. The insoluble matter rate of the adhesive was calculated in consideration of the insoluble matter rate of  $\text{CaCO}_3$ . The pH of the solution after boiling treatment was measured. Fourier Transform Infrared Spectroscopy (FT-IR) analysis of the insoluble matter was conducted. In manufacture of the particleboard,  $\text{CaCO}_3$  powder was added into recycled wood particles. The adhesive was sprayed onto the particles at 20wt% solid content based on the dried particles. The weight ratios of  $\text{CaCO}_3$  to the solid-based adhesive were from 0 to 40wt%. After drying the particles and mat-forming, the mat was hot-pressed at 200°C for 10 min. The pH value of the solution after TS test was measured as well as some physical properties such as TS, bending and internal bond strength. In addition, FT-IR analysis of the particleboard was conducted.

**Results and discussion**

The pH value of the adhesive increased as  $\text{CaCO}_3$  content increased both in Groups A and B. This means that the acidic property of the adhesive became weak with increasing  $\text{CaCO}_3$  content, irrespective of conditioning. In Group A, the insoluble matter rate of the adhesive was over 70%, irrespective of  $\text{CaCO}_3$  content, and was higher than that of Group B. It was clarified that in addition of  $\text{CaCO}_3$ , drying the mixture solution immediately was effective.

The pH value of the solution after TS test increased as  $\text{CaCO}_3$  content increased. This means that the acidic property of the particleboard became weak with increasing  $\text{CaCO}_3$  content. Furthermore, some mechanical properties of particleboard with certain  $\text{CaCO}_3$  content slightly improved. The reason seemed to be that  $\text{CaCO}_3$  could offset the acidic property of the particleboard, and would react with ADP to generate calcium phosphate such as hydroxyapatite.

Based on the results above,  $\text{CaCO}_3$  addition was effective in weakening the acidic property of adhesive. The insoluble matter rate of the adhesive showed a high value if the mixture solution was dried immediately. In addition,  $\text{CaCO}_3$  addition was also effective for offsetting the acidic property and improving some mechanical properties of the particleboard.

## ABSTRACTS (MASTER THESIS)

**Study on production of high strength material by  
using of kozo (*Broussonetia kazinoki* × *B. papyrifera*)**

**(Graduate School of Agriculture, Laboratory of Sustainable Materials,  
RISH, Kyoto University)**

**Yuto Yoshioka**

### Introduction

Natural fiber composite materials, made from natural fibers and resins, have recently been studied. It has been required for reducing the environmental loading to increase the ratio of fibers to resins in the materials. The influence of contact, interlocking, and voids among fibers, on the material strength is expected to increase with the increase in the fiber ratio. Single fiber (pulp) is therefore required to have high strength, moderate length, and flexibility. The raw material of Japanese paper, pulp of kozo (*Broussonetia kazinoki* × *B. papyrifera*) is expected to be suitable for these requirements. The purpose of this study is to establish the process of producing the high strength materials by using the kozo pulp. In this report, the influence of the contact and voids among fibers on the mechanical properties of the material was examined.

### Materials and methods

Kozo pulp was purchased from Kurotani Washi Cooperative Association (Ayabe, Japan). Specimens numbered from ① to ④ were prepared according to the manufacturing procedure as shown in Fig.1. Part of this procedure was based on the general method to produce fiber board in wet forming process. In the impregnation step (Fig.1), methyl methacrylate (MMA) with 1 wt% azo type polymerization initiator was impregnated into the squeezed cake, and was polymerized at 85 °C for 24h in the polymerization step. Density of each specimen was evaluated by external dimensions and mass of the specimens. Bending modulus of elasticity (MOE) and modulus of rupture (MOR) were evaluated by three point bending test.

### Results and discussion

All the physical properties (density, MOE, and MOR) of specimen ② were higher than those of specimen ①. This indicates the contact among fibers was promoted by vacuum drying of the squeezed cake with the clamping pressure maintained. All the physical properties of specimen ③ were higher than those of specimen ②. This indicates that the MMA filled the residual voids without dissolving the contact among fibers. MOE and MOR of specimen ④ was lower than those of specimen ③, while density of ④ was higher than ③. This may be due to both the breakage and separation of the fibers.

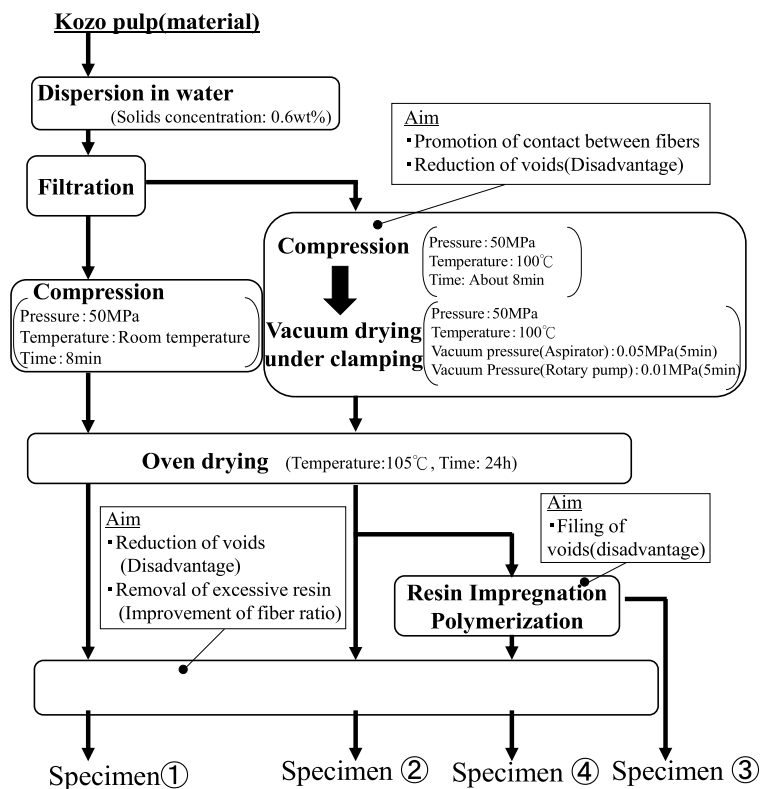


Figure 1. Manufacturing procedure

## ABSTRACTS (MASTER THESIS)

**Effect of water hammer on liquid permeation into wood in impregnation process**

(Graduate School of Agriculture,  
Laboratory of Sustainable Materials, RISH, Kyoto University)

**Kamii Nakamura**

**Introduction**

Impregnation of wood with chemical liquids has been used to improve the disadvantages of wood. After the impregnation process, however, there often exist some areas without being filled with the liquid, leading to the inadequate improvement. This is mainly caused by the obstacle that blocks the liquid flow, e.g., the aspirated pits in tracheid of coniferous wood. This study focuses on the water hammer to penetrate the obstacle as follows. If the liquid fills up the cell cavities between the wood surface and the tip of the liquid permeation in wood, or the obstacles, the abrupt increase in the liquid pressure from one to another on the wood surface is expected to cause the damping oscillation in the liquid pressure at the obstacles, which is expected to penetrate them. The purpose of this study is to promote the liquid permeation into wood by applying the water hammer. The test equipment was fabricated to generate the water hammer. The change in pressure with time was examined for various conditions of the equipment, and was analyzed using the fluid dynamics. Effect of the water hammer on the liquid permeation into wood was also examined.

**Materials and methods**

The test equipment is shown in Figure 1. Distilled water was used as a liquid.

To generate water hammer, vessel B filled with liquid at an ordinary pressure (0.1 MPa) was connected by a valve to vessel A filled with liquid at higher pressure (1.1 MPa). The change in liquid pressure in the vessel B as a function of time was measured just after the valve was opened with various rate. The maximum pressure and the maximum pressure-increasing rate was estimated from the temporal change in pressure, and analyzed by the fluid dynamics.

To examine liquid permeation, wood samples with a dimension of 15 mm (T) × 15 mm (R) × 100 mm (L) were prepared from a block of yellow cedar (*Chamaecyparis nootkatensis* Spach), and dried at 105 °C for 24 h to oven-dry state. The container with the dried samples inside was evacuated by a rotary pump for 1 h, injected with distilled water so that all the samples were immersed in the liquid, and introduced with the air to be an ordinary pressure. The samples were subsequently remained to be immersed in the liquid for 48 h. A sample after immersed was fixed directly under the pressure gauge  $P_1$  in the vessel B with an ordinary pressure (Fig. 1). The valve was opened with various rate after the vessel A at higher pressure (1.1 MPa) inside. Amount of the liquid taken up to the sample was measured for each rate.

**Results and discussion**

The pressure  $P_1$  without specimens showed damping oscillation behavior when the valve was opened quickly, called quick pressurization. While with slow opening of the valve, called slow pressurization, the pressure gradually increased to a constant value. These findings indicate that the water hammer occurred by the quick pressurization. The amount of the liquid taken up to the wood sample, however, showed no significant difference between the quick and slow pressurization.

With the increase in the maximum pressure-increasing rate, the maximum pressure increased up to about 1.1 times larger than the equilibrium pressure. It was indicated from analyzing this relation that the maximum pressure can reach to twice the equilibrium pressure. Thus, there remains the possibility that the water hammer in this experiment is not so much large as affecting the penetration of the obstacle in wood. Being based on the analysis, the valve opening rate and the aperture of the valve are required to be higher in order to enhance the strength of the water hammer.

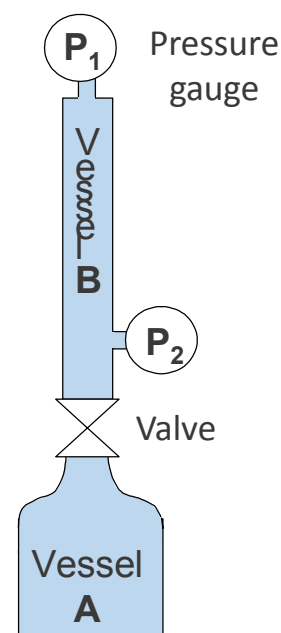


Figure 1. Schematic diagram for test equipment.

## ABSTRACTS (MASTER THESIS)

**Development of natural wood adhesive composed of sucrose and ammonium nitrate**

(Graduate School of Agriculture,  
Laboratory of Sustainable Materials, RISH, Kyoto University)

Mitsuki Nomura

**Introduction**

Increasing demand of wood-based material is expected because of global population increase and economic growth. However, general wood-based materials are made using synthetic adhesives derived from fossil resources. Considering future of fossil resources, it is desirable to replace synthetic adhesive with natural adhesive based on non-fossil resources.

Recently, research on utilization of sucrose as wood adhesives has been investigated. The purpose of this research is to develop a natural adhesive composed of sucrose and ammonium nitrate (AN). It is possible that AN promotes curing of sucrose and brings self-bonding of wood. In this study, the curing properties of sucrose and AN mixture was investigated, and the physical properties of wood-based molding glued with sucrose and AN were clarified.

**Methods**

Mixture of sucrose and AN with various weight ratios (AN ratios were 0~30wt%) was dissolved in distilled water, which was used as an adhesive. The adhesive was freeze-dried, and the thermal properties were investigated by DSC and TGA. Insoluble matter rate to boiling water for heated adhesive was calculated. In the preparation of wood-based molding, the adhesive was mixed with wood powder. Solid content of adhesive was 20wt% to wood powder. After drying, the mixture was poured into a dumbbell-shape mold for JIS7139-1966 type A3, and hot-pressed. The bending test, insoluble matter rate measurement and FT-IR analysis of the wood-based molding were performed.

**Results and discussion**

It was clarified that sucrose and AN mixtures have endothermic and exothermic reactions with weight loss between 130~160°C. In the higher AN ratio, the marked behavior of those reactions was recognized. Fig. 1 shows insoluble matter rate of adhesive heated at 180°C for 20min. The adhesive with AN ratio of 5 wt% showed low value. However, the insoluble matter rate increased with increasing AN ratio, indicating that AN promoted the polymerization of sucrose. Fig. 2 shows insoluble matter rate of wood-based molding. Even though AN ratio in solid content of adhesive was low, insoluble matter rate was high value. This tendency was very different from the heated adhesive, indicating AN contributed to self-bonding of wood. The bending properties of wood-based moldings were improved with increasing AN ratio in solid content of adhesive until 10wt%. However, higher AN ratio than 20wt% brought lower bending properties. Based on the results of FT-IR, formations of ester linkage and furan compound were presumed.

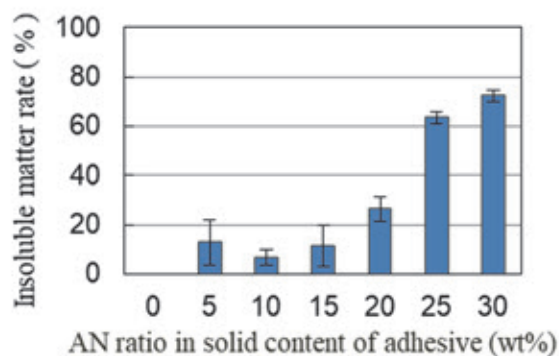


Fig. 1: Insoluble matter rare of heated adhesive.  
(Heat treatment : 180°C,20 min)

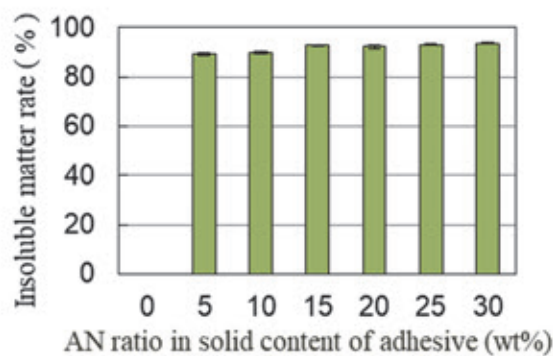


Fig. 2: Insoluble matter rare of moldings.  
(Hot press : 180°C,20 min)

## ABSTRACTS (MASTER THESIS)

**Compressive fracture behavior of CLT wall panel under horizontal loading**

(Graduate School of Agriculture,  
Laboratory of Structural Function, RISH, Kyoto University)

Youta Ueda

**Introduction**

As a way to open up new possibilities for wood buildings with low environmental impact, Cross-laminated timber (CLT) that can effectively utilize low-quality materials and enable a reasonable wall structure has attracted attention, and mid-rise building technology is under development. In the shaking table experiment of the 5 story CLT building, a compression failure was caused at around the hole for fasteners at the bottom of the wall panel of first floor, and it became a criterion for seismic performance. This study aimed to verify this phenomenon which is considered as one of design criteria.

**Methods**

In order to reproduce a compression failure at the bottom of wall panel, a static horizontal loading test of a 5-layer 5-ply CLT wall panel with length 1,000 mm × height 2,700 mm × thickness 150 mm was conducted. Also, the presence or absence of hole for tensile bolt connector was set as parameter. In the loading method, pulling side cyclic loading was applied controlled by apparent displacement based on stroke displacement of the actuator. The lift-up displacement due to the locking of the panel was restrained by tie-rods, HD hardware so as to cause a collapse at panel leg. Simultaneously, the numerical analysis by elasto-plastic finite element model was carried out for the model of specimen. In the FE analysis, the influence of the restraint condition and the vertical force of the top of the specimen was confirmed.

**Results and discussion**

In the fracture behavior, after the crack was observed near the hole, the outermost lamina was deflected out of plane and collapsed by local buckling, which was similar to the destructive behavior of shaking table experiment. The load-displacement relationship showed elastic load increase up to deformation of 1/30 rad, followed by no clear load reduction until 1/20 rad with high deformability. The specimens with holes showed about 20% lower ultimate strength in comparison of the specimens with and without holes. It was thought that the vicinity of the hole collapsed prior to the crush of the contact surface at the bottom of the panel. From the stress distribution of the specimen measured by the strain gauge, the internal stress flow was observed that occurred from the position of the tie rod at the top of the specimen toward the leg compression side. So it was concluded that the resistance mechanism of the compression struts was formed by tie rods bearing the large tension force. Results of FE analysis were in good agreement with experimental results. In order to confirm the influence of constrained conditions, a model only tie rods works as constraint hardware was analyzed. As a result, it was found that the contribution of the hold-down fastener to the horizontal resistance is smaller than that of the tie rod. In order to simulate the actual shaking table experiment condition, in which the tensile restraint conditions are different from wall test, we performed advanced FE analysis with applying the vertical constant load of 0 to 2,000 kN as the parameter. The results are shown in Fig. 1. Up to vertical load condition of 1,500 kN, the higher the vertical load, the more the lifting is restrained which resulted in the higher yield load. However, in condition of 2,000 kN, both rigidity and yield load became smaller compared with that of 1,500 kN. Based on this result, it was confirmed that the crushing of the leg in the shaking table experiment was caused by the influence of the fluctuating axial force due to the horizontal force.

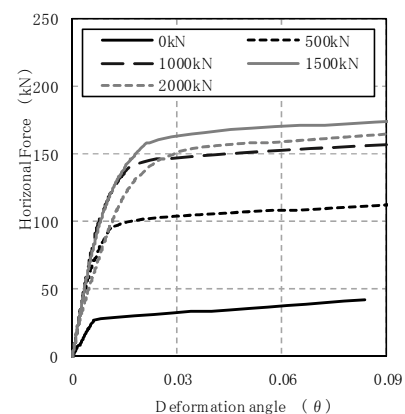


Figure 1. Relation between load and deformation angle.

---

ABSTRACTS (MASTER THESIS)

---

**Study on acceleration mechanism of radiation belt electrons  
through interaction with sub-packet chorus emissions**

**(Graduate School of Engineering,  
Laboratory of Computer Simulation for Humanospheric Sciences,  
RISH, Kyoto University)**

**Ryoko Hiraga**

We conduct test particle simulations to examine the mechanism how relativistic electrons are accelerated by sub-packet chorus waves. As the analysis of recent observations [1], amplitude of an element of chorus wave (an element with a rising tone frequency) consists of many shortwave packets, which we call a sub-packet chorus wave. In this simulation, we reproduce the rapid fluctuations in the wave amplitude model and phase discontinuities due to the sub-packet structure, in order to examine how they influence the nonlinear trapping processes for efficient acceleration of relativistic electrons such as relativistic turning acceleration RTA [2] and ultra-relativistic acceleration URA [3]. To conduct comprehensive examinations, we follow more than nine million test particles with various initial conditions covering an energy range from 100 keV to 6 MeV and equatorial pitch angles from  $10^\circ$  to  $89^\circ$ . The test particles are interacting with a single element of sub-packet chorus wave set up with the maximum amplitude of about 2 nT and the frequency increase from about 1.3 kHz to 3.8 kHz over 0.25s. Relativistic electrons are accelerated by about 150 keV under preferable conditions. The energy increase verifies the high efficiency of acceleration by wave-particle interaction. It is achieved by a short time interaction less than 1s with a single element of chorus wave with a rapidly fluctuating sub-packet structure. By analyzing the detailed behavior of the accelerated electrons, we find successive entrapping of resonance electrons resulting in efficient acceleration by consecutive multiple sub-packets.

**References**

- [1] Foster et al., 2017.
- [2] Omura et al., 2007.
- [3] Summers and Omura, 2007.



---

**ABSTRACTS (MASTER THESIS)**

---

**Study on substorm evolution process by global MHD simulation**

**(Graduate School of Engineering,  
Laboratory of Computer Simulation for Humanospheric Sciences,  
RISH, Kyoto University)**

**Naoki Kamiyoshikawa**

Substorm is a remarkable disturbance occurring in the Earth's magnetosphere. A large amount of energy ( $\sim 10^{11}$  W) is consumed in the ionosphere during the substorm. A problem is how the energy comes from. Recent global magnetohydrodynamics (MHD) simulation is capable of reproducing features of auroral substorms. The substorms are known to develop when the interplanetary magnetic field (IMF) is southward and the solar wind speed is high. However, the relationship between the solar wind parameter and the magnitude of the substorm is little known. First, we studied the influence of solar wind condition on the substorm evolution by introducing 3 cases of solar wind speed (300, 500, and 700 km/s) and 5 cases of interplanetary magnetic field (IMF) (-1, -3, -5, -7, and -9 nT). When the solar wind speed is 700 km/s and IMF Bz is -9 nT, the onset occurs earliest the AE index is highest, and the evolution is fastest. Secondly, transport of energy from the solar wind to the ionosphere is examined. It is found that about 1/3 of the solar wind kinetic energy is converted the electromagnetic energy in the cusp-mantle dynamo region. About 1/200 of the solar wind kinetic energy is found to be consumed in the ionosphere. The electromagnetic energy is stored in the lobe during the growth phase, and it is released in the expansion phase. The released energy appears to be insufficient to the electromagnetic energy consumed in the ionosphere. Continuous transport from the cusp-mantle dynamo is found to contribute to the energy supply in to the ionosphere for any solar wind conditions. Thirdly, we studied the influence of the boundary conditions of the global MHD simulation on the evolution of the substorm. The substorm is known to be caused by the consequence of the solar wind-magnetosphere interaction. The contribution from the Earth is not well known. We change the inner boundary that is located on the sphere with a radius of  $\sim 3 R_E$ . In Case 1, the pressure gradient in the radial direction is introduced, resulting in the acceleration of plasma toward the ionosphere. In Case 2, no pressure gradient is introduced. The simulation in Case 1 results in a rapid development of the auroral electrojet, which is resemble to typical variation of the auroral electrojet as seen by the AL index during the substorm expansion. Case 2 results in a relatively slow development of auroral electrojet. It is concluded that continuous inhalation of plasma from the magnetosphere to the ionosphere may play a role in the rapid development of the auroral electrojet.

## ABSTRACTS (MASTER THESIS)

## Study on the improvement of RF-DC conversion efficiency of microwave rectifiers with pulse modulation

(Graduate School of Engineering,  
Laboratory of Applied Radio Engineering for Humanosphere, RISH, Kyoto University)

Takashi Hirakawa

### Introduction

Currently, the necessity of the Internet of things (IoT) technique is increasing. IoT requires a flexible configuration of sensor networks, which is hindered by wired-charging sensors. The microwave wireless charging (MWPT) can be the solution to this problem. Although MWPT enables integrating communications and battery-less motion of the sensor network, it interferes with communications and its charging efficiency is lower than the wired charging. So improvement of the transmission efficiency is very important for practical use of MWPT. MWPT has many loss components. This study focused on radio frequency to direct current (RF-DC) conversion efficiency of rectifiers. In former study, input waves which have high peak-to-average power ratio (PAPR) is effective for improving the RF-DC conversion efficiency of rectifiers. Pulse modulation can make higher the PAPR of input waves. So we studied about the rectifiers with pulse modulated input as shown in Fig. 1 in this thesis.

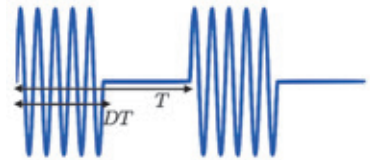


Figure 1. Pulse modulated wave

### Circuit design and Experiments

We designed the single-shunt rectifier for continuous wave (CW) input which has 10mW input power and 2.45 GHz frequency. Figure 2 shows the designed circuit. As a load of this rectifier, the resistance and 100 uF capacitance are connected in parallel. Figure 3. shows the simulation and experimental results of RF-DC conversion efficiency with continuous input. In these simulations and experiments, we changed the average power and load impedance. This result shows the same tendency of all lines. Next, we experimented the RF-DC conversion efficiency of this rectifier with pulse modulated input. We changed the duty ratio of pulse modulated waves and load impedance. Duty ration  $D$  means the on-time to off-time ratio as shown in Fig. 1. In all cases the average power is fixed as 1 mW. Therefore, the peak power becomes the  $1/D$  mW. Figure 4. shows the experimental result of RF-DC conversion efficiency with pulse modulated input. The smaller duty ratio is, the larger peak RF-DC conversion efficiency and optimum impedance become. Optimum impedance becomes  $1/D$  times as that with continuous wave input. In addition, the peak RF-DC conversion efficiency with duty ratio equals to 1mW compete with that with 10mW continuous input. As a result, we can achieve the RF-DC conversion efficiency with low input using pulse modulation.

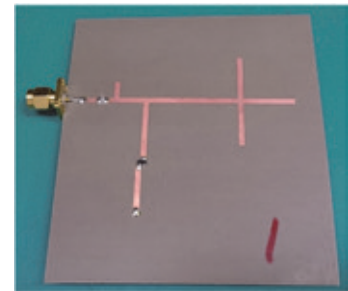


Figure 2. The designed and experimented circuit

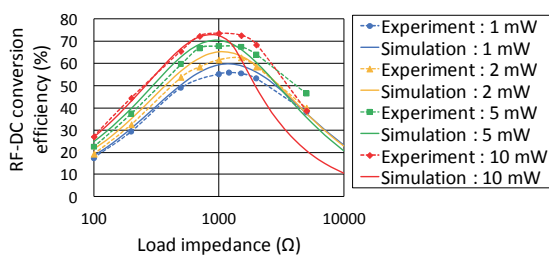


Figure 3. Experimental result of the rectifier with continuous input.

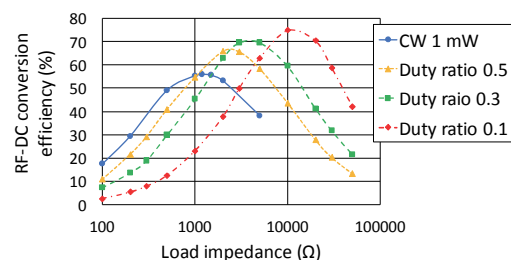


Figure 4. Experimental result of the rectifier with pulse modulated input.

## ABSTRACTS (MASTER THESIS)

## Study on a harmonic-based retrodirective system for microwave power transfer

(Graduate School of Engineering,  
Laboratory of Applied Radio Engineering for Humanosphere, RISH, Kyoto University)

Shogo Kawashima

### Introduction

Recently, wireless power transfer (WPT) techniques has attracted much attention. Microwave power transfer, one of the type of WPT, has some feature that is able to transfer with a long distance. Some applications such as a small airplane or smartphone have been proposed and developed. A Retrodirective system can be used for beam steering in a microwave power transfer system. The target sends a pilot signal, and microwaves are radiated from the direction of arrival (DOA). In this paper, we proposed a harmonics-based retrodirective system (HBRS). Reradiation harmonics from rectennas are adopted for the pilot signal in the HBRS. As such, it is not necessary to prepare the pilot signal source. In this paper, we constructed an HBRS which is consist from a rectenna, a DOA estimating system, and a transmitting system.

### The system configuration and the experimental results

At first, the harmonic re-radiation characteristics of a  $\lambda/2$  dipole rectenna was measured. Based on the re-radiation characteristics, we constructed an interferometry estimation system of second-harmonic DOA. The phase difference between two antennas were detected by phase comparator. Experimental results revealed that the detected directions of second-harmonic DOA were almost similar to a pilot signal DOA. The measurement errors of DOA were analyzed by electromagnetic simulation and were found to be caused by mutual coupling of the harmonic receiving antennas. In order to decrease these errors, correction function was introduced to the system. As a transmitter, a phased array antenna with 2 thin horn antennas was designed. The beam steering range of this phased array antenna was  $25^\circ$ . From the rectenna, the DOA estimating system, and the phased array antenna, integrated experiments was conducted. Figure 1 shows the picture. The results are showed in Figure 2 and Figure 3. Compared to the results without tracking, the rectenna was powered in a wide range with the HBRS tracking. Compared to the results with hand tracking, the results of the HBRS were almost similar. In addition, this paper proposed the method for estimating the initial direction of a target. In this method, initial power is transmitted in wider directivity by using one element of array antenna. This method was verified by experiments. Finally, the HBRS system adopted for experiments of powering a small airplane. However, The error of the DOA estimation differed from the previous experimental results with one rectenna because of the obscurity of re-radiation characteristics. In order to construct an HBRS, it is necessary to design the system entirely including rectennas.

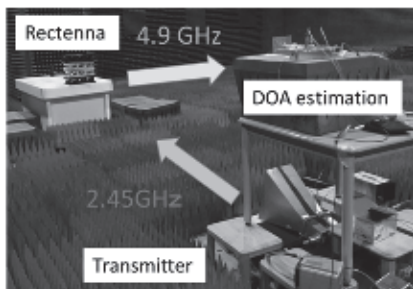


Figure 1.  
The experimental system of HBRS.

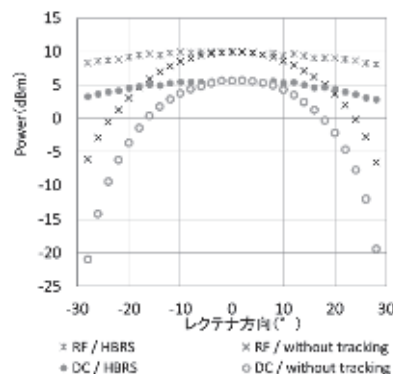


Figure 2. Experimental results without tracking and with HBRS.

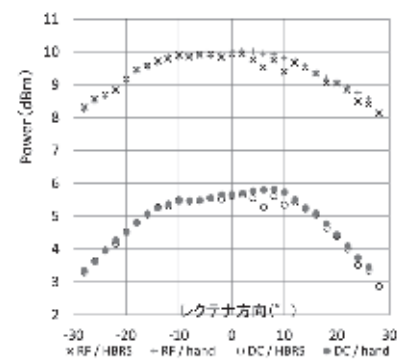


Figure 3. Experimental results with HBRS and with hand tracking.

## ABSTRACTS (MASTER THESIS)

**Development of microwave heating devices using electromagnetic coupling**

**(Graduate School of Engineering,  
Laboratory of Applied Radio Engineering for Humanosphere, RISH, Kyoto University)**

**Daichi Nishio**

**Introduction**

Microwave enables directly and selective heating that is different from conventional heating by heat transfer. Therefore microwave heating has been used in various fields recently. Cavity resonators are generally used as microwave heating devices. However, they are difficult to uniformly heat multiple samples at the same time. Moreover, the resonator requires the metal shield, which expands the size of cavity. Thus, conditions of the heated object in the cavity are hardly observed. A new heating device using electromagnetic coupling is developed in order to solve the above problem. Electromagnetic coupling techniques are often used in fields of wireless power transfer. It is possible to transmit energy without radiating electromagnetic wave using resonators coupling each other. Using this technique, a proposed heating device enables to heat samples in the open space with less microwave leakage.

**The results of simulations and experiments**

In this paper, heating devices using 2.45 GHz half-wavelength resonators are designed with a band pass filters design theory. We designed two types of devices to heat a heating sample and compared with each other from the perspective of heat efficiency and microwave leakage. One is a device using narrow side coupling and the other one is a device using broad side coupling. The simulation model of the device using broad side coupling is shown in Figure 1. HFSS (High Frequency Structural Simulator) using finite element method was used for simulation. As the results of simulation, although heat efficiency of the latter one is lower than former one, the microwave leakage is lower than former one. Therefore, broadside coupling type device was selected to experiment heating samples. In order to meet the radio wave protection guideline, the input power is limited below 30W and in this case absorption power is 6.31 W. This power is enough to heat 4.3mL pure water to 100 °C. We also designed the device to uniformly heat two samples. Modifying the resonator position, heating efficiency became higher and microwave leakage became lower. As the results, this device enables to heat two pure water to 80 °C in order to meet the JIS standard of microwave oven. The real device that can heat two pure water uniformly at the same time is shown in Figure 2. Moreover, the experimental results of heating two pure water samples showed that changing microwave frequency is valid for improvement of heating efficiency.

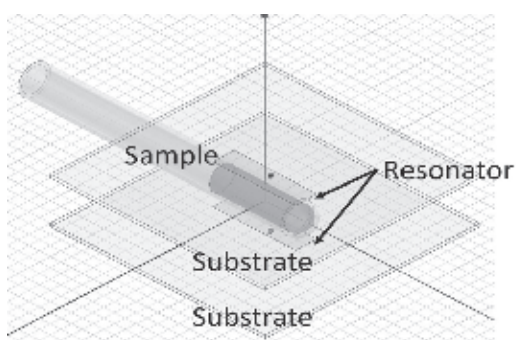


Figure 1. Simulation model of a heating device using broad side coupling

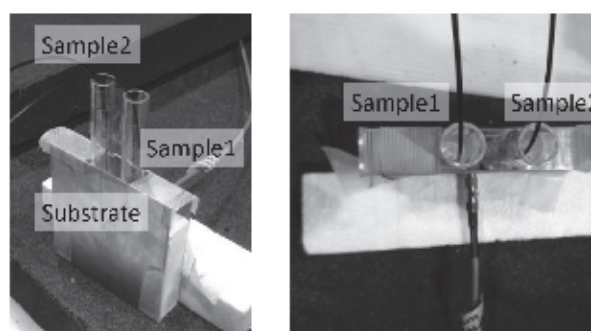


Figure 2. The experimental device

## ABSTRACTS (MASTER THESIS)

**Study on a phase-controlled magnetron for wireless power transfer**

(Graduate School of Engineering,  
Laboratory of Applied Radio Engineering for Humanosphere, RISH, Kyoto University)

**Bo Yang**

**Introduction**

Magnetrons have been widely used as microwave heating applications typified as microwave ovens. The advantages of magnetrons include high efficiency, low cost, and high output power. However, the magnetrons as transmitters have a wide bandwidth, difficult phase control, poorly stable output frequency, and high phase noise. We developed a 5.8 GHz phase controlled magnetron (PCM) system which can control the output phase in a stable frequency and output power. With 5 W (Pi/Po: -18.2dB) injection power, the phase-locked stability of the PCM was lower than  $\pm 1^\circ$ . The response time was less than 100  $\mu$ s. The PCM output could be varied from 160W to 329 W in a phase and power stability state with 10 W (Pi/Po: -15.2dB) injection power.

**The results of simulations and experiments**

In this study, utilizing the injection locking method and the phase locked loop method (PLL). The injection locking method is injecting a reference signal to the magnetron to lock the oscillation frequency. Therefore, controlling the reference signal parameters achieves the frequency and phase synchronization of the magnetron output. An analog phase shifter was set to control the phase of the injection signal in the 5.8 GHz PCM. The magnetron output is fed back to control the phase shifter, then a feedback loop is constituted for controlling the phase. This PLL method does not require the characteristics of the anode current and the magnetron oscillation frequency. We designed and demonstrated a 5.8 GHz PCM system. In this system, the gain margin Gm was 38.6 dB and the phase margin Pm was 63.7°. A photo of the 5.8 GHz PCM is shown in Fig. 1.

The anode current was set 150 mA to make the magnetron worked in the rated condition. The injection power was 5 W. The output power was 329 W within 1% stability. The filament current of the magnetron was 7.4 A by AC 3.35 V. Before the PLL circuit worked, we observed the phase of the magnetron output with the noisy. When turning on the PLL circuit, the magnetron was in a phase-locked state. The measured magnetron phase and power are shown in Fig. 2. The noise disappeared and the output power was in a stable state. Here, the phase of magnetron output was locked in a narrow range. Figure 2 shows the phase when the PLL circuit was working. The phase-locked stability was lower than  $\pm 1^\circ$ .



Fig.1: Photo of a 5.8 GHz PVPCM system (1: 5.8 GHz magnetron, 2: directional coupler, 3: dummy load, 4: current meter, 5: circulator, 6: spectrum analyzer.)

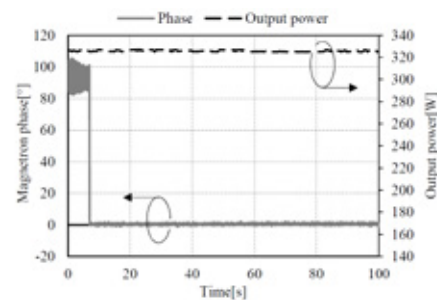


Fig.2: Magnetron phase and output power when the PLL circuit start working.

---

ABSTRACTS (MASTER THESIS)

---

**Study on 3D shape estimation of space debris using MU radar**

**(Graduate School of Engineering,  
Laboratory of Space Systems and Astronautics, RISH, Kyoto University)**

**Naruomi Ikeda**

Recently, the amount of space debris has been rapidly increasing, and this is becoming an obstacle for space exploration. Many organizations are observing space debris and storing such data, however, there was a collision between an active satellite and satellite debris in 2009 regardless of these efforts. This indicates that the present observation network is not sufficient to completely avoid space accidents, and we need to improve and expand the observation network. The aim of this study is to develop a method of estimating the three dimensional shape of space debris using the Middle and Upper atmosphere (MU) RADAR, which is a major observation facility in the Shigaraki MU Observatory of the Research Institute for Sustainable Humanosphere (RISH), Kyoto University. Since atmosphere radar is already in use around the world, by applying this method, we can expand the observation network for space debris without constructing a new observation facility. However, atmosphere radar has poor range resolution compared to conventional radar for space debris observation, and a special signal processing method must be developed. In the previous research using MU radar, the Single- Range Doppler Interferometry (SRDI) method had been proposed to estimate the shape of space debris. In the SRDI method, the shape of space debris can be estimated from a 2D imaging that uses the information of actuating Doppler spectrogram caused by its spin motion. Also, shape estimation method using Radar Cross Section (RCS) had been proposed. In the RCS method, the shape of space debris can be estimated using the information of actuating echo of the target, which is also generated from the spin motion of the target. In this thesis, the basic idea and some results of shape estimation using both SRDI and RCS method are presented. Furthermore, a three dimensional shape estimation method which combines SRDI method and RCS method is described. In order to validate the accuracy of our method, we made actual observation using MU radar and we successfully estimated three dimensional shape of some targets.

---

ABSTRACTS (MASTER THESIS)

---

**Study on feasibility of debris removal method by laser**

**(Graduate School of Engineering,  
Laboratory of Space Systems and Astronautics, RISH, Kyoto University)**

**Yuta Kobayashi**

Currently, there are numerous space debris around the Earth. Space debris are artifacts such as discarded satellites, rockets damaged by an accident and small pieces generated by a collision. Observable debris from the ground exists more than 20,000. The number of debris smaller than 10 cm are estimated to be more than tens of millions. Those debris are difficult to be observed from the ground. Debris are moving at a very high speed of about 7 - 8 km/s. Even small debris hit the satellite directly, there is a risk of serious damage. For this reason, research on debris removal method have been progressed. As one of them, removal method by laser ablation has been studied. Laser ablation is a phenomenon that the part of an object spurts out as plasma when it is irradiated with a strong laser beam. In this way it is possible to change the speed of an object, it is expected to be applied as a debris removal method. In the previous study, the project is proposed that putting a satellite into orbit with an optical observation device and laser irradiation device. The system will detect debris which is difficult to observe from ground and remove the debris by laser irradiation. However, debris removal effect is not considered in detail. Thus in our study, we construct the orbit simulation of a satellite and debris. We evaluated debris removal effect of the method by the simulation.

We perform simulation about existing debris and debris fragment, and investigated the effect of remediation for various debris orbital plane. As a result, we found that it is possible to remove 2% of all debris for 4 week simulation. It mean that we can remove more than 20% of debris around the Earth for 1 year. From this fact, we can conclude that our proposing method using laser ablation is effective for debris remediation around the Earth.

---

ABSTRACTS (MASTER THESIS)

---

**Study on orbital evolution of small space debris  
in consideration of the Lorentz force**

**(Graduate School of Engineering,  
Laboratory of Space Systems and Astronautics, RISH, Kyoto University)**

**Keisuke Akari**

The effects of the Lorentz force on micron-sized space debris has been studied. Their motion can be affected by the Lorentz force because space debris are charged by an interaction with the ambient plasma. In addition, the electromagnetic influence becomes remarkable for smaller debris. Thus, in this study, an orbital model considering the Lorentz force has been developed. Performing the orbital calculation with the model, two significant results have been obtained. The Lorentz force merely rotates orbital planes of debris and strongly shorten time required particular debris to re-enter the atmosphere.

First, the Lorentz force simply rotates orbital planes of small space debris. The Lorentz force causes a monotonically decrease of the right ascension of the ascending node and thus their orbital plane rotates against the Earth's rotation axis. On the contrary, the Lorentz force does not cause the meaningful secular changes in the orbital inclination, even though both the deviation of the actual geomagnetic field from dipole magnetic field and the charge variation during their orbital motion are taken into consideration. As a result, it can be thought that the orbital distribution doesn't change because all orbital planes of debris merely rotate due to the Lorentz force.

Secondly, the Lorentz force generates sparse regions of micron-sized debris because the Lorentz force strongly shortens their lifetime in a particular orbit. Simulation results show that the Lorentz force generally decrease the lifetime of debris and the effect becomes greater for debris in orbits with an orbital inclination of approximately 60 or 120 degrees. This means that it is difficult for micron-sized debris to survive in regions with the declination of around  $\pm 60$  degrees. As a result, debris' flux density is thought to be relatively smaller in the area. Therefore, it can be thought that the Lorentz force is likely to change the orbital distribution in the perspective of the lifetime variation.